

University of Windsor

Scholarship at UWindor

Electronic Theses and Dissertations

Theses, Dissertations, and Major Papers

2003

Syntheses and applications of group VI and VIII-X heterocyclic-phosphinimine complexes.

Liam P. Spencer
University of Windsor

Follow this and additional works at: <https://scholar.uwindsor.ca/etd>

Recommended Citation

Spencer, Liam P., "Syntheses and applications of group VI and VIII-X heterocyclic-phosphinimine complexes." (2003). *Electronic Theses and Dissertations*. 3685.
<https://scholar.uwindsor.ca/etd/3685>

This online database contains the full-text of PhD dissertations and Masters' theses of University of Windsor students from 1954 forward. These documents are made available for personal study and research purposes only, in accordance with the Canadian Copyright Act and the Creative Commons license—CC BY-NC-ND (Attribution, Non-Commercial, No Derivative Works). Under this license, works must always be attributed to the copyright holder (original author), cannot be used for any commercial purposes, and may not be altered. Any other use would require the permission of the copyright holder. Students may inquire about withdrawing their dissertation and/or thesis from this database. For additional inquiries, please contact the repository administrator via email (scholarship@uwindsor.ca) or by telephone at 519-253-3000ext. 3208.

Syntheses and Applications of Group VI and VIII-X Heterocyclic-Phosphinimine Complexes

By
Liam P. Spencer

A Thesis
Submitted to the Faculty of Graduate Studies and Research
Through the Department of Chemistry and Biochemistry
in Partial Fulfillment of the Requirements for
the Degree of Master of Science at the
University of Windsor

Windsor, Ontario, Canada
December, 2002



National Library
of Canada

Bibliothèque nationale
du Canada

Acquisitions and
Bibliographic Services

Acquisitions et
services bibliographiques

395 Wellington Street
Ottawa ON K1A 0N4
Canada

395, rue Wellington
Ottawa ON K1A 0N4
Canada

Your file *Votre référence*
ISBN: 0-612-92452-1
Our file *Notre référence*
ISBN: 0-612-92452-1

The author has granted a non-exclusive licence allowing the National Library of Canada to reproduce, loan, distribute or sell copies of this thesis in microform, paper or electronic formats.

L'auteur a accordé une licence non exclusive permettant à la Bibliothèque nationale du Canada de reproduire, prêter, distribuer ou vendre des copies de cette thèse sous la forme de microfiche/film, de reproduction sur papier ou sur format électronique.

The author retains ownership of the copyright in this thesis. Neither the thesis nor substantial extracts from it may be printed or otherwise reproduced without the author's permission.

L'auteur conserve la propriété du droit d'auteur qui protège cette thèse. Ni la thèse ni des extraits substantiels de celle-ci ne doivent être imprimés ou autrement reproduits sans son autorisation.

In compliance with the Canadian Privacy Act some supporting forms may have been removed from this dissertation.

Conformément à la loi canadienne sur la protection de la vie privée, quelques formulaires secondaires ont été enlevés de ce manuscrit.

While these forms may be included in the document page count, their removal does not represent any loss of content from the dissertation.

Bien que ces formulaires aient inclus dans la pagination, il n'y aura aucun contenu manquant.

Canada

© 2002 Liam Spencer

Abstract

A class of phosphinimine-based group VI and VIII-X late transition metal (LTM) complexes has been synthesized and evaluated for olefin polymerisation activity. The phosphinimine ligand has been designed to incorporate an imine moiety; a functional group which has been successfully applied in very active LTM olefin catalytic systems. Heterocycles, such as pyridine and imidazole are used to accomplish the integration of an imine group into the ligand. Phosphines employing the heterocyclic group are oxidized by phenyl azides in excellent yields to form phosphinimine ligands. These phosphinimine ligands react with several LTM's, the complexes of which are identified by single crystal diffraction studies, elemental analysis, NMR and IR spectroscopy, and magnetic susceptibility measurements. In contrast to highly active imine-based systems, we find iron(II) and nickel(II) complexes with bulky phosphinimine-based ligands oligomerise ethylene to form C₄ alkenes with moderate activities.

Computational calculations were performed to determine the effects of a phosphinimine-based ligand on a cationic nickel(II) centre. The presence of a phosphorus atom in the backbone of the ligand creates an increase in negative charge on the nickel atom, in contrast to that seen in imine ligands. This increase in charge suppresses electron donation from the incoming ethylene molecule to the metal centre, thus creating a weak metal-ethylene bond. The addition of electron-withdrawing substituents such as fluorine on the phosphorus appears to increase the positive charge on the nickel(II) atom, hence allowing for a stronger metal-ethylene interaction. Attempts to make a fluorinated phosphinimine have so far been unsuccessful, due to an inability to oxidize the phosphine to the corresponding phosphinimine ligand.

In addition to neutral analogues, we find the imidazolyl-phosphinimine ligand can be advantageously altered to possess anionic character. Metal complexes involving a phosphinimine-imidazolate ligand can be formed with rhodium(I), rhodium(III), chromium(III), and nickel(II) metals. It was determined that, similar to neutral iron(II) and nickel(II) imidazolyl-metal complexes, the nickel(II) imidazolate complex oligomerises ethylene with a low activity ($18.9 \text{ g}\cdot\text{mmol}^{-1}\cdot\text{hr}^{-1}\cdot\text{atm}^{-1}$).

Dedication

This work is dedicated to the two important women in my life. To my mother, Carolyn Norris, you have always been there for me and I greatly appreciate all that you have given me (especially my sense of humour (“Illegitimus Non Carborundum”)). If it wasn't for you momma, I hesitate to think where I would be. To my girlfriend, Pauline Vykruta, your approach to life is truly inspirational. You have challenged me in many ways, and I look forward to spending my life with you, miláčku.

Acknowledgements

I wish to acknowledge first and foremost, Dr. Douglas Stephan. When I first came to Windsor as an undergraduate, I was amazed by the passion that he has for chemistry. Despite his immensely busy schedule, he always found time to listen to my ideas (and problems) and offer words of encouragement and hope. In the words of a colleague, you truly have made learning in this environment “a grad student’s dream”, Doug.

I would like to thank those people who I have worked with: Drs. Aaron Hoskin, Chris Ong, Silke Courtenay, Jim Kickham; and those who I currently work with: Dr. Pingrong Wei, Dr. Todd Graham, Dr. Denise Walsh, and Chad Beddie (PhD), Emily Hollink (PhD), Sarah Smith (PhD), Steve Clemens (MSc), Katie Chan (MSc), Lourisa Cabrera (MSc), Ramadan Ali Altwer (MSc), Jason Masuda (MSc), and Jenny McCahill (MSc). Each of you has taught me something which I will remember. Equally important, I would also like to thank all the members of the Loeb group.

The department of Biochemistry and Chemistry has also been an immense help in making my stay here easy and enjoyable. I would especially like to thank James Gauld (my second boss) for his patience and his advice not only with calculations, but also for friendship. I would also like to thank Mike Fuerth for all his NMR assistance, and everyone in the CCC. Sharon Horne, and Kimberly Lefebvre also require thanks for being patient with me during tough health times.

Finally, I would like to thank my roommates; past and present: Greg (John Earl) Davidson, Niroshan Ramachandran, and Steve Clemens. You have made my stay in

Ontario a memorable one, and have filled me with stories to tell the ages (good and bad, but mostly good). I appreciate everything you guys have done for me.

Table of Contents

	Page
Abstract	iv
Dedication	vi
Acknowledgements	vii
List of Figures	xiv
List of Tables.....	xv
List of Schemes	xvi
Abbreviations	xvii

Chapter One**Introduction**

1.1	The Development of ETM Olefin Polymerisation Catalysts.....	2
1.2	The Beginning of Late Transition Metal Catalysis.....	5
1.3	Further Developments In LTM Catalysis	10
1.4	Reported Chemistry of Phosphinimine metal complexes in olefin polymerisation.....	13
1.5	General Synthesis of Phosphinimine Ligands	17
1.6	Scope of this Work.....	18

Chapter 2**Synthesis of Selected Group VIII-X Pyridyl Phosphinimine Complexes**

2.1	Introduction	19
2.2	Experimental Section	
	General data.....	19

Synthesis of 2,6-diisopropylphenyl azide N ₃ -2,6- ⁱ Pr ₂ C ₆ H ₃ 28 and N ₃ -2,6-Me ₂ C ₆ H ₃ 29	21
Synthesis of 2-bromo-6-benzylpyridine [2-Br-6-Bn]py 30	21
Synthesis of 2-bromo-6-trimethylsilylpyridine [2-Br-6-TMS]py 31	22
Synthesis of 2-amino-6-phenylpyridine [2-NH ₂ -6-Ph]py 32	22
Synthesis of 2-bromo-6-phenylpyridine [2-Br-6-Ph]py 33	22
Synthesis of 2-(diphenylphosphino)-pyridine (2-py)PPh ₂ 26 , [6-Me-2-PPh ₂]py 34 , [6-Bn-2-PPh ₂]py 35 , [6-TMS-2-PPh ₂]py 36 , and [6-Ph-2-PPh ₂]py 37	22
Synthesis of [2-PPh ₂ N-2,6-Me ₂ C ₆ H ₃]py 38 , [2-PPh ₂ N-2,6- ⁱ PrC ₆ H ₃]py 39 , [2-PPh ₂ N-TMS]py 40 , [6-Me-2-PPh ₂ N-2,6-Me ₂ C ₆ H ₃]py 41 , [6-Me-2-PPh ₂ N-2,6- ⁱ PrC ₆ H ₃]py 42 , [6-TMS-2-PPh ₂ N-2,6-Me ₂ C ₆ H ₃]py 43 , [6-TMS-2-PPh ₂ N-2,6- ⁱ PrC ₆ H ₃]py 44 , [6-Bn-2-PPh ₂ N-2,6-Me ₂ C ₆ H ₃]py 45 , [6-Bn-2-PPh ₂ N-2,6- ⁱ PrC ₆ H ₃]py 46 , [6-Ph-2-PPh ₂ N-2,6-Me ₂ C ₆ H ₃]py 47 , and [6-Ph-PPh ₂ N-2,6- ⁱ PrC ₆ H ₃]py 48	24
Synthesis of [2-PPh ₂ N-TMS]pyPdCl ₂ 49	28
Synthesis of [2-PPh ₂ N-2,6-Me ₂ C ₆ H ₃]pyNiBr ₂ 50 , [2-PPh ₂ N-2,6- ⁱ Pr ₂ C ₆ H ₃]pyNiBr ₂ 51 , [6-Me-2-PPh ₂ N-2,6-Me ₂ C ₆ H ₃]pyNiBr ₂ 52 , [6-Me-2-PPh ₂ N-2,6-Pr ₂ C ₆ H ₃]pyNiBr ₂ 53 , [6-TMS-2-PPh ₂ N-2,6-Me ₂ C ₆ H ₃]pyNiBr ₂ 54 , [6-TMS-2-PPh ₂ N-2,6- ⁱ Pr ₂ C ₆ H ₃]pyNiBr ₂ 55 , [6-Bn-2-PPh ₂ N-2,6-Me ₂ C ₆ H ₃]pyNiBr ₂ 56 , [6-Bn-2-PPh ₂ N-2,6- ⁱ Pr ₂ C ₆ H ₃]pyNiBr ₂ 57 , [6-Ph-2-PPh ₂ N-2,6-Me ₂ C ₆ H ₃]pyNiBr ₂ 58 , and [6-Ph-2-PPh ₂ N-2,6- ⁱ Pr ₂ C ₆ H ₃]pyNiBr ₂ 59	29
Synthesis of [2-PPh ₂ N-2,6-Me ₂ C ₆ H ₃]pyFeCl ₂ 60 , [2-PPh ₂ N-2,6- ⁱ Pr ₂ C ₆ H ₃]pyFeCl ₂ 61 , [6-Me-2-PPh ₂ N-2,6-Me ₂ C ₆ H ₃]pyFeCl ₂ 62 , [6-Me-2-PPh ₂ N-2,6- ⁱ Pr ₂ C ₆ H ₃]pyFeCl ₂ 63 , [6-TMS-2-PPh ₂ N-2,6-Me ₂ C ₆ H ₃]pyFeCl ₂ 64 , [6-TMS-2-PPh ₂ N-2,6- ⁱ Pr ₂ C ₆ H ₃]pyFeCl ₂ 65 ,	

[6-Bn-2-PPh ₂ N-2,6-Me ₂ C ₆ H ₃]pyFeCl ₂ 66 ,	
[6-Bn-2-PPh ₂ N-2,6- ⁱ Pr ₂ C ₆ H ₃]pyFeCl ₂ 67 ,	
[6-Ph-2-PPh ₂ N-2,6-Me ₂ C ₆ H ₃]pyFeCl ₂ 68 , and	
[6-Ph-2-PPh ₂ N-2,6- ⁱ Pr ₂ C ₆ H ₃]pyFeCl ₂ 69	30
Synthesis of [6-Ph-2-P(C ₆ F ₅) ₂]py 70	32
Procedure for ethylene polymerisation	32
Procedure for ethylene oligomerisation	33
Computational Details.....	34
X-ray Data Collection and Reduction.....	34
Structure Solution and Refinement.....	35
2.3 Results and Discussion	
Synthesis and Characterization of Pyridyl-Phosphinimine Metal Complexes.	38
Ethylene Polymerisation and Oligomerisation Study of Pyridyl-phosphinimine Metal Complexes	49
Computational Study of Diimine (NCCN) and Phosphinimine-imine (NPCN) Ligands and Nickel(II) Complexes.....	51
Attempted Synthesis of Fluorinated Pyridyl-phosphinimine Ligands.....	54
2.4 Summary and Conclusions	56

Chapter 3

Synthesis of Selected Group VI and VIII-X Imidazolyl and Imidazolate- Phosphinimine Complexes

3.1 Introduction	57
3.2 Experimental section	
General Data	57
Synthesis of 1-methyl-2-(diphenylphosphino)imidazole [1-Me-2-PPh ₂]imidazole 73 , [1-Me-4,5-Ph ₂ -2-PPh ₂]imidazole 74 , and [1-Me-2-PPh ₂]benzimidazole 75 ...	58
Synthesis of [1-Me-2-PPh ₂ N-2,6-Me ₂ C ₆ H ₃]imid 76 ,	
[1-Me-2-PPh ₂ N-2,6- ⁱ PrC ₆ H ₃]imid 77 ,	
[1-Me-4,5-Ph ₂ -2-PPh ₂ N-2,6-Me ₂ C ₆ H ₃]imid 78 ,	

[1-Me-4,5-Ph ₂ -2-PPh ₂ N-2,6- ⁱ PrC ₆ H ₃]imid 79 ,	
[1-Me-2-PPh ₂ N-2,6-Me ₂ C ₆ H ₃]benzimid 80 ,	
[1-Me-2-PPh ₂ N-2,6- ⁱ PrC ₆ H ₃]benzimid 81 , and	
[1-Me-4- ^t Bu-2-PPh ₂ N-2,6- ⁱ PrC ₆ H ₃]imid 82	59
Synthesis of [1-Me-2-PPh ₂ N-2,6- ⁱ Pr ₂ C ₆ H ₃]imidPdCl ₂ 83	62
Synthesis of [1-Me-2-PPh ₂ N-2,6-Me ₂ C ₆ H ₃]imidNiBr ₂ 84 ,	
[1-Me-2-PPh ₂ N-2,6- ⁱ Pr ₂ C ₆ H ₃]imidNiBr ₂ 85 ,	
[1-Me-2-PPh ₂ N-2,6-Me ₂ C ₆ H ₃]benzimidNiBr ₂ 86 ,	
[1-Me-2-PPh ₂ N-2,6- ⁱ Pr ₂ C ₆ H ₃]benzimidNiBr ₂ 87 ,	
[1-Me-4,5-Ph ₂ -2-PPh ₂ N-2,6-Me ₂ C ₆ H ₃]imidNiBr ₂ 88 ,	
[1-Me-4,5-Ph ₂ -2-PPh ₂ N-2,6- ⁱ Pr ₂ C ₆ H ₃]imidNiBr ₂ 89 , and	
[1-Me-4- ^t Bu-2-PPh ₂ N-2,6- ⁱ Pr ₂ C ₆ H ₃]imidNiBr ₂ 90	63
Synthesis of [1-Me-2-PPh ₂ N-2,6-Me ₂ C ₆ H ₃]imidFeCl ₂ 91 ,	
[1-Me-2-PPh ₂ N-2,6- ⁱ Pr ₂ C ₆ H ₃]imidFeCl ₂ 92 ,	
[1-Me-2-PPh ₂ N-2,6-Me ₂ C ₆ H ₃]benzimidFeCl ₂ 93 ,	
[1-Me-2-PPh ₂ N-2,6- ⁱ Pr ₂ C ₆ H ₃]benzimidFeCl ₂ 94 ,	
[1-Me-4,5-Ph ₂ -2-PPh ₂ N-2,6-Me ₂ C ₆ H ₃]imidFeCl ₂ 95 ,	
[1-Me-4,5-Ph ₂ -2-PPh ₂ N-2,6- ⁱ Pr ₂ C ₆ H ₃]imidFeCl ₂ 96 , and	
[1-Me-4- ^t Bu-2-PPh ₂ N-2,6- ⁱ Pr ₂ C ₆ H ₃]imidFeCl ₂ 97	64
Synthesis of [1-H-2-PPh ₂ N-2,6-Me ₂ C ₆ H ₃]imid 98	65
Synthesis of Na[2-PPh ₂ N-2,6-Me ₂ C ₆ H ₃]imid· THF 99	66
Synthesis of [2-PPh ₂ N-2,6-Me ₂ C ₆ H ₃]imidRhCp*Cl 100 , and	
[2-PPh ₂ N-2,6-Me ₂ C ₆ H ₃]imidCrCp*Cl 101	66
Synthesis of [2-PPh ₂ N-2,6-Me ₂ C ₆ H ₃]imidRhCOD 102	67
Synthesis of [2-PPh ₂ N-2,6-Me ₂ C ₆ H ₃]imidNi(allyl) 103	68
Procedure for ethylene polymerisation and oligomerisation.....	68
3.3 Results and Discussion	
Neutral Imidazolyl-phosphinimine Ligands	71
Anionic Imidazolyl-phosphinimine Ligands	78
Ethylene Polymerisation Study of Imidazolyl-phosphinimine Metal Complexes.	89
3.4 Summary and Conclusions	91

Chapter 4

Summary and Future Outlook.....	92
References.....	95
<i>Curriculum Vitae</i>	104

List of Figures

Figure	Description	Page
1.1	Nickel(II) and palladium(II) diimine catalysts (4 and 5 , respectively).....	7
1.2	Various phosphinimine-based ligands examined for LTM olefin polymerisation.....	14
2.1	ORTEP drawing of 34	39
2.2	ORTEP drawing of 49	43
2.3	ORTEP drawing of 54-CH₂Cl₂	46
2.4	ORTEP drawing of 57	47
2.5	ORTEP drawing of 69-H₂O	48
2.6	Orbital diagrams of the lone pairs on (a) nitrogen, and (b) phosphorus in the PNCN ligand	52
2.7	Orbital diagrams of (a) bonding and (b) antibonding lone pairs on the NCCN ligand	53
3.1	ORTEP drawing of 83-CH₃CN	74
3.2	ORTEP drawing of 96	76
3.3	ORTEP drawing of 97	77
3.4	ORTEP drawing of 99	80
3.5	ORTEP drawing of 100	83
3.6	ORTEP drawing of 101	84
3.7	ORTEP drawing of 102	87

List of Tables

Table	Description	Page
2.1	Crystallographic Parameters for 34, 49, 54, 57, 69	36
2.2	Ethylene polymerisation by Cp_2ZrCl_2 and nickel/iron pyridyl-phosphinimine complexes 54, 55, 58, 59, 64, 65, 68, and 69	49
2.3	Ethylene oligomerisation results of activated nickel/iron pyridyl-phosphinimine complexes 59 and 69	50
2.4	Lone pair energies and nickel atomic charge of ligands and cationic metal complexes.....	53
3.1	Crystallographic Parameters for 83, 96, 97, 99, 100, 101 and 102	69
3.2	Ethylene polymerisation by nickel/iron pyridyl-phosphinimine complexes 89, 90, and 97	90
3.3	Ethylene oligomerisation results of activated nickel/iron pyridyl-phosphinimine complexes 89 and 97	91

List of Schemes

Scheme	Description	Page
1.1	Heterogeneous olefin polymerisation by TiCl_4	2
1.2	Activation of Cp_2ZrCl_2 by excess MAO.....	3
1.3	Proposed mechanism of LTM olefin polymerisation	9
1.4	The Staudinger reaction between a trivalent phosphorus atom and an organic azide proceeding through a phosphazide intermediate	17
1.5	The Kirsanov reaction between a pentavalent phosphorus atom and a primary amine.	18
2.1	Synthesis of 6-substituted-2-pyridyldiphenylphosphines	38
2.2	Synthesis of 2,6-disubstituted phenylazides.....	40
2.3	Synthesis of pyridyl-phosphinimines 38-48	41
2.4	Synthesis of palladium-phosphinimine complex 49	42
2.5	Synthesis of First Row Group VIII and X transition metal pyridyl-phosphinimines	44
2.6	Attempted synthesis of a fluorinated-phosphinimine ligand utilizing 70	55
3.1	Synthesis of substituted 1-methyl-2-(diphenylphosphino)imidazoles 73-75	71
3.2	Synthesis of neutral substituted imidazolyl-phosphinimine ligands 76-82	72
3.3	Synthesis of the imidazolyl-phosphinimine palladium complex 83	73
3.4	General synthesis of metal complexes 84-97	75
3.5	Synthesis of 1-H-imidazolyl-phosphinimine ligand 98	79
3.6	Synthesis of phosphinimine-imidazolate ligand 99	81
3.7	Synthesis of Rh(III) and Cr(III) phosphinimine-imidazolate metal complexes	82
3.8	Reaction of 99 with a $[(\text{COD})\text{RhCl}]_2$	85
3.9	The reaction between 99 and $[(\text{allyl})\text{NiBr}]_2$	88

Abbreviations

Å	Angstrom
Ar	aryl
atm	atmosphere
B3LYP	Hybrid Density Functional Theory Method with Becke 3 exchange with Lee, Yang, Parr correlation
BM	Bohr Magneton
Bn	benzyl (-CH ₂ (C ₆ H ₅))
br	broad
Co.	company
Cp*	pentamethylcyclopentadienyl anion (η^5 -C ₅ Me ₅)
d	doublet
dd	doublet of doublets
dt	doublet of triplets
°	Degree
°C	degrees of Celsius
δ	chemical shift
Da	Daltons
DEAC	diethylaluminum chloride
DFT	Density Functional Theory
DME	dimethoxyethane
EA	elemental analysis
eq	equivalent

ETM	early transition metal
F_c	calculated structure factor
F_o	observed structure factor
g	grams
η	hapto
G98	Gaussian 98
GC	gas chromatography
h	hour
HF	Hartree-Fock
HOMO	highest occupied molecular orbital
Hz	Hertz
i.d.	internal diameter
imid	imidazole
IR	Infrared
ⁱ Pr	iso-propyl (-CH(CH ₃) ₂)
J	coupling constant
LANL2DZ	Los Alamos National Lab 2 Double Zeta
LTM	late transition metal
LUMO	lowest unoccupied molecular orbital
m	multiplet
MAO	methylaluminumoxane
Me	methyl (-CH ₃)
MHz	Megahertz

min	minutes
mL	millilitre
mm	millimetre
mmol	millimols
MS	mass spectrometry
NBO	natural bond orbital
NMR	Nuclear Magnetic Resonance
ORTEP	Oak Ridge Thermal Ellipsoid Plot
Ph	phenyl (-C ₆ H ₅)
ppm	parts per million
PDI	polydispersity index
POV	Persistence of Vision
psi	pounds per square inch
py	pyridine
R	agreement factor
R _w	weighted agreement factor
s	singlet
sept	septet
^t Bu	tertiary butyl (-C(CH ₃) ₃)
THF	tetrahydrofuran
α	alpha
β	beta
γ	gamma

Chapter One

Introduction

Polyethylene is ubiquitous in modern society having found widespread household and industrial applications. Indeed, there is a growing interest in it as providing an alternative to glass, metal, paper and concrete.¹ Consequently, the demand for polyethylene has been projected at 50 million metric tons annually by the year 2003.² Early transition metal (ETM) catalysts have been commercially used to produce polyethylene due to their long lifetime and high activity.³⁻⁷ However, such catalysts suffer inherent drawbacks of sensitivity to moisture, oxygen, and impurities in monomer feed.⁸

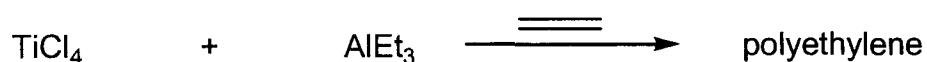
Developments in the field of polymerisation catalysis have generally focussed on obtaining greater control of the polymer's characteristics, the ability to incorporate combinations of monomers, and the development of effective catalysts able to tolerate a variety of functional groups. Late transition metal (LTM) catalysts provide attractive alternatives as they are less oxophilic than ETM's and are more tolerant of functional groups. These attributes make LTM catalysts likely targets for the development of new polymers for novel applications .

In this chapter, technological advances regarding LTM olefin polymerisation catalysis are highlighted. In addition, previous research of metallocenes and non-metallocene-based metal complexes is included along with the early discoveries of LTM olefin polymerisation. The synthesis and the reported use of the phosphinimine ligand in

olefin polymerisation is also described to demonstrate the virtually unexplored nature of this area.

1.1 The Development of ETM Olefin Polymerisation Catalysts

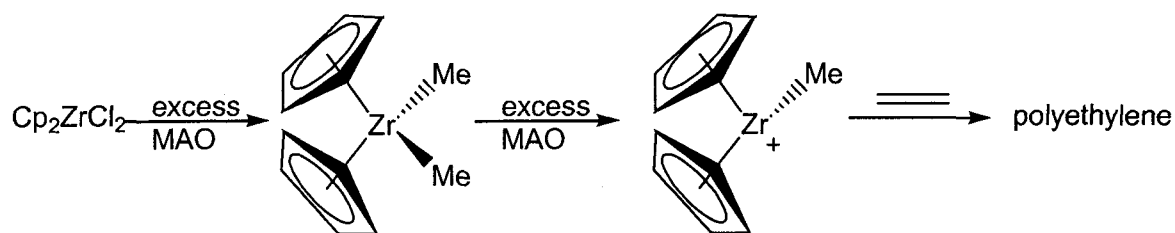
The discovery that ETM's could polymerise α -olefins into polyolefins by Ziegler and Natta⁹ has had a tremendous impact both industrially and academically. Prior to Ziegler's discovery, polyethylene was produced using a free-radical process under forcing conditions (e.g. 3500 atm at 300°C).¹⁰ However, Ziegler-Natta catalysts demonstrated that ethylene could be polymerised under milder conditions in the presence of TiCl_4 with AlEt_3 activation (Scheme 1.1). Unfortunately, the discovery by Ziegler and Natta was based on an ill-defined heterogeneous system, whose mode and mechanism still remain a topic of current research.



Scheme 1.1 Heterogeneous olefin polymerisation by TiCl_4 .

Developments derived from the original Ziegler-Natta catalyst dealt with the discovery of a well-defined homogeneous olefin polymerisation catalyst. Kaminsky³ reported that Cp_2ZrCl_2 could be activated with methylaluminoxane (MAO) to give a cationic zirconium alkyl species capable of polymerizing ethylene (Scheme 1.2). It is generally accepted that the role of MAO is to create a dialkyl species that quickly undergoes alkyl abstraction by the same aluminum cocatalyst to produce a cationic metal centre.¹¹ Chain termination is believed to occur by either: (1) β -hydrogen elimination to

yield an unsaturated polymer chain end and a metal hydride cation, or (2) alkyl chain transfer to the non-coordinating counterion thus, providing a metal alkyl cation.

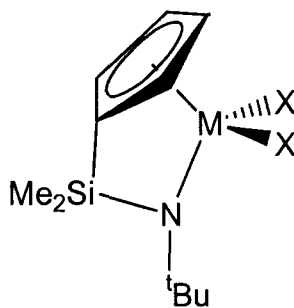


Scheme 1.2 Activation of Cp_2ZrCl_2 by excess MAO.

Further work by Sinn,⁴ Brintzinger,^{5,7} Kaminsky,^{4,7} and Ewan¹² showed that metallocenes activated with aluminoxanes produced catalysts with high catalytic activities and long lifetimes. The accepted industry standard is Cp_2ZrCl_2 , which has a reported activity of $895 \text{ g}\cdot\text{mmol}^{-1}\cdot\text{hr}^{-1}$ at atmospheric ethylene pressure with MAO activation.⁸ In addition, modification of the Cp ligand resulted in catalysts which could produce polymers with specific characteristics.¹³ Furthermore, changing the olefin from ethylene to propylene allowed for stereospecific polymerisation which produced a variety of novel polymers with varying uses and characteristics.^{5,12}

The idea that modified metallocene catalysts could create unique polymers shifted research efforts towards the development of non-metallocene based ligands and metal complexes. There are numerous examples of non-metallocene ligands that can complex with ETM's to produce complexes capable of being highly active olefin polymerisation catalysts.⁸ Perhaps the most recognized example of a non-metallocene catalyst is the “constrained geometry catalyst” designed at Dow and Exxon. This catalyst 1 and

derivatives thereof, are highly active in the both the polymerisation of ethylene ($1500 \text{ g}\cdot\text{mmol}\cdot\text{hr}^{-1}\cdot\text{bar}^{-1}$) and copolymerisation of ethylene with 1-hexene comonomer.^{14,15,16}



1

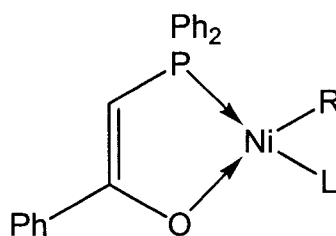
Of central importance in both ETM metallocene and non-metallocene catalysts is the role that the ligand plays. It has been determined that the ligand affects the metal centre in various ways, by: (1) control over the metal coordination number; (2) control over the metal coordination geometry; (3) control over the formal oxidation state of the metal; and (4) steric protection of the active site, which in some cases can influence stereoselectivity.⁸ In designing a ligand system, both electronic and steric effects must be considered in order to synthesize a highly active olefin polymerisation catalyst.

As briefly mentioned earlier, polymerisations with ETM systems have several potential drawbacks. ETM's have an increased electrophilic nature which makes them prone to poisoning by most functionalized olefins. However, there are some examples of copolymerisation under special circumstances.¹⁷⁻²⁶ Furthermore, these systems are air and moisture sensitive, in particular the catalytically active cationic metal species, which can cause deactivation of the catalyst. Late transition metal complexes offer solutions to these problems as they are generally less oxophilic and hydrophobic than ETM's and can tolerate a variety of polar functional groups. This allows the incorporation of polar

functionalities into the resultant polymer, thus providing avenues to synthesizing polymers with potentially unique properties unavailable to ETM catalysts.

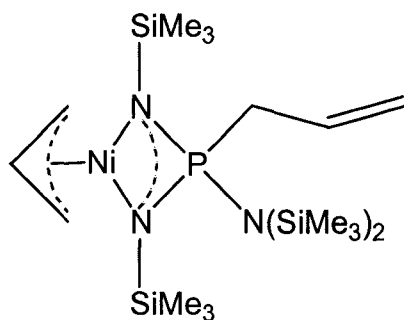
1.2 The Beginning of Late Transition Metal Catalysis

Late transition metal complexes can be exploited to make polymers and oligomers not accessible by early transition metal compounds. In contrast to their ETM counterparts, LTM's show an increased tendency to chain terminate *via* β -hydride elimination. When the rate of this process becomes competitive with the rate of propagation process, formation of short chain polymers, called oligomers results. Arguably, the first recognized industrial applications of LTM catalysis was the Shell Higher Olefin Process (SHOP) developed by Keim *et al.*²⁷ This process is based on a neutral nickel catalyst containing a P—O chelate (**2**, R = solvent, L = PPh₃), that oligomerises ethylene to form linear C₄-C₂₀ chains under extreme conditions or in the presence of a phosphine scavenger.



Nitrogen-based ligands with bulky substituents have been garnering attention for the past 20 years as potential tools in LTM olefin polymerisation. Keim *et al.* were the first group to extend their research to encompass polymerisation of olefins with bulky

nitrogen chelates by employing a bulky iminophosphorane amidato ligand to form the nickel complex **3**.²⁸

**3**

Compound **3** was shown to be a single component catalyst for the polymerisation of ethylene, having a reported activity of 1000 mol ethylene/mol nickel at 70°C and 50 bar. The corresponding palladium complex did not catalyze the polymerisation of ethylene. Although low activities were found, results from these experiments suggested nitrogen-based ligands in LTM complexes could polymerise ethylene.

A significant breakthrough in LTM olefin polymerisation catalysis was the development of nickel and palladium diimine complexes by Brookhart *et al.*²⁹⁻³⁶ Brookhart anticipated that “harder” nitrogen-based ligands with increased steric demand might lead to higher molecular weight polymers. To satisfy this condition, Brookhart proposed the syntheses of cationic methyl complexes incorporating bulky nitrogen-based diimine ligands (Figure 1.1).

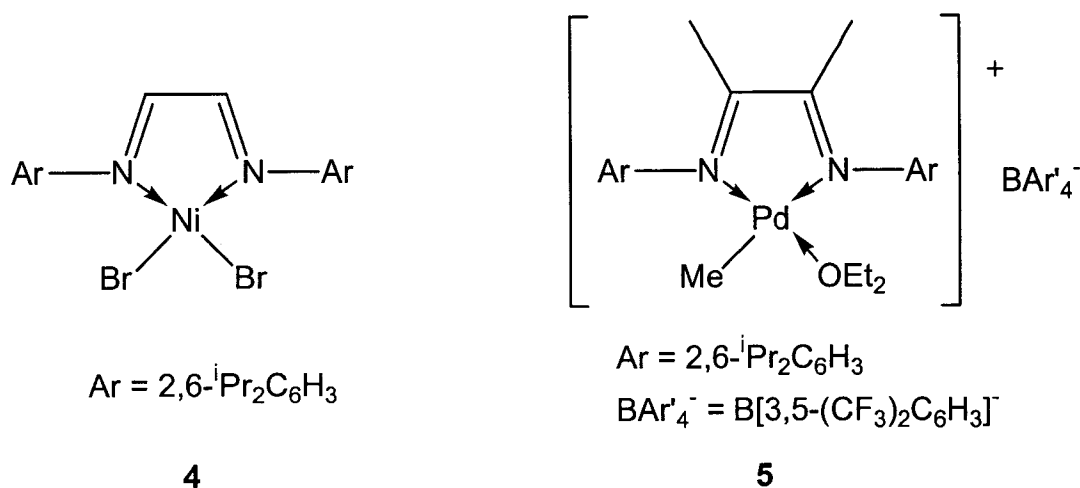


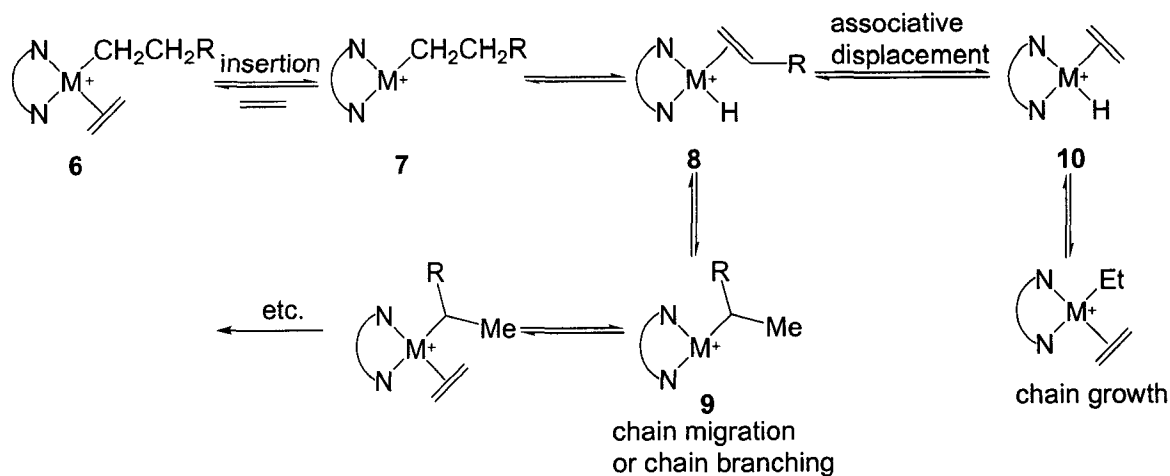
Figure 1.1 Nickel(II) and palladium(II) diimine catalysts (**4** and **5**, respectively).

The ethylene polymerisation activity of complex **4** was 11,000 g·mmol⁻¹·hr⁻¹ at 25°C and 1 atm when activated by methylaluminoxane (MAO); however, the corresponding palladium complex **5** has an activity of 26.6 g·mmol⁻¹·hr at 25°C and 1 atm. The activity of **4** and its derivatives is drastically reduced upon increasing pressure and temperature, indicative of a weak dative bond between the nitrogen and nickel atoms.

Analysis of the polyethylene obtained from **4** and **5** indicated extensive, randomly dispersed branching of variable length along the main chain. Brookhart noted that reducing the steric bulk of neutral α -diimine ligands reduces the degree of branching and the molecular weight.²⁹ From these results, it was determined that both the ligand and the metal play key roles and that the following specific features of the catalyst are required for the polymerisation of ethylene: (1) an electrophilic cationic metal centre to allow the binding of ethylene; (2) steric bulk to protect the metal centre from undergoing deactivation pathways present in earlier processes; and (3) the presence of a non-coordinating counterion to provide a coordination site for incoming ethylene.

Mechanistic studies performed by Brookhart *et al.* (Scheme 1.3)²⁹ showed that an alkyl-ethylene metal species (6) is the resting state of the active catalyst species. The ethylene moiety can then insert into the M—C bond creating a growing alkyl chain (7). This process of coordination and insertion can continue to create a linear alkyl unit or alternatively, the alkyl chain can undergo β -hydride elimination to form a metal hydride species (8). This hydride can then either undergo reinsertion with opposite stereochemistry to form a methyl branch on the chain (9), or another olefin unit can associatively displace the alkyl unit to create a new alkyl chain (10). The elimination of the alkyl chain by associative displacement is known as chain growth, whereas formation of methyl (and longer side chains) groups is known as chain branching.

Since the LTM complexes in question are square planar, the steric environment created by the ligand affects both associative displacement and chain transfer. Brookhart²⁹⁻³¹ suggested that substituents on the aryl ring, by virtue of their perpendicular orientation with respect to the ligand plane, block the approach of olefins from above and below the plane. This allows the rate of chain propagation to be faster than the rate of chain migration, thus producing high molecular weight polymers. In addition, they also showed that varying the pressure and temperature led to different degrees of branching and density in the polymer produced.

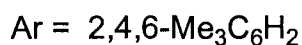
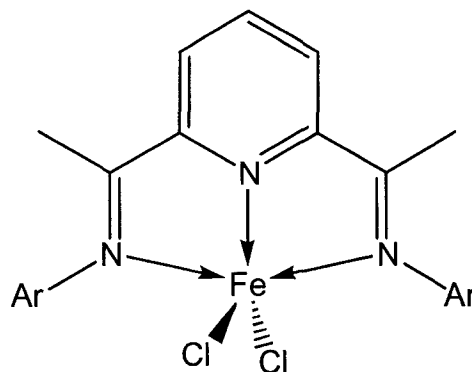


Scheme 1.3 Proposed mechanism of LTM olefin polymerisation.

Brookhart *et al.*³⁷ and Gibson *et al.*³⁸ extended the above considerations with nickel and palladium catalysts to encompass iron and cobalt. A bis(imino)pyridyl ligand was used to form iron(II) and cobalt(II) complexes much like Brookhart's original nickel(II) complex. Not only could this ligand be modified to exist as an aldimine or ketimine, but modification of the steric bulk above and below the metal-ligand plane affected activity, molecular weight, and molecular weight distribution. The most active catalyst reported is that of the iron ketimine complex **11** ($206,000 \text{ g}\cdot\text{mmol}^{-1}\cdot\text{hr}^{-1}$) with MAO activation at 35°C and a TMA scavenger.

The behaviour of these catalysts towards olefin polymerisation is very different from that of nickel(II) diimine compounds. The activity of **11** increases when there is a decrease in steric bulk from isopropyl to methyl groups in the *ortho* position on the aryl ring.^{37,39} Furthermore, the polyethylene formed is highly linear. In both the iron and cobalt examples, the electronic environment of the metal centre is significantly different

from that of the nickel and palladium cases; therefore, it is no surprise that not only are the activities different, but also the polymer characteristics.

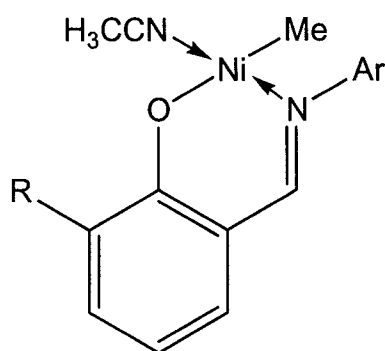


11

Clearly, the steric and electronic properties of the ligand are of paramount importance for the successful polymerisation of ethylene by LTM complexes. Phosphinimine groups may be tailored to offer a steric environment similar to diimine ligands but they differ in other characteristics such as π -acceptor ability and donor strength. This class of ligands are readily-accessible, yet have been virtually unexploited.

1.3 Further Developments In LTM Catalysis

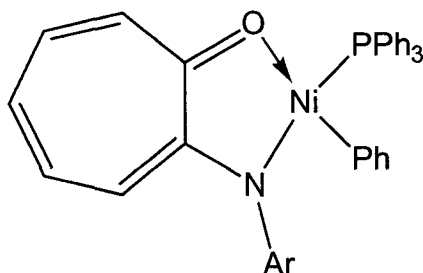
Recent research in LTM catalysis has involved development of single-component catalysts. Pioneering work in this field was performed by Grubbs *et al.*,⁴⁰ who demonstrated that a N—O salicylaldiminato ligand could react to form a nickel(II) species (**12**, R = anthracenyl, Ar = 2,6-ⁱPr₂C₆H₃) similar to the complex Keim reported earlier.²⁷



12

These complexes are very active and produce highly linear polyethylene with 5-20 branches per 1000 carbon atoms ($M_w > 250,000$). In the absence of cocatalysts, these species have an indefinite lifetime and are capable of producing activities up to $6400 \text{ g}\cdot\text{mmol}^{-1}\cdot\text{hr}^{-1}$ at 250 psig of ethylene. These values are comparable to the industrial standard Cp_2ZrCl_2 metallocene and other LTM catalysts such as Brookhart's.²⁹ In addition, these catalysts are also very tolerant of functional groups, and maintain high activity in the presence of ketones, esters, and ethers. Addition of water or other protic solvents gradually decomposes the catalyst, while addition of monomers such as norbornadienes, carbon monoxide, and other functional olefins results in the incorporation of these compounds into the growing polymer chain.

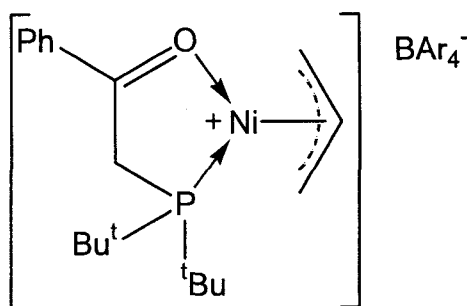
Brookhart *et al.*⁴¹ then developed a very similar catalyst with the aim of synthesizing a catalyst similar to that of Grubbs, employing similar steric bulk restraints, but with a reduced number of atoms in the chelating ring; five instead of six. This was accomplished by the synthesis of a 2-(2,6-diisopropylanilino)tropone nickel(II) complex (13, $\text{Ar} = 2,6\text{-}i\text{-Pr}_2\text{C}_6\text{H}_3$).



13

Comparison of **12** and **13** shows that the five-membered chelate ring complex **13** is a superior ethylene polymerisation catalyst. In the absence of activator, complex **13** has an activity of $8800 \text{ g}\cdot\text{mmol}^{-1}\cdot\text{hr}^{-1}$, with a substantially higher molecular weight polymer than obtained for **12**. It was also determined that altering the temperature and pressure gives the resultant polymer very different characteristics. Increasing the pressure caused a decrease in the amount of branching, while increasing the temperature resulted in an increase in polymer branching. The addition of polar functional groups (ethyl acetate or THF) in fact *increases* the activity of **13**, whereas addition of water decreases the activity by 3.5-4.5 times.

Both of the above examples in this section feature an anionic ligand bound to a nickel(II) centre; a “neutral” nickel(II) catalyst. Brookhart has recently developed a very active P—O chelating cationic nickel(II) complex (**14**, Ar = 3,5- $\text{C}_6\text{H}_3(\text{CF}_3)_2$), which is very active in the absence of cocatalyst.⁴²

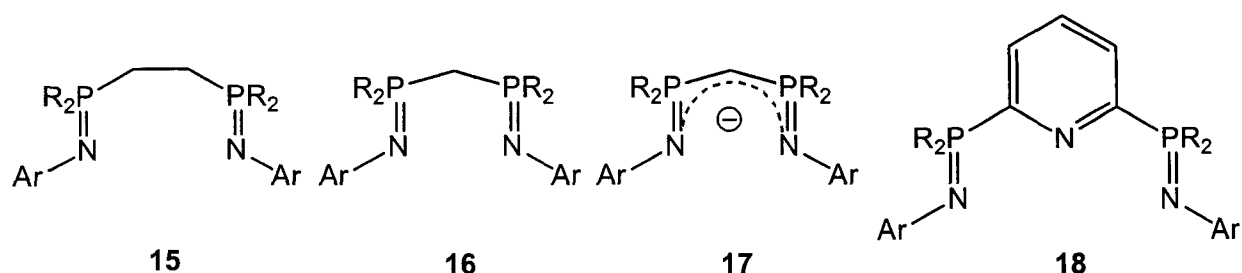


14

The highest recorded activity under optimal conditions (27.2 atm ethylene, toluene, 26°C) was $698 \text{ g}\cdot\text{mmol}^{-1}\cdot\text{hr}^{-1}\cdot\text{atm}^{-1}$. The polymer obtained was highly linear with 6-8 methyl chains per 1000 carbon atoms. This catalyst remains active even in the presence of ethyl acetate. The palladium analog generates low molecular weight PE oligomers with an average molecular weight around 350.

1.4 Reported Chemistry of Phosphinimine LTM and Main Group metal complexes in olefin polymerisation

There are numerous examples of phosphinimine, or iminophosphorane complexes exhibiting different coordination geometries to metal centres;⁴³⁻⁴⁵ however, few have been examined for the potential to polymerise olefins. Bochmann *et al.* has reported the synthesis of Group IX and X first row transition metal complexes with: (1) bis(aryliminophosphoranyl)ethane **15** and methane **16** ligands; (2) bis(aryliminophosphoranyl)methanide ligands **17**; and (3) bis(aryliminophosphoranyl)-pyridyl ligands **18** (Figure 1.2).⁴⁶

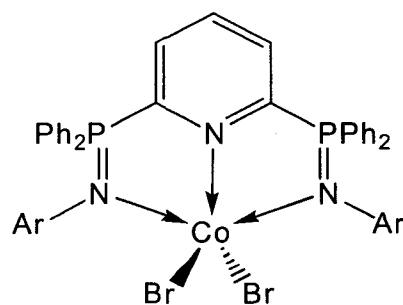


R = Ph, Cy

Ar = 2,6-ⁱPr₂C₆H₃, 2,4,6-Me₃C₆H₂

Figure 1.2 Various phosphininimine-based ligands examined for LTM olefin polymerisation.

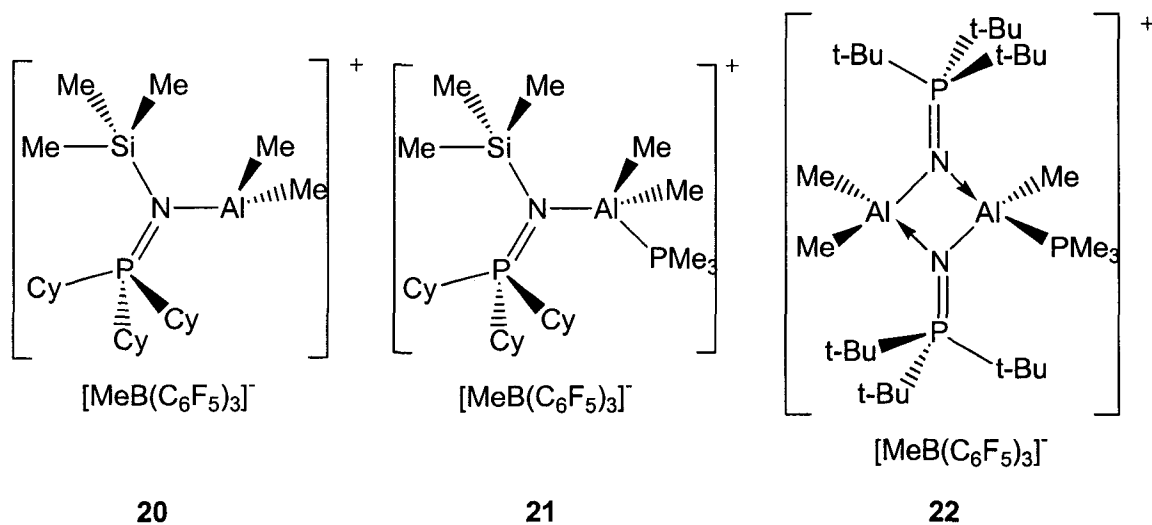
The bis(iminophosphoranyl)pyridyl ligands **15-18** mirror the bis(imino)pyridyl ligands developed by Brookhart and Gibson, except that the C=N groups are replaced by P=N groups. Activation of the cobalt bis(iminophosphoranyl)pyridyl compounds with MAO in toluene at 50°C at 10 bar ethylene results in activities of 5-30 g·mmol⁻¹·hr⁻¹·bar⁻¹ for complex **19**. The corresponding iron and vanadium complexes with the same ligand and the same conditions show activities of 6 and 140 g PE/mmol cat·hr·bar, respectively. The polymer obtained from the vanadium catalyst has a molecular weight of 382,000 and a polydispersity of 2.3. It is interesting to note that at low ethylene pressures, no consumption was noted.



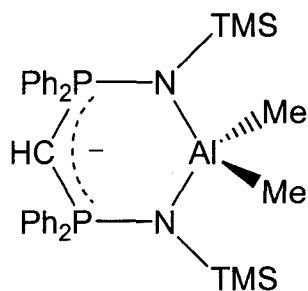
19

These results are very surprising in light of the results obtained by Brookhart and Gibson involving bis(imino)pyridyl complexes.^{37,38} Bochmann *et al.* explained that the very low activities could be attributed to the insolubility of the metal complexes in the solvent used; however, no discussion of other solvents or electronic ligand differences were given. Polymerisations of any other metal-ligand complexes yielded negligible polymer.

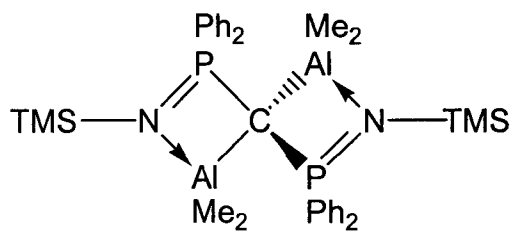
Main group aluminum complexes have been reported by Stephan *et al.* which contain monodentate phosphinimine and bidentate bisphosphinimine ligands.⁴⁷ Unfortunately, cationic complexes **20**, **21** and **22** failed to polymerise ethylene at 1 atm and 25°C.



However, Cavell's research group has reported aluminum complexes **23** and **24** using bidentate ligands formed by the reaction of two equivalents of TMA with a bidentate bisphosphinimine ligand.^{48,49} When activated at 164°C with $[\text{Ph}_3\text{C}][\text{B}(\text{C}_6\text{F}_5)_4]$ under 200 psig of ethylene, the reported activity of **24** is $520 \text{ g}\cdot\text{mmol}^{-1}\cdot\text{hr}^{-1}\cdot\text{atm}^{-1}$.

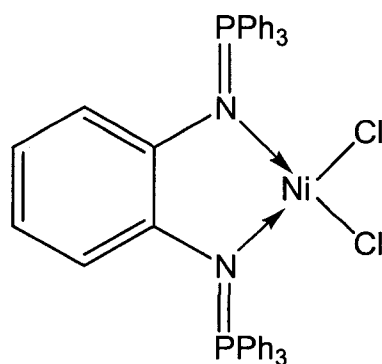


23



24

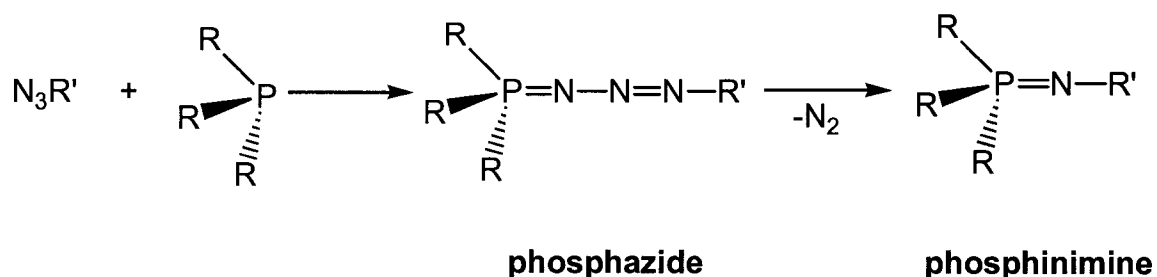
Souza and Reau *et al.* have recently reported the synthesis of nickel(II) 1,2-di(iminophosphorane) complexes and their use in ethylene oligomerisation.⁵⁰ Activation of these nickel(II) complexes with diethylaluminum chloride (DEAC) resulted in C₄ and C₆ oligomer formation. Variables such as activator, pressure, temperature, and the ratio of nickel(II) catalyst to aluminum cocatalyst were varied to determine the optimal oligomerisation conditions. Activation of the nickel(II) dichloride complexes with TMA did not oligomerise ethylene, while the use of MAO as an activator gave rise to systems with reduced activities compared to DEAC activation. A maximum activity of 344 g·mmol⁻¹·hr⁻¹·atm⁻¹ was obtained with **25** under optimal conditions (50°C, 11 atm ethylene, Al:N ration of 200:1).



25

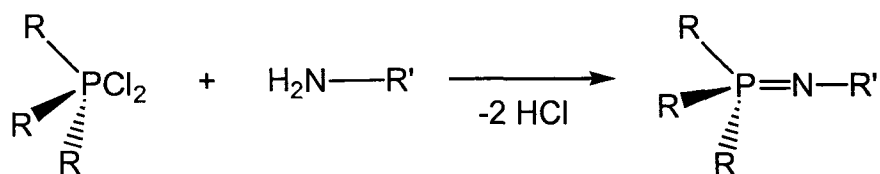
1.5 General Synthesis of Phosphinimine Ligands

The imination of trivalent phosphorus complexes with organic azides was discovered by Staudinger in 1919.⁵¹ This reaction employs a two-step process beginning with electrophilic attack on a trivalent phosphorus atom by an organic azide. An intermediate phosphazide molecule is formed, which can then eliminate dinitrogen to form a phosphinimine functional group (Scheme 1.4). The existence of the phosphazide intermediate has been well-documented with many examples reported.⁵² The stability of such complexes is determined by both electronic (delocalization of cationic charge on the phosphorus atom) and steric factors (shielding of the phosphorus atom by bulky substituents).



Scheme 1.4 The Staudinger reaction between a trivalent phosphorus atom and an organic azide proceeding through a phosphazide intermediate.

In 1950 Kirsanov discovered a new oxidative imination reaction resulting in renewed interest in phosphinimine molecules⁵³ involving the imination of phosphorus pentachloride and its derivatives with amine compounds (Scheme 1.5). Kirsanov's research compliments that of Staudinger and allows the synthesis of most phosphinimine, or iminophosphorane, compounds.



Scheme 1.5 The Kirsanov reaction between a pentavalent phosphorus atom and a primary amine.

1.6 Scope of this Work

This thesis describes the synthesis of pyridyl- and imidazolyl-phosphines, their oxidation to the corresponding phosphinimines, and their reactions with selected group VI, VIII, IX and X transition metals. The purpose of this strategy is to create novel ligands which incorporate phosphinimines with the previously successful imine functionalities. Metal compounds with these ligands are anticipated to polymerise or oligomerise ethylene with activities similar or superior to previously reported catalysts.²⁹⁻⁴²

Chapter Two

Synthesis of Selected Group VIII and X Pyridyl Phosphinimine Complexes

2.1 Introduction

Nitrogen-based ligands have been at the forefront of developments in LTM olefin polymerisation. In particular, Brookhart has shown that α -diimine nickel catalysts exhibit a high activity for ethylene oligomerisation and polymerisation.²⁹ The analogous phosphinimines are a readily accessible class of nitrogenous ligands, which have only recently been examined for their catalytic potential.⁴⁶⁻⁵⁰ This class of ligand can offer a steric environment similar to diimine ligands, but with marked differences in donor strength and π -acceptor capacity.

In this chapter, we examine the synthesis of both sterically bulky pyridyl phosphinimine ligands and their group VIII and X metal complexes. The potential for activated metal precursors to polymerize and oligomerize ethylene was also evaluated. In order to better understand the ligand effect on the activated metal centre, computational methods were used to examine the lone pair orbital energies of several types of imine and phosphinimine ligands. The atomic charge on nickel in the $[\text{NiCH}_3(\text{ligand})]^+$ activated species was also investigated.

2.2 Experimental Section

General Data All preparations were performed under a dry, O_2 -free nitrogen atmosphere employing either Schlenk line techniques, a Mbraun inert atmosphere glovebox, or a

Vacuum Atmospheres Co. glovebox unless otherwise stated. Unless otherwise mentioned all organic chemicals were reagent grade and used as received from Aldrich Chemical Co., and all phosphines and metal compounds were used as received from Strem Chemical Co. Diethyl ether, ethanol, hexane, petroleum ether (bp 35-60°C), methylene chloride, and toluene were either dried according to literature techniques⁵⁴ or obtained directly from an Innovative Technologies solvent purification system. 2-Pyridyldiphenylphosphine **26**⁵⁵ and bis(pentafluorophenyl)chlorophosphine **27**⁵⁶ were prepared according to literature techniques. ¹H, ¹³C{¹H}, and ³¹P{¹H} NMR spectra were recorded on Bruker Avance 300 operating at 300, 75, and 121 MHz, respectively. Several ¹H, ¹³C{¹H}, and ³¹P{¹H} NMR spectra were recorded on a Bruker Avance 500 MHz spectrometer operating at 300, 121, and 202 MHz, respectively. Trace amounts of protonated solvents were used as references and chemical shifts reported relative to SiMe₄. ³¹P{¹H} spectra were externally referenced to 85% H₃PO₄. The ¹³C{¹H} resonances reported are all singlets unless otherwise noted. Elemental analyses were carried out by Guelph Chemical Labs Inc., Guelph, Ontario, Canada or the Centre for Catalysis and Materials Research (CCMR), Windsor, Ontario, Canada. GC analysis was performed with a Shimadzu GC-9A apparatus with a Quadrex Corporation fused silica glass capillary column (methyl silicone, 25 metres long, i.d. 0.25 mm and film thickness of 1.00 μm) working at 35°C for 15 min. then heating at 25°C min⁻¹ up to 275°C. IR spectroscopy was performed on a Bruker Infrared Fourier Transform Spectrometer VECTOR 22. Unpaired electron measurements were made with a Johnson Matthey magnetic susceptibility balance (Evans design).

Synthesis of 2,6-diisopropylphenyl azide N_3 -2,6- 1Pr_2C_6H_3 28, N_3 -2,6- $Me_2C_6H_3$ 29

Compounds **28** and **29** were prepared by similar methods, thus only one representative procedure is described. A mixture of 2,6-diisopropylaniline (10.0 g, 56.4 mmol) and $NaNO_2$ (4.3 g, 62.3 mmol) were added to a cooled ($-30^\circ C$) acidic (40 mL conc. HCl and 40 mL distilled H_2O) solution of $NaBF_4$ (12.4 g, 112.9 mmol). After several minutes of stirring, a yellow precipitate gradually formed, which was stirred at $-30^\circ C$ for 30 minutes. The tetrafluoroborate salt was filtered quickly in air, and washed with cold H_2O . The yellow sticky powder was added to a cooled ($0^\circ C$) aqueous solution (100 mL) of NaN_3 (11.0 g, 169.2 mmol). After vigorous gas evolution, the orange mixture was stirred overnight at room temperature. The product was extracted from the aqueous layer with diethyl ether (3 x 30 mL), and dried with $MgSO_4$. The solution was filtered, and the solvent removed to give a light red oil (9.5 g, 83%). The oil was not purified due to the risk of explosion. **28**: 1H NMR ($CDCl_3$, $25^\circ C$, δ): 1.28 (d, 12H, $-CH(CH_3)_2$), 3.38 (sept, 2H, $-CH(CH_3)_2$), 7.07-7.21 (m, 3H, $-C_6H_3$). **29**: 1H NMR ($CDCl_3$, $25^\circ C$, δ): 2.21 (s, 6H, $-CH_3$), 6.67 (t, 1H, $-paraC_6H_3$), 6.96 (d, 2H, $-metaC_6H_3$).

Synthesis of 2-bromo-6-benzylpyridine [2-Br-6-Bn]py 30 Compound **30** was prepared according to a literature method;⁵⁷ however, NMR data was not reported. **30**: 1H NMR ($CDCl_3$, $25^\circ C$, δ): 4.15 (s, 2H, $-CH_2$), 7.01 (d, 1H, $-pyH_5$), 7.23-7.27 (m, 2H, $-pyH_3, H_4$), 7.31-7.34 (m, 4H, $-ArH$), 7.42 (m, 1H, $-ArH$).

Synthesis of 2-bromo-6-trimethylsilylpyridine [2-Br-6-TMS]py 31 Compound **31** was prepared according to a literature method,⁵⁸ however, NMR data was not given. **31**: ¹H NMR (C₆D₆, 25°C, δ): 0.20 (s, 9H, -Si(CH₃)₃), 6.60 (m, 1H, -pyH₅), 6.91-6.96 (m, 2H, -pyH₃, H₄).

Synthesis of 2-amino-6-phenylpyridine [2-NH₂-6-Ph]py 32 Compound **32** was prepared according to a literature method,⁵⁹ however, NMR data was not reported. **32**: ¹H NMR (CDCl₃, 25°C, δ): 4.50 (br s, 2H, -NH₂), 6.46 (d, 1H, -pyH₃), 7.10 (m, 1H, -pyH₄), 7.37 (d, 1H, -pyH₅), 7.44 (m, 2H, -PhH), 7.51 (t, 1H, -PhH), 7.95 (m, 2H, -PhH).

Synthesis of 2-bromo-6-phenylpyridine [2-Br-6-Ph]py 33 Compound **33** was prepared according to a literature method;⁵⁹ however, NMR data was not reported. **33**: ¹H NMR (CDCl₃, 25°C, δ): 7.42-7.51 (m, 4H, -PhH, -pyH₄, H₅), 7.62 (t, 1H, -PhH), 7.69 (m, 1H, -pyH₃), 8.00 (m, 2H, -PhH).

Synthesis of 2-(diphenylphosphino)pyridine (2-py)PPh₂ 26, [6-Me-2-PPh₂]py 34, [6-Bn-2-PPh₂]py 35, [6-TMS-2-PPh₂]py 36, and [6-Ph-2-PPh₂]py 37 Compounds **26**, and **34** to **37** were prepared using similar routes using a modified procedure, thus only one representative procedure is described. To a stirred THF solution (100 mL) of diphenylphosphine (2.66 g, 14.3 mmol) was added an equimolar amount (5.7 mL) of a 2.5 M hexane solution of n-butyllithium and the deep red solution stirred overnight at room temperature. To this solution was added dropwise a 20 mL THF solution of 2-bromopyridine (2.26 g, 14.3 mmol). After stirring overnight, the solvent was removed *in*

vacuo and ethanol (30 mL) was added to quench the reaction. The solvent was again removed *in vacuo* and ether was added (30 mL), and the solution was then filtered. Removal of the ether *in vacuo* yielded a colourless oily solid, which was recrystallized with CH₂Cl₂ and hexane. **26**: 80% yield based on Ph₂PH. ³¹P{¹H} NMR (C₆D₆, 25°C, δ): -3.2 (s). ¹H NMR (CDCl₃, 25°C, δ): 6.49 (m, 1H, -pyH₅), 6.87 (m, 1H, -pyH₄), 7.04-7.09 (m, 7H, -metaPPh₂, -paraPPh₂, -pyH₃), 7.50-7.53 (m, 4H, -orthoPPh₂), 8.49 (d, 1H, -pyH₆).

34: Yield = 70%, colourless crystals. ³¹P{¹H} NMR (*d*₈-THF, 25°C, δ): -4.0 (s). ¹H NMR (*d*₈-THF, 25°C, δ): 2.48 (s, 3H, -CH₃), 6.82 (d, 1H, 9.0 Hz, -pyH₅), 7.11 (m, 1H, -pyH₄), 7.34 (m, 10 H, -PPh₂), 7.28 (m, 1H, -pyH₃). ¹³C{¹H} NMR (*d*₈-THF, 25°C, δ): 24.4, 120.4, 124.7 (d, J_{C-P} 2.9 Hz), 128.3, 128.7 (d, J_{C-P} 19.4 Hz), 132.4 (d, J_{C-P} 2.7 Hz), 130.2 (d, J_{C-P} 10.4 Hz), 136.0, 158.5 (d, J_{C-P} 9.8 Hz), 162.9 (d, J_{C-P} 4.2 Hz).

35: Yield = 65%, white solid. ³¹P{¹H} NMR (C₆D₆, 25°C, δ): -3.2 (s). ¹H NMR (C₆D₆, 25°C, δ): 4.05 (s, 2H, -CH₂), 6.67 (d, 1H, -pyH₅), 6.94 (t, 1H, 8.9 Hz, -pyH₄), 6.99 (d, 1H, 9.0 Hz, -pyH₃), 7.17-7.23 (m, 11H, -metaPPh₂, -paraPPh₂, -ArH), 7.59-7.63 (m, 4H, -orthoPPh₂). ¹³C{¹H} NMR (C₆D₆, 25°C, δ) 44.1, 117.6, 123.9, 125.9 (d, J_{C-P} 3.5 Hz), 126.1, 127.4, 130.6, 131.3 (d, J_{C-P} 19.0 Hz), 134.1, 135.5, 136.5 (d, J_{C-P} 10.0 Hz), 139.5, 158.3 (d, J_{C-P} 9.8 Hz), 161.1 (d, J_{C-P} 4.5 Hz).

36: Yield = 75%, golden oil. The oil was purified by flash column chromatography on silica using hexanes. ³¹P{¹H} NMR (C₆D₆, 25°C, δ): -3.3(s). ¹H NMR (C₆D₆, 25°C, δ): 0.24 (s, 9H, -Si(CH₃)₃), 6.95 (m, 2H, -pyH_{4,5}), 7.06-7.11 (m, 7H, -metaPPh₂, -paraPPh₂, -pyH₃), 7.55 (m, 4H, -orthoPPh₂). ¹³C{¹H} NMR (CDCl₃, 25°C, δ): -1.9, 126.7, 127.0,

128.3 (d, J_{C-P} 3.3 Hz), 128.7, 133.2 (d, J_{C-P} 19.1 Hz), 134.2 (d, J_{C-P} 19.1 Hz), 137.1 (d, J_{C-P} 10.5 Hz), 163.2 (d, J_{C-P} 4.1 Hz), 168.9 (d, J_{C-P} 9.8 Hz).

37: Yield = 65%, cream-colored solid. $^{31}\text{P}\{^1\text{H}\}$ NMR (CDCl_3 , 25°C, δ): -3.0 (s). ^1H NMR (CDCl_3 , 25°C, δ): 7.07 (m, 1H, -py H_5), 7.36-7.39 (m, 6H, -metaPPh $_2$, -ArH), 7.39-7.41 (m, 2H, -paraPPh $_2$), 7.42 (m, 1H, -py H_4), 7.45-7.50 (m, 4H -orthoPPh $_2$), 7.63 (m, 1H, -py H_3), 7.65 (m, 1H, -ArH), 8.00 (m, 2H, -ArH). $^{13}\text{C}\{^1\text{H}\}$ NMR (CDCl_3 , 25°C, δ): 118.7, 126.4, 126.9, 128.4 (d, J_{C-P} 3.5 Hz), 128.6, 128.9, 129.0, 134.3 (d, J_{C-P} 19.3 Hz), 136.2 (d, J_{C-P} 2.7 Hz), 136.6 (d, J_{C-P} 10.7 Hz), 139.0, 157.1 (d, J_{C-P} 12.2), 163.4 (d, J_{C-P} 4.5 Hz).

Synthesis of [2-PPh $_2$ N-2,6-Me $_2$ C $_6$ H $_3$]py 38, [2-PPh $_2$ N-2,6- i PrC $_6$ H $_3$]py 39, [2-PPh $_2$ N-TMS]py 40, [6-Me-2-PPh $_2$ N-2,6-Me $_2$ C $_6$ H $_3$]py 41, [6-Me-2-PPh $_2$ N-2,6- i PrC $_6$ H $_3$]py 42, [6-TMS-2-PPh $_2$ N-2,6-Me $_2$ C $_6$ H $_3$]py 43, [6-TMS-2-PPh $_2$ N-2,6- i PrC $_6$ H $_3$]py 44, [6-Bn-2-PPh $_2$ N-2,6-Me $_2$ C $_6$ H $_3$]py 45, [6-Bn-2-PPh $_2$ N-2,6- i PrC $_6$ H $_3$]py 46, [6-Ph-2-PPh $_2$ N-2,6-Me $_2$ C $_6$ H $_3$]py 47, [6-Ph-2-PPh $_2$ N-2,6- i PrC $_6$ H $_3$]py 48 Compounds **38** to **48** were prepared by similar methods, thus only one representative procedure is described. To a toluene solution (50 mL) of diphenyl-2-pyridylphosphine (1.0 g, 3.8 mmol) was added a THF solution of **29** (1.12 g, 7.6 mmol). The solution was stirred at room temperature for several hours, and the solvent was removed to give a brown oil. Petroleum ether was added to the mixture, which was stirred for several hours and then stored at -30°C overnight. Filtration gave a cream-colored solid, which was washed several times with hexane. **38**: Yield = 95%, cream-colored solid, $\nu_{P=N}$ 1329 cm^{-1} . $^{31}\text{P}\{^1\text{H}\}$ NMR (C_6D_6 , 25°C, δ): -17.0 (s). ^1H NMR (C_6D_6 , 25°C, δ): 2.42 (s, 6H, -(CH $_3$) $_2$), 6.57-6.60 (m, 1H, -

pyH₅), 7.00 (t, 1H, -NArH), 7.09-7.12 (m, 7H, -metaPPh₂, -NArH, -pyH₄), 7.28 (m, 2H, -paraPPh₂), 8.05-8.10 (m, 4H, -orthoPPh₂), 8.40 (m, 1H, -pyH₃), 8.45 (m, 1H, -pyH₆).
¹³C{¹H} NMR (CDCl₃, 25°C, δ) 22.0, 119.1, 124.3 (d, J_{C-P} 2.8 Hz), 127.9, 128.5, 128.7 (d, J_{C-P} 19.1 Hz), 131.0 (d, J_{C-P} 2.4 Hz), 132.2 (d, J_{C-P} 7.5 Hz), 132.8 (d, J_{C-P} 9.1 Hz), 134.8 (d, J_{C-P} 98.9 Hz), 135.7 (d, J_{C-P} 8.9 Hz), 147.9, 149.5 (d, J_{C-P} 20.0 Hz), 158.6 (d, J_{C-P} 136.9 Hz).

39: Yield = 95%, cream-colored solid, ν_{P=N} 1333 cm⁻¹. ³¹P{¹H} NMR (C₆D₆, 25°C, δ): -6.9 (s). ¹H NMR (C₆D₆, 25°C, δ): 1.14 (d, 12H, -CH(CH₃)₂), 3.66 (sept, 2H, -CH(CH₃)₂), 6.47-6.52 (m, 1H, -pyH₅), 6.97-7.04 (m, 7H, -metaPPh₂, -NArH), 7.10 (m, 1H, -pyH₄), 7.25-7.28 (m, 2H, -paraPPh₂), 7.89-7.99 (m, 4H, -orthoPPh₂), 8.28-8.34 (m, 2H, -pyH₃).
¹³C{¹H} NMR (CDCl₃, 25°C, δ): 24.4, 29.7, 120.4, 123.7, 124.7 (d, J_{C-P} 2.9 Hz), 128.7, 129.2 (d, J_{C-P} 19.1 Hz), 131.4 (d, J_{C-P} 2.4 Hz), 133.2 (d, J_{C-P} 9.1 Hz), 134.8 (d, J_{C-P} 99.4 Hz), 136.0 (d, J_{C-P} 6.9 Hz), 142.8 (d, J_{C-P} 6.9 Hz), 144.9, 150.1 (d, J_{C-P} 20.0 Hz), 158.5 (d, J_{C-P} 139.0 Hz).

40: Yield = 99% cream-colored solid, ν_{P=N} 1350 cm⁻¹. ³¹P{¹H} NMR (C₆D₆, 25°C, δ): -4.9 (s). ¹H NMR (CDCl₃, 25°C, δ): 0.39 (s, 9H, -SiMe₃), 6.50 (m, 1H, -NArH), 7.00-7.15 (m, 8H, -metaPPh₂, -paraPPh₂, -NArH, -pyH₅), 7.94-7.99 (m, 4H, -orthoPPh₂), 8.33 (m, 1H, -pyH₄), 8.42 (m, 1H, -pyH₃). ¹³C{¹H} NMR (CDCl₃, 25°C, δ): 4.8 (d, J_{C-P} 2.7 Hz), 124.5 (d, J_{C-P} 2.5 Hz), 128.5, 131.3 (d, J_{C-P} 2.1 Hz), 133.0 (d, J_{C-P} 9.9 Hz), 135.9 (d, J_{C-P} 9.3 Hz), 136.1 (d, J_{C-P} 99.7 Hz), 149.9 (d, J_{C-P} 19.4 Hz), 159.0 (d, J_{C-P} 135 Hz).

41: Yield = 85%, cream-colored solid, ν_{P=N} 1342 cm⁻¹. ³¹P{¹H} NMR (CDCl₃, 25°C, δ): -16.5 (s). ¹H NMR (CDCl₃, 25°C, δ): 2.40 (s, 6H, -(CH₃)₂), 2.61 (s, 3H, -CH₃), 6.62-6.65 (m, 1H, -NArH), 7.00 (m, 2H, -NArH), 7.09-7.12 (m, 7H, -metaPPh₂, -paraPPh₂, -pyH₅),

7.28 (m, 2H, -pyH_{3,4}), 8.05-8.10 (m, 4H, -orthoPPh₂). ¹³C{¹H} NMR (CDCl₃, 25°C, δ): 22.0, 25.0, 119.0, 124.1 (d, J_{C-P} 2.7 Hz), 127.9, 128.1 (d, J_{C-P} 19.0 Hz), 131.3 (d, J_{C-P} 2.5 Hz), 132.0, 132.2, 132.8 (d, J_{C-P} 9.1 Hz), 134.3 (d, J_{C-P} 98.5 Hz), 135.0 (d, J_{C-P} 8.5 Hz), 147.1, 149.2 (d, J_{C-P} 20.5 Hz), 158.4 (d, J_{C-P} 135.4 Hz).

42: Yield = 80%, cream-colored solid, $\nu_{\text{P=N}}$ 1340 cm⁻¹. ³¹P{¹H} NMR (CDCl₃, 25°C, δ): -13.6 (s). ¹H NMR (CDCl₃, 25°C, δ): 1.28 (d, 6.9 Hz, 12H, -CH(CH₃)₂), 2.55 (s, 3H, -CH₃), 3.40 (sept, 8.7 Hz, 2H, -CH(CH₃)₂), 6.79 (m, 1H, -NArH), 6.95 (d, 7.4 Hz, 2H, -NArH), 7.14 (m, 1H, -pyH₅), 7.19 (m, 1H, -pyH₄), 7.39 (m, 4H, -metaPPh₂), 7.46 (m, 2H, -paraPPh₂), 7.63 (m, 1H, -pyH₃), 7.70 (m, 4H, -orthoPPh₂). ¹³C{¹H} NMR (CDCl₃, 25°C, δ): 24.0, 26.0, 30.2, 120.3, 123.5, 124.5 (d, J_{C-P} 2.8 Hz), 128.5, 129.9 (d, J_{C-P} 18.9 Hz), 131.5 (d, J_{C-P} 2.5 Hz), 133.0, 133.6, 134.4 (d, J_{C-P} 99.0 Hz), 135.0 (d, J_{C-P} 7.1 Hz), 144.1, 150.5 (d, J_{C-P} 20.0 Hz), 159.2 (d, J_{C-P} 138.5 Hz).

43: Yield = 90%, cream-colored solid, $\nu_{\text{P=N}}$ 1339 cm⁻¹. ³¹P{¹H} NMR (C₆D₆, 25°C, δ): -16.6 (s). ¹H NMR (C₆D₆, 25°C, δ): 0.23 (s, 9H, -Si(CH₃)₃), 2.46 (s, 6H, -CH₃), 7.03-7.14 (m, 9H, -metaPPh₂, -paraPPh₂, -NArH), 7.33 (m, 1H, -pyH₅), 8.04-8.13 (m, 5H, -orthoPPh₂ and -pyH₄), 8.40 (m, 1H, -pyH₃). ¹³C{¹H} NMR (CDCl₃, 25°C, δ): -2.0, 20.6, 118.5, 127.3 (d, J_{C-P} 20.3 Hz), 127.8, 127.9 (d, J_{C-P} 12.3 Hz), 129.0 (d, J_{C-P} 2.7 Hz), 131.0 (d, J_{C-P} 1.6 Hz), 132.0 (d, J_{C-P} 16.7 Hz), 132.6 (d, J_{C-P} 8.9 Hz), 133.9 (d, J_{C-P} 8.5 Hz), 134.0 (d, J_{C-P} 100.1 Hz), 147.4, 157.5 (d, J_{C-P} 131.9 Hz), 168.7 (d, J_{C-P} 17.0 Hz).

44: Yield = 92%, cream-colored solid, $\nu_{\text{P=N}}$ 1332 cm⁻¹. ³¹P{¹H} NMR (CDCl₃, 25°C, δ): -12.6 (s). ¹H NMR (CDCl₃, 25°C, δ): 0.19 (s, 9H, -Si(CH₃)₃), 0.91 (d, 8.7 Hz, 12H, -CH(CH₃)₂), 3.35 (sept, 8.7 Hz, 2H, -CH(CH₃)₂), 6.85 (m, 1H, -NArH), 6.97 (m, 2H, -NArH), 7.27-7.54 (m, 7H, -metaPPh₂, -paraPPh₂, -pyH₅), 7.69 (m, 1H, -pyH₄), 7.72-7.79

(m, 4H, *-orthoPPh₂*), 7.95 (m, 1H, *-pyH₃*). $^{13}\text{C}\{^1\text{H}\}$ NMR (CDCl_3 , 25°C, δ): -2.0, 23.6, 28.6, 118.9, 122.6, 127.3 (d, $J_{\text{C-P}}$ 20.3 Hz), 127.8 (d, $J_{\text{C-P}}$ 11.9 Hz), 128.8 (d, $J_{\text{C-P}}$ 2.9 Hz), 130.8 (d, $J_{\text{C-P}}$ 2.0 Hz), 132.6 (d, $J_{\text{C-P}}$ 9.0 Hz), 133.7 (d, $J_{\text{C-P}}$ 8.6 Hz), 133.9 (d, $J_{\text{C-P}}$ 100.8 Hz), 142.5 (d, $J_{\text{C-P}}$ 7.0 Hz), 144.2, 157.0 (d, $J_{\text{C-P}}$ 131.5 Hz), 168.7 (d, $J_{\text{C-P}}$ 17.0 Hz).

45: Yield = 88%, cream-colored solid, $\nu_{\text{P=N}}$ 1355 cm^{-1} . $^{31}\text{P}\{^1\text{H}\}$ NMR (d_8 -THF, 25°C, δ): -17.2 (s). ^1H NMR (d_8 -THF 25°C, δ): 1.97 (s, 6H, $-(\text{CH}_3)_2$), 4.08 (s, 2H, $-\text{CH}_2$), 6.46 (t, 1H, $-\text{NArH}$), 6.77 (d, 2H, $-\text{NArH}$), 7.13-7.20 (m, 5H, $-\text{CH}_2\text{Ph}$), 7.27-7.44 (m, 5H, *-orthoPPh₂*, *-pyH₃*), 7.73 (m, 1H, *-pyH₄*), 7.76-7.80 (m, 4H, *-PPh₂*), 8.04 (t, 1H, 9.0 Hz, *-pyH₃*). $^{13}\text{C}\{^1\text{H}\}$ NMR (d_8 -THF 25°C, δ) 21.1, 44.1, 117.6, 123.9, 125.9 (d, $J_{\text{C-P}}$ 19.3 Hz), 126.1, 127.4, 127.8 (d, $J_{\text{C-P}}$ 11.9 Hz), 128.1, 129.0, 130.6, 131.3 (d, $J_{\text{C-P}}$ 7.2 Hz), 132.3 (d, $J_{\text{C-P}}$ 9.1 Hz), 135.5 (d, $J_{\text{C-P}}$ 99.4 Hz), 136.5 (d, $J_{\text{C-P}}$ 9.2 Hz), 139.5, 147.4, 157.4 (d, $J_{\text{C-P}}$ 135.4 Hz), 161.1 (d, $J_{\text{C-P}}$ 19.5 Hz).

46: Yield = 85%, cream-colored solid, $\nu_{\text{P=N}}$ 1330 cm^{-1} . $^{31}\text{P}\{^1\text{H}\}$ NMR (d_8 -THF, 25°C, δ): -16.5 (s). ^1H NMR (d_8 -THF 25°C, δ): 0.86 (d, 6.9 Hz, 12H, $-\text{CH}(\text{CH}_3)_2$), 3.32 (sept, 6.9 Hz, 2H, $-\text{CH}(\text{CH}_3)_2$), 4.08 (s, 2H, $-\text{CH}_2$), 6.64 (m, 1H, $-\text{NArH}$), 6.84 (m, 2H, $-\text{NArH}$), 7.12-7.18 (m, 5H, $-\text{CH}_2\text{Ph}$), 7.28-7.46 (m, 8H, *-metaPPh₂*, *-paraPPh₂*, *-pyH₃*), 7.69-7.78 (m, 5H, *-orthoPPh₂*, *-pyH₄*), 7.97 (m, 1H, *-pyH₃*). $^{13}\text{C}\{^1\text{H}\}$ NMR (CDCl_3 , 25°C, δ): 23.1, 29.6, 45.2, 119.7, 123.2, 125.0, 127.0 (d, $J_{\text{C-P}}$ 9.6 Hz), 127.2 (d, $J_{\text{C-P}}$ 9.6 Hz), 128.9 (d, $J_{\text{C-P}}$ 11.9 Hz), 129.3, 130.1, 131.7, 133.5 (d, $J_{\text{C-P}}$ 9.0 Hz), 135.5 (d, $J_{\text{C-P}}$ 99.8 Hz), 137.5 (d, $J_{\text{C-P}}$ 9.2 Hz), 140.6, 142.8 (d, $J_{\text{C-P}}$ 7.0 Hz), 145.3, 157.5 (d, $J_{\text{C-P}}$ 136.1 Hz), 162.4 (d, $J_{\text{C-P}}$ 18.9 Hz).

47: Yield = 92%, white solid, $\nu_{\text{P=N}}$ 1342 cm^{-1} . $^{31}\text{P}\{^1\text{H}\}$ NMR (CDCl_3 , 25°C, δ): -11.9 (s). ^1H NMR (CDCl_3 , 25°C, δ): 2.07 (s, 6H, $-\text{Me}_2$), 6.66 (m, 1H, $-\text{NArH}$), 6.93 (m, 2H, -

NArH), 7.38-7.44 (m, 7H, *-metaPPh₂*, -ArH, -pyH₅), 7.50 (m, 2H, *-paraPPh₂*), 7.80-7.88 (m, 8H, *-orthoPPh₂*, -ArH, -pyH₄), 8.05 (m, 1H, -pyH₅). ¹³C{¹H} NMR (CDCl₃, 25°C, δ): 21.4, 118.5, 121.0, 126.6, 126.8, 127.7, 128.0 (d, J_{C-P} 11.9 Hz), 128.7, 129.3, 131.0, 131.1, 132.6 (d, J_{C-P} 9.2 Hz), 133.5 (d, J_{C-P} 100.1 Hz), 136.7 (d, J_{C-P} 7.6 Hz), 138.4, 147.2, 156.6 (d, J_{C-P} 19.1 Hz), 157.0 (d, J_{C-P} 131.8 Hz).

48: Yield = 95%, white solid, $\nu_{\text{P=N}}$ 1357 cm⁻¹. ³¹P{¹H} NMR (CDCl₃, 25°C, δ): -11.9 (s). ¹H NMR (CDCl₃, 25°C, δ): 0.90 (d, 6.8 Hz, 2H, -CH(CH₃)₂), 3.97 (sept, 6.8 Hz, 2H, -CH(CH₃)₂), 6.84 (dt, 7.7 Hz, 1.6 Hz, 1H, -NArH), 6.99 (dd, 7.5 Hz, 0.9 Hz, 2H, -NArH), 7.37-7.43 (m, 7H, *-metaPPh₂*, -ArH, -pyH₅), 7.49 (m, 2H, *-paraPPh₂*), 7.75-7.80 (m, 4H, *-orthoPPh₂*), 7.81-7.85 (m, 4H, -ArH, -pyH₄), 7.91 (m, 1H, -pyH₃). ¹³C{¹H} NMR (CDCl₃, 25°C, δ): 22.8, 28.6, 119.1, 120.9, 122.7, 125.9, 126.6, 128.0 (d, J_{C-P} 11.4 Hz), 128.7, 129.4, 131.1, 132.6 (d, J_{C-P} 7.4 Hz), 133.9 (d, J_{C-P} 100.1 Hz), 136.8 (d, J_{C-P} 7.5 Hz), 138.4, 142.7, 144.1, 156.0 (d, J_{C-P} 130.2 Hz), 156.7 (d, J_{C-P} 19.1 Hz).

Synthesis of [2-PPh₂N-TMS]pyPdCl₂ 49 To a toluene suspension (10 mL) of PdCl₂(PhCN)₂ (50 mg, 0.13 mmol) was added **40** (44 mg, 0.13 mmol) dissolved in 5 mL toluene. The orange solution was stirred overnight, and the solvent removed until a few mL's remained. Diethyl ether was added to give a red precipitate, which was then filtered. The solid was washed with diethyl ether (3 x 5 mL), dried *in vacuo*, and recrystallized by slow diffusion of a saturated CH₂Cl₂ layer into hexane to give dark red crystals (76% yield). ³¹P{¹H} NMR (CD₂Cl₂, 25°C, δ): 27.9(s). ¹H NMR (CD₂Cl₂, 25°C, δ): 0.07 (s, 9H, -Si(CH₃)₃), 7.36 (m, 2H, -pyH₃), 7.65 (m, 4H, *-metaPPh₂*), 7.77 (t, 2H, *-paraPPh₂*), 7.84-7.88 (m, 4H, *-orthoPPh₂*), 8.00 (m, 2H, -pyH_{4,5}), 9.30 (d, 1H, 9.0 Hz, -

pyH₆). ¹³C {¹H} NMR (CD₂Cl₂, 25°C, δ): 4.5 (d, J_{C-P} 2.6 Hz), 127.3, 128.5 (d, J_{C-P} 121.1 Hz), 128.3, 129.5 (d, J_{C-P} 12.8 Hz), 133.8 (d, J_{C-P} 11.4 Hz), 134.3 (d, J_{C-P} 2.2 Hz), 138.6 (d, J_{C-P} 10.2 Hz), 153.7 (d, J_{C-P} 10.4 Hz), 159.0 (d, J_{C-P} 130.4 Hz). Anal. Calcd. for C₂₀H₂₃Cl₂N₂PPdSi (527.79): C, 45.51; H, 4.39; N, 5.31. Found: C, 45.02; H, 4.33; N, 5.34.

Synthesis of [2-PPh₂N-2,6-Me₂C₆H₃]pyNiBr₂ 50, [2-PPh₂N-2,6-ⁱPr₂C₆H₃]pyNiBr₂ 51, [6-Me-2-PPh₂N-2,6-Me₂C₆H₃]pyNiBr₂ 52, [6-Me-2-PPh₂N-2,6-Pr₂C₆H₃]pyNiBr₂ 53, [6-TMS-2-PPh₂N-2,6-Me₂C₆H₃]pyNiBr₂ 54, [6-TMS-2-PPh₂N-2,6-ⁱPr₂C₆H₃]pyNiBr₂ 55, [6-Bn-2-PPh₂N-2,6-Me₂C₆H₃]pyNiBr₂ 56, [6-Bn-2-PPh₂N-2,6-ⁱPr₂C₆H₃]pyNiBr₂ 57, [6-Ph-2-PPh₂N-2,6-Me₂C₆H₃]pyNiBr₂ 58, [6-Ph-2-PPh₂N-2,6-ⁱPr₂C₆H₃]pyNiBr₂ 59 Compounds **50** to **59** were prepared by similar methods, thus only one representative procedure is described. To a slight excess of **38** (1.05 eq., 200 mg, 0.29 mmol) and NiBr₂(DME) (86 mg, 0.278 mmol) was added 10 mL CH₂Cl₂. The blue suspension was stirred overnight, and then was concentrated to several mL's *in vacuo*. Diethyl ether (10 mL) was added and the mixture filtered to give a light blue powder. **50-CH₂Cl₂**: Yield = 90%, blue powder, $\nu_{P=N}$ 1213 cm⁻¹, μ_{eff} 2.90. Anal. Calcd. for C₂₆H₂₅Br₂Cl₂NiN₂P (685.87): C, 45.53; H, 3.67; N, 4.08. Found: C, 45.26; H, 3.59; N, 4.16.

51: Yield = 95%, blue powder, $\nu_{P=N}$ 1244 cm⁻¹, μ_{eff} 2.95. Anal. Calcd. for C₂₉H₃₁Br₂NiN₂P (657.05): C, 53.01; H, 4.76; N, 4.26. Found: C, 53.21; H, 4.75; N, 4.21.

52: Yield = 85%, light green powder, $\nu_{P=N}$ 1193 cm⁻¹, μ_{eff} 3.10. Anal. Calcd. for C₂₆H₂₅Br₂NiN₂P (614.97): C, 50.78; H, 4.10; N, 4.56. Found: C, 50.58; H, 4.84; N 3.96.

53: Yield = 80%, light blue powder, $\nu_{\text{P=N}}$ 1242 cm^{-1} , μ_{eff} 3.20. Anal. Calcd. for $\text{C}_{30}\text{H}_{33}\text{Br}_2\text{NiN}_2\text{P}$ (671.07): C, 53.69; H, 4.96; N, 4.17. Found: C, 53.57; H, 4.85; N 4.39.

54-CH₂Cl₂: Yield = 75%, royal blue crystals, $\nu_{\text{P=N}}$ 1217 cm^{-1} , μ_{eff} 3.07. Anal. Calcd. for $\text{C}_{28}\text{H}_{31}\text{Br}_2\text{NiN}_2\text{PSi}$ (673.12): C, 49.96; H, 4.64; N, 4.16. Found: C, 49.66; H, 4.92; N, 3.90.

55-1/2CH₂Cl₂: Yield = 74%, blue-green powder, $\nu_{\text{P=N}}$ 1255 cm^{-1} , μ_{eff} 3.23. Anal. Calcd. for $\text{C}_{32}\text{H}_{39}\text{Br}_2\text{NiN}_2\text{PSi}$ (779.71): C, 50.83; H, 5.43; N, 3.59. Found: C, 50.53; H, 5.09; N, 3.45.

56: Yield = 84%, blue powder, $\nu_{\text{P=N}}$ 1216 cm^{-1} , μ_{eff} 3.15. Anal. Calcd. for $\text{C}_{32}\text{H}_{29}\text{Br}_2\text{NiN}_2\text{P}$ (691.06): C, 55.62; H, 4.23; N, 4.05. Found: C, 55.58; H, 4.72; N, 3.62.

57: Yield = 78%, dark blue crystals, $\nu_{\text{P=N}}$ 1258 cm^{-1} , μ_{eff} 2.97. Anal. Calcd. for $\text{C}_{36}\text{H}_{37}\text{Br}_2\text{NiN}_2\text{P}$ (747.17): C, 57.87; H, 4.99; N, 3.75. Found: C, 57.91; H, 5.27; N, 3.46.

58-H₂O: Yield = 90%, purple powder, $\nu_{\text{P=N}}$ 1217 cm^{-1} , μ_{eff} 2.95. Anal. Calcd. for $\text{C}_{31}\text{H}_{27}\text{Br}_2\text{NiN}_2\text{P}$ (677.03): C, 53.57; H, 4.21; N, 4.03. Found: C, 54.00; H, 4.50; N, 3.70.

59: Yield = 92%, blue-green powder, $\nu_{\text{P=N}}$ 1241 cm^{-1} , μ_{eff} 2.91. Anal. Calcd. for $\text{C}_{35}\text{H}_{35}\text{Br}_2\text{NiN}_2\text{P}$ (733.14): C, 57.34; H, 4.81; N, 3.82. Found: C, 57.35; H, 5.16; N, 3.58.

Synthesis of [2-PPh₂N-2,6-Me₂C₆H₃]pyFeCl₂ **60**, [2-PPh₂N-2,6-ⁱPr₂C₆H₃]pyFeCl₂ **61**, [6-Me-2-PPh₂N-2,6-Me₂C₆H₃]pyFeCl₂ **62**, [6-Me-2-PPh₂N-2,6-ⁱPr₂C₆H₃]pyFeCl₂ **63**, [6-TMS-2-PPh₂N-2,6-Me₂C₆H₃]pyFeCl₂ **64**, [6-TMS-2-PPh₂N-2,6-ⁱPr₂C₆H₃]pyFeCl₂ **65**, [6-Bn-2-PPh₂N-2,6-Me₂C₆H₃]pyFeCl₂ **66**, [6-Bn-2-PPh₂N-2,6-ⁱPr₂C₆H₃]pyFeCl₂ **67**, [6-Ph-2-PPh₂N-2,6-Me₂C₆H₃]pyFeCl₂ **68**, [6-Ph-2-PPh₂N-2,6-ⁱPr₂C₆H₃]pyFeCl₂ **69** Compounds **60** to **69** were prepared by similar methods, thus only one representative

procedure is described. To a slight excess of **38** (1.05 eq, 200 mg, 0.39 mmol) and FeCl₂ (47 mg, 0.37 mmol) was added 10 mL THF. The orange suspension was stirred overnight, and then was concentrated to several mL's *in vacuo*. Diethyl ether (10 mL) was added and the mixture filtered to give an orange powder. **60**: Yield = 92%, orange powder, $\nu_{\text{P=N}}$ 1211 cm⁻¹, μ_{eff} 4.95. Anal. Calcd. for C₂₅H₂₃Cl₂FeN₂P (509.19): C, 58.97; H, 4.55; N, 5.50. Found: C, 58.99; H, 4.73; N, 5.17.

61: Yield = 87%, light-orange solid, $\nu_{\text{P=N}}$ 1237 cm⁻¹, μ_{eff} 5.04. Anal. Calcd. for C₂₉H₃₁Cl₂FeN₂P (565.29): C, 61.62; H, 5.53; N, 4.96. Found: C, 61.91; H, 5.42; N, 4.86.

62: Yield = 95%, dull orange solid, $\nu_{\text{P=N}}$ 1188 cm⁻¹, μ_{eff} 5.12. Anal. Calcd. for C₂₆H₂₅Cl₂FeN₂P (523.21): C, 59.68; H, 4.82; N, 5.35. Found: C, 59.50; H, 4.75; N, 5.55.

63: Yield = 85%, orange solid, $\nu_{\text{P=N}}$ 1242 cm⁻¹, μ_{eff} 5.24. Anal. Calcd. for C₃₀H₃₃Cl₂FeN₂P (579.32): C, 62.20; H, 5.74; N, 4.84. Found: C, 62.32; H, 5.93; N, 4.50.

64: Yield = 76%, orange-red crystals, $\nu_{\text{P=N}}$ 1213 cm⁻¹, μ_{eff} 5.07. Anal. Calcd. for C₂₈H₃₁Cl₂FeN₂PSi (581.37): C, 57.85; H, 5.37; N, 4.82. Found: C, 57.86; H, 5.45; N, 4.84.

65: Yield = 72%, orange crystals, $\nu_{\text{P=N}}$ 1254 cm⁻¹, μ_{eff} 4.99. Anal. Calcd. for C₃₂H₃₉Cl₂FeN₂PSi (637.48): C, 60.29; H, 6.17; N, 4.39. Found: C, 60.07; H, 6.15; N, 4.12.

66-CH₂Cl₂: Yield = 67%, deep orange crystals, $\nu_{\text{P=N}}$ 1215 cm⁻¹, μ_{eff} 5.14. Anal. Calcd. for C₃₃H₃₁Cl₄FeN₂P (684.24): C, 57.93; H, 4.57; N, 4.09. Found: C, 57.27; H, 5.14; N, 3.56.

67-CH₂Cl₂: Yield = 76%, orange crystals, $\nu_{\text{P=N}}$ 1258 cm⁻¹, μ_{eff} 5.20. Anal. Calcd. for C₃₇H₃₉Cl₄FeN₂P (740.35): C, 60.03; H, 5.31; N, 3.78. Found: C, 59.82; H, 5.61; N, 3.39.

68-H₂O: Yield = 55%, dark orange crystals, $\nu_{\text{P=N}}$ 1242 cm⁻¹, μ_{eff} 5.35. Anal. Calcd. for C₃₁H₂₉Cl₂FeN₂OP (603.30): C, 61.72; H, 4.85; N, 4.64. Found: C, 61.60; H, 5.08; N, 4.19.

69-H₂O: Yield = 65%, dark orange crystals, $\nu_{\text{P=N}}$ 1217 cm⁻¹, μ_{eff} 5.19. Anal. Calcd. for C₃₅H₃₇Cl₂FeN₂OP (659.41): C, 63.75; H, 5.66; N, 4.25. Found: C, 63.69; H, 5.68; N, 4.13.

Synthesis of [6-Ph-2-P(C₆F₅)₂]py 70 PhMgBr (1.0 M in THF, 1.1 mL, 1.1 mmol) was added dropwise to a stirred THF solution (10 mL) of **33** (0.25 g, 1.1 mmol) over a period of 15 minutes to give a deep yellow solution. The solution was stirred overnight with no observable change in colour. A THF solution (5 mL) of **27** (402 mg, 1.1 mmol) was then added dropwise and the deep red solution was stirred overnight. The solvent was removed *in vacuo* and the residual oil was extracted with pentane several times. The pentane extracts were cooled to -35°C and filtered to give the white solid **70** (450 mg), which was washed several times with cold pentane. Yield = 92%. ³¹P{¹H} NMR (CDCl₃, 25°C, δ): -45.0 (quint, $J_{\text{P-F}}$ 30.0 Hz). ¹H NMR (CDCl₃, 25°C, δ): 7.39-7.51 (m, 2H, -ArH), 7.56 (m br, 2H, -ArH), 7.65 (t, 7.8 Hz, 1H, -pyH₅), 7.69 (d, 7.7 Hz, 1H, -pyH₄), 8.00 (m, 2H, -pyH₃).

Procedure for ethylene polymerisation

A 500 mL Parr stainless steel autoclave equipped with mechanical stirring and pressure gauge was heated (~110°C) under vacuum for >2 hours. The temperature of the autoclave was regulated by a thermal jacket. The autoclave was cooled to the desired

temperature and 500 equivalents of MAO dissolved in toluene was added under N₂. The solution was stirred for an additional hour, and a toluene suspension of the catalyst was added. The vessel was then quickly pressurized with 300 psi ethylene, and the reaction stirred for 30 minutes. The polymerisation was stopped by venting the volatiles at room temperature, followed by quenching of the reaction solution with acidified MeOH and the solution filtered. The organic layer was separated, dried with Na₂SO₄, filtered and the solvent removed to give traces of a sticky, gummy polymer. The trace amounts of polymer were redissolved in hexane, filtered again to remove any residual catalyst, and the solvent removed.

Procedure for ethylene oligomerisation

A 500 mL Parr stainless steel autoclave was heated (~110°C) under vacuum for >2 hours. After cooling the autoclave to the desired temperature, a toluene solution of the activator (DEAC, MAO) was added under N₂. The solution was stirred for an additional hour, and a toluene/chlorobenzene solution of metal complex was added. The vessel was quickly pressurized with 300 psi, and the reaction stirred for 30 minutes. The autoclave was cooled to -78°C, and the volatiles slowly vented. Ethanol (20 mL) and an internal standard were added (toluene for DEAC activation or diethyl ether for MAO activation) to quench the reaction, and the mixture slowly warmed to -30°C over 10 minutes. The composition of the alkenes formed was determined by GC and NMR spectroscopy.

Computational Details

Optimized geometries of $[\text{NiCH}_3(\text{ligand})]^+$, ligand = diimine (NCCN), phosphinimine-imine (NPCN) and fluorinated phosphinimine-imine (NPF₂CN), were obtained using the Gaussian 98^{60a} suite of programs. The hybrid DFT method, B3LYP⁶¹ (as implemented in G98)^{60b}, was employed in conjunction with the 6-31G(d) basis set for the ligand, and the LANL2DZ basis set for nickel. This latter basis set uses the effective core potentials developed by Hay and Wadt.⁶² NBO analysis was also performed on the optimized structure to determine the natural charge on the nickel atom.

The optimized geometry of the nickel complex was used to determine the orbital energies of the ligand. After the cartesian coordinates were determined for each optimized structure, the nickel and methyl moieties were removed. A single point energy calculation was then performed on the resulting constrained ligand geometries using the Hartree-Fock (HF) method and the 6-31G(d) basis set to determine the lone pair orbital energy. Lone pair diagrams were generated using POV-ray.

X-ray Data Collection and Reduction.

The crystals was manipulated and mounted in a glass capillary in a glovebox, thus maintaining a dry, O₂-free environment. The diffraction study was performed with a Siemens SMART System CCD diffractometer. The data were collected for a hemisphere of data in 1329 frames with 10-second exposure times. Atomic coordinates and equivalent isotropic displacement parameters are given in Table 2 (Supplementary data). Selected interatomic bond distances and angles are given in Table 3. Anisotropic displacement factors are given in Table 4, and hydrogen coordinates and isotropic

displacement parameters are given in Table 5. The observed extinctions were consistent with the space group. A measure of decay was obtained by re-collecting the first 50 frames of each data set. The intensities of reflections within these frames showed no statistically significant change over the duration of the data collection. An empirical absorption correction based on redundant data was applied to the data set. Subsequent solution and refinement was performed using the SHELXTL solution package.

Structure Solution and Refinement.

Non-hydrogen atomic scattering factors were taken from the literature tabulations.¹ The heavy atom positions were determined using direct methods. The remaining non-hydrogen atoms were located from successive difference Fourier map calculations. The refinements were carried out by using full-matrix least squares techniques on F , minimizing the function $\omega(|F_o| - |F_c|)^2$ where the weight ω is defined as $4F_o^2/2\sigma(F_o^2)$ and F_o and F_c are the observed and calculated structure factor amplitudes. In the final cycles of each refinement, all non-hydrogen atoms were assigned anisotropic temperature factors. No disorder was indicated by the difference maps or the thermal parameters. Carbon-bound hydrogen atom positions were calculated and allowed to ride on the carbon to which they are bonded assuming a C-H bond length of 0.95 Å. Hydrogen atom temperature factors were fixed at 1.10 times the isotropic temperature factor of the carbon atom to which they are bonded. The hydrogen atom contributions were calculated, but not refined.

Table 2.1 Crystallographic Parameters for 34, 49, 54, 57, 69

	34	49
Formula	C ₁₈ H ₁₆ NP	C ₂₀ H ₂₃ Cl ₂ N ₂ PPdSi
MW	277.29	527.76
a(Å)	11.076(7)	9.426(14)
b(Å)	9.274(6)	15.17(2)
c(Å)	15.069(10)	15.75(2)
α(deg)		90.83(3)
β(deg)		91.56(3)
γ(deg)		90.18(3)
Cryst syst	Orthorhombic	Triclinic
Space group	Pna2(1)	P-1
Vol(Å) ³	1547.9(16)	2252(6)
D _{calcd} (g cm ⁻³)	2.380	1.556
Z	8	4
Abs. coeff., μ, mm ⁻¹	0.334	1.193
Data collected	6177	9555
Data F _o ² >3σ(F _o ²)	2130	6438
Variables	181	487
R ^a (%)	3.1	2.6
R _w ^a (%)	6.8	6.8
Goodness of Fit	1.057	1.082

^aAll data collected at 20°C with Mo Kα radiation (λ = 0.71073 Å), $R = \frac{\sum ||F_o| - |F_c||}{\sum |F_o|}$, $R_w = \left[\frac{\sum [\omega(F_o^2 - F_c^2)^2]}{\sum [\omega F_o^2]^2} \right]^{0.5}$

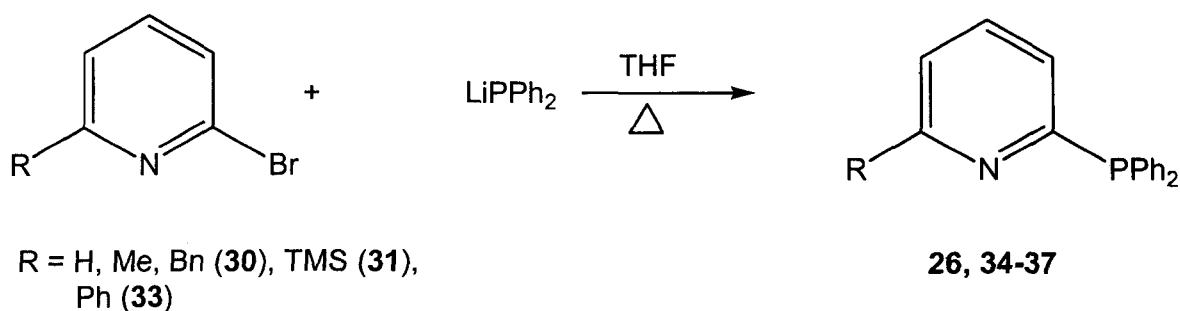
	54-CH ₂ Cl ₂	57	69-H ₂ O
Formula	C ₃₀ H ₃₃ Br ₂ Cl ₂ Br ₂ NiPSi	C ₃₆ H ₃₇ Br ₂ N ₂ NiP	C ₃₅ H ₃₇ Cl ₂ FeN ₂ OP
MW	758.06	747.18	659.39
a(Å)	10.109(6)	20.150(14)	9.019(5)
b(Å)	20.839(14)	9.089(6)	17.963(9)
c(Å)	15.184(9)	18.691(12)	21.636(11)
α(deg)			
β(deg)	92.665(13)	102.377(14)	99.174(10)
γ(deg)			
Cryst syst	Monoclinic	Monoclinic	Monoclinic
Space group	P2(1)/n	P2(1)/c	P2(1)/c
Vol(Å) ³	3195(4)	3344(4)	3460(3)
D _{calcd} (g cm ⁻³)	1.576	1.484	1.266
Z	4	4	4
Abs. coeff., μ, mm ⁻¹	3.385	3.045	0.665
Data collected	13144	13895	14586
Data F _o ² >3σ(F _o ²)	4564	4822	4891
Variables	343	379	379
R ^a (%)	7.9	6.2	5.2
R _w ^a (%)	20.2	8.7	15.9
Goodness of Fit	1.023	1.051	1.073

^aAll data collected at 20°C with Mo Kα radiation (λ = 0.71073 Å), R = Σ||F_o|-|F_c|| / Σ|F_o|, R_w = [Σ[ω(F_o²-F_c²)²] / Σ[(ωF_o²)²]]^{0.5}

2.3 Results and Discussion

Synthesis and Characterization of Pyridyl-Phosphinimine Metal Complexes

Substituted pyridyl-phosphines can be synthesized in reasonable yields by the reaction of lithium diphenylphosphide with the desired substituted bromopyridine (Scheme 2.1).⁵⁵ ^1H NMR spectroscopy shows the expected substitution on the pyridine ring, in addition to two equivalent phenyl groups located on the phosphorus atom. Assignment of pyridine and phosphine protons in ^1H NMR spectra were made according to chemical shifts reported in similar species.⁵⁵ The ^{31}P NMR spectra of **26**, and **34-37** feature single resonances around -3.5 ppm, which are in agreement for similarly reported compounds.⁵⁵ X-ray quality crystals of **34** were grown from a saturated THF solution and identified by a single crystal diffraction study (Figure 2.1). The solid state structure of **34** clearly indicates the presence of a methyl group in the 6-position of the pyridine ring. As expected, the geometry at the phosphorus atom is pseudo-tetrahedral; determined from the angles formed around P(1) ($100.64(17)^\circ$ - $102.41(16)^\circ$). These angles are in close agreement with angles found for 2-pyridyldiphenylphosphine ($101.7(1)^\circ$ - $103.3(1)^\circ$).⁶³



Scheme 2.1 Synthesis of 6-substituted-2-pyridyldiphenylphosphines.

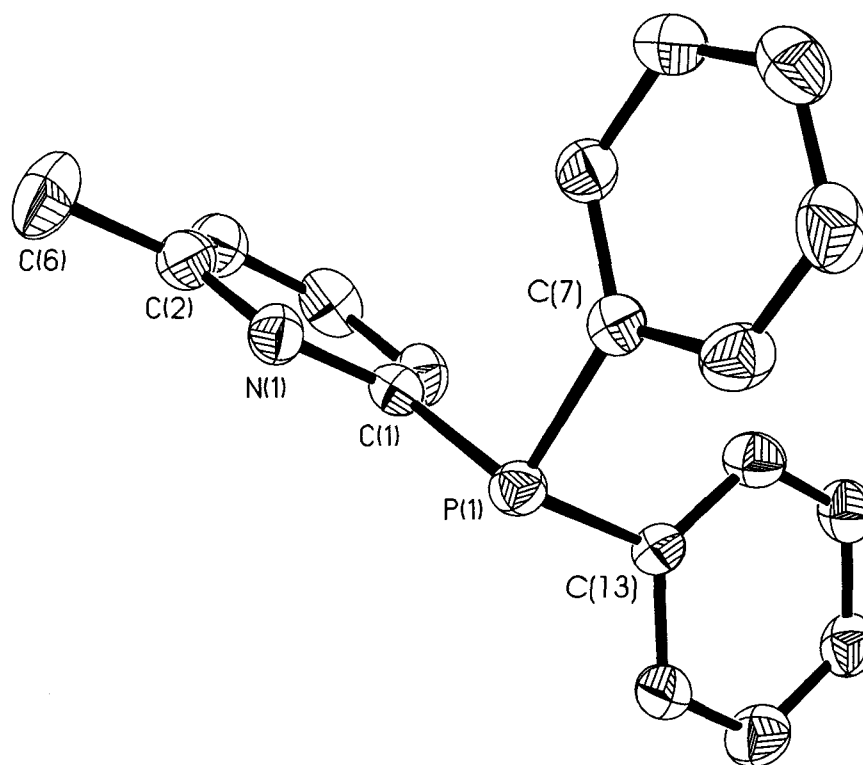
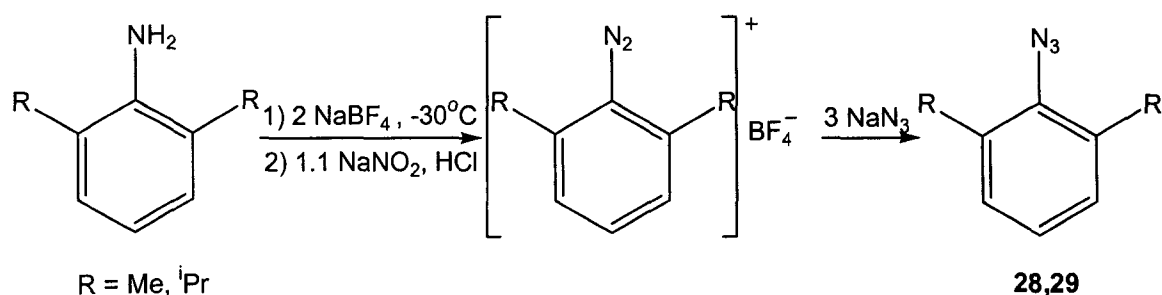


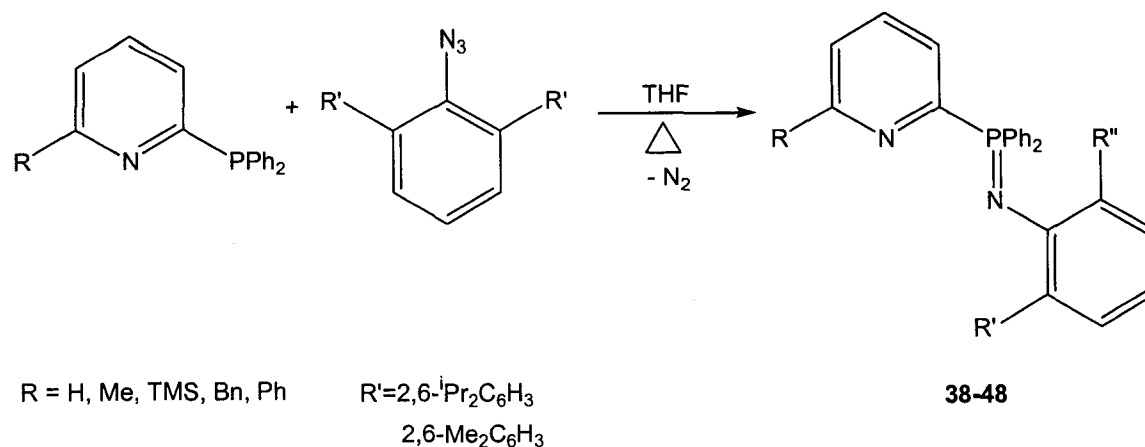
Figure 2.1 ORTEP drawing of **34**, 30% thermal ellipsoids are shown. Hydrogen atoms have been omitted for clarity. P(1)-C(1) 1.846(3) Å, P(1)-C(7) 1.852(4) Å, N(1)-C(1) 1.352(4) Å, N(1)-C(1) 1.352(4) Å, C(2)-C(6) 1.513(5) Å, C(1)-C(13) 1.853(4) Å, C(1)-P(1)-C(7) 102.41(16)°, C(1)-P(1)-C(13) 101.01(16)°, C(7)-P(1)-C(13) 100.64(17)°, N(1)-C(2)-C(6) 116.4(3)°.

Substituted phenyl azides are synthesized by a derivation of a published method.⁶⁴ The previously published syntheses^{46,65} of 2,6-diisopropylphenyl azide suffer from decreased yields and the presence of impurities. This new method allows isolation of an air stable diazonium tetrafluoroborate salt, which can undergo nucleophilic displacement with an azide anion to form **28** and **29** in yields greater than 85%, with only trace amounts of impurities (Scheme 2.2).

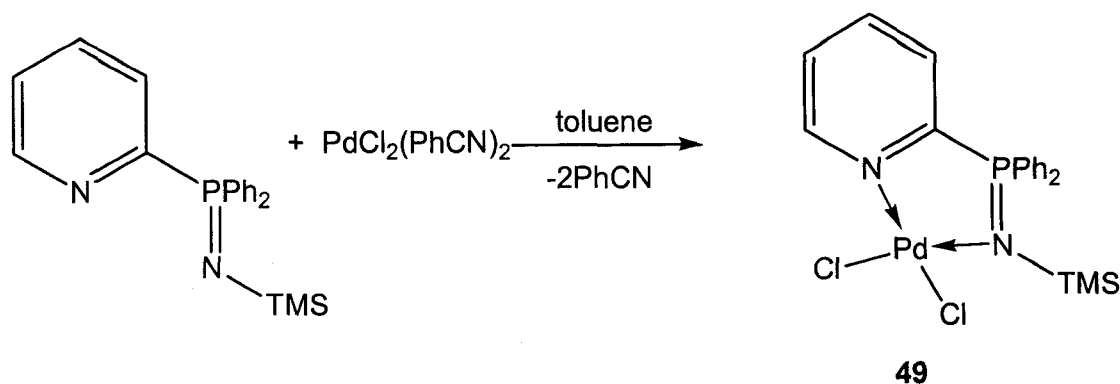


Scheme 2.2 Synthesis of 2,6-disubstituted phenyl azides.

Oxidation of phosphines with organic azides proceeds cleanly to give phosphinimine ligands **38-48** in excellent yields after recrystallization (Scheme 2.3). Upon oxidation there is a slight upfield shift in the ³¹P spectra (5-10 ppm) of all complexes, representing the formation of a P=N bond. ¹H NMR spectroscopy clearly shows the presence of isopropyl or methyl groups, in addition to the desired substitution on the pyridine group. IR analysis of **38-48** indicates strong P=N stretching frequencies around 1329-1357 cm⁻¹, in agreement with previous results.^{43-48,66}

**Scheme 2.3** Synthesis of pyridyl-phosphinimines **38-48**.

Phosphinimine ligands can react with group VIII and X metal halides in appropriate solvents to give both paramagnetic and diamagnetic complexes. Reaction of the ligand **40** and $\text{PdCl}_2(\text{PhCN})_2$ gives a square planar, diamagnetic compound that can be identified by NMR spectroscopy (Scheme 2.4). The ^1H NMR spectrum of complex **49** shows very little shift in the ligand resonances after palladium coordination; however, the ^{31}P NMR spectrum displays a singlet with a resonance 30 ppm downfield relative to the ligand. This phenomenon is not unexpected, as it is been shown that coordination of a *P,N*-chelated iminophosphorane ligand to palladium causes a ^{31}P shift of the complexed ligand to a higher frequency.⁶⁷



Scheme 2.4 Synthesis of a palladium(II) pyridyl phosphinimine complex (**49**).

The formulation of **50** was confirmed crystallographically from crystals obtained from the diffusion of a saturated CH_2Cl_2 layer into hexane. The geometry about the palladium metal centre appears to be pseudo-square planar with the pyridyl-phosphinimine ligand coordinating in a bidentate fashion (Figure 2.2). The palladium-phosphinimine five-membered metallacycle is not planar, having a torsion angle formed by Pd(1)-N(2)-C(13)-P(1) of 4.3° and a mean deviation from the plane of 0.0847 \AA . Such a distortion is not surprising as Arques *et al.* have described this phenomenon for related complexes.⁶⁷ The two Pd—Cl bond lengths and Pd—N distances are relatively close, suggesting the *trans*-influences of the two nitrogen donor atoms are similar. The Pd—N_{phosphinimine} bond is also similar to those described by Arques for palladium complexes of the *P,N*-chelated iminophosphorane ligand and by Liu *et al.*⁶⁸ for palladium complexes of exocyclic *P,N*-chelated iminophosphorane ligands. The P=N bond is slightly longer in the palladium complex **49** ($1.578(3) \text{ \AA}$) than the reported ligand $\text{CH}_2(\text{Ph}_2\text{P}=\text{NC}_6\text{H}_4\text{Me-4})_2$ ⁴³ ($1.568(2) \text{ \AA}$). In comparison with formal P—N bond length calculations (a formal single bond value of 1.77 \AA and a double bond of 1.57 \AA),^{43,69} it

appears that the ligand loses some double bond character upon coordination to the palladium metal centre.

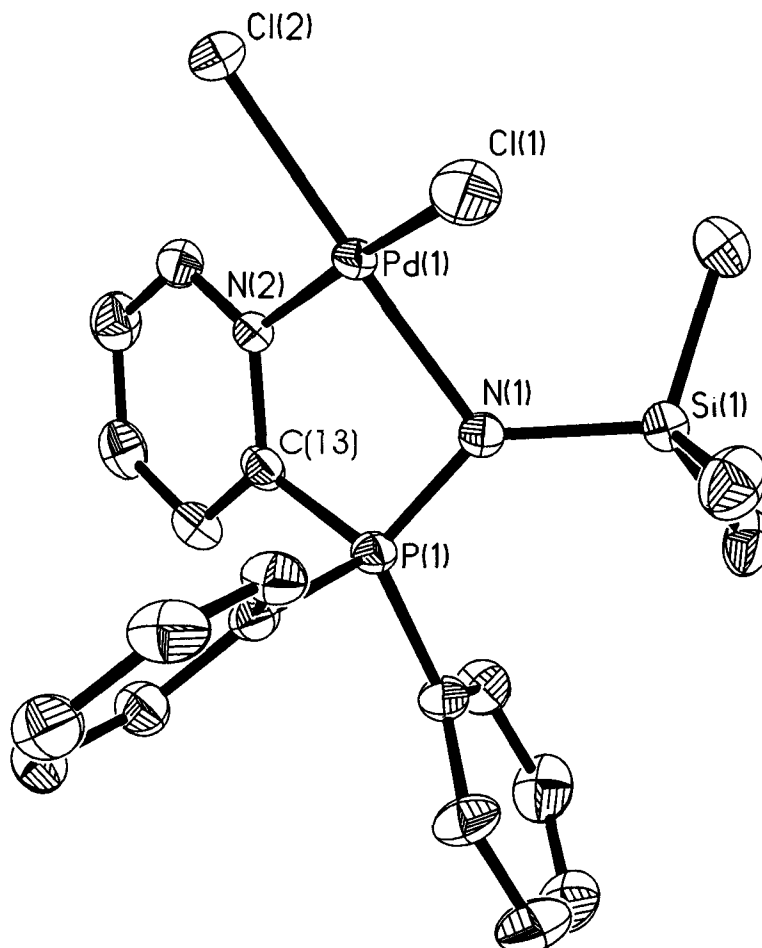
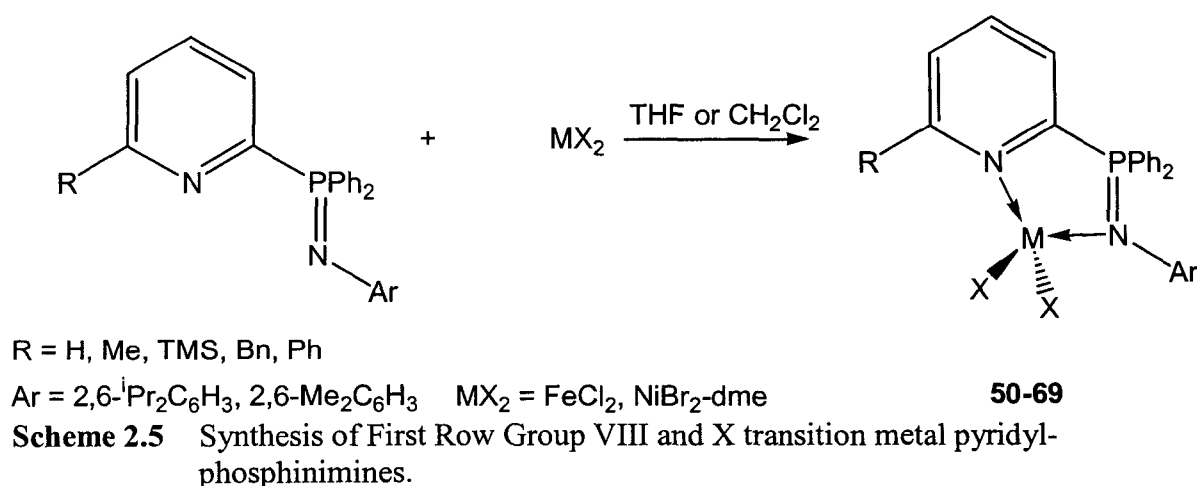


Figure 2.2 ORTEP drawing of **49**, 30% thermal ellipsoids are shown. Hydrogen atoms have been omitted for clarity. Pd(1)-N(1) 2.063(3) Å, Pd(1)-N(2) 2.056(4) Å, Pd(1)-Cl(1) 2.286(3) Å, Pd(1)-Cl(2) 2.280(2) Å, P(1)-N(1) 1.578(3) Å, N(1)-Si(1) 1.751(3) Å, N(2)-C(13) 1.361(4) Å, P(1)-C(13) 1.813(4) Å, N(2)-Pd(1)-N(1) 85.20(12)°, N(2)-Pd(1)-Cl(2) 93.12(10)°, N(1)-Pd(1)-Cl(1) 92.64(11)°, Cl(2)-Pd(1)-Cl(1) 89.45(9)°, Si(1)-N(1)-Pd(1) 121.77(15)°, P(1)-N(1)-Pd(1) 103.40(15)°, C(13)-N(2)-Pd(1) 114.6(2)°, N(1)-P(1)-C(13) 104.34(16)°, N(2)-C(13)-P(1) 111.0(2)°.

Iron(II) and nickel(II) complexes **50-69** were synthesized from the reaction between ligands **38, 39, 41-48** and appropriate metal halides (Scheme 2.5). The formulations of these metal complexes were determined by IR spectroscopy, magnetic susceptibility, elemental analysis, and X-ray crystallography. Due to the paramagnetic nature of the products, attempts to identify these compounds with NMR spectroscopy were difficult. IR spectroscopy of all iron(II) and nickel(II) complexes show P=N stretching frequencies between 1190-1250 cm^{-1} . In comparison with the IR spectra of the free ligands, coordination of the ligand to the metal centre shifts the P=N frequency to lower wavenumbers ($\sim 100 \text{ cm}^{-1}$), which is greater than previously reported results.^{29,31} This finding suggests a loss of P=N double bond character upon ligand coordination, which is in agreement with the X-ray structure determinations (Figures 2.3-2.5) of **54, 57,** and **69**. Magnetic susceptibility measurements show average values of 5.13 BM for iron(II) complexes and 3.04 BM for nickel(II) complexes, which compare well with theoretical calculations for d_6 and d_8 tetrahedral metal compounds (4.90 BM and 2.83 BM, respectively).



Only recently have the solid state structures of Ni-phosphinimine complexes been reported;⁵⁰ however, no elucidations of iron(II) phosphinimine complexes have been made. The formulations of **54**, **57**, and **69** were verified by a single crystal diffraction study. As expected, the geometry about the metal atoms is pseudo-tetrahedral, with two halides and a bidentate pyridyl-phosphinimine ligand completing the coordination sphere. Phosphinimine (P=N) bond lengths varied between 1.586(9) Å and 1.615(7) Å, which agrees with the average P=N bond lengths (1.610(6) Å) reported by Bochmann *et al.* for similar compounds.⁴⁶ These P=N bond lengths also parallel distances found by Elsevier *et al.* for the rhodium complex $[(\text{CH}_2(\text{Ph}_2\text{P}=\text{NC}_6\text{H}_4\text{Me-4})_2\text{Rh}(\text{COD}))]$,²⁹ and are slightly longer than the P=N bond length reported for the ligand $\text{CH}_2(\text{Ph}_2\text{P}=\text{NC}_6\text{H}_4\text{Me-4})_2$ (1.568(2) Å).⁴³

The arrangement of the NPCN-metal five-membered chelating ring and the orientation of bulky substituent groups in **54**, **57**, and **69** warrants further discussion. The metal-ligand chelating ring adopts a non-planar orientation, similar to complex **49**, with a mean deviation from the plane of 0.0556 Å, 0.0881 Å, and 0.1026 Å, for **54**, **57**, and **69**, respectively. Bulky groups in the six position of the pyridine ring orient in a fashion to minimize steric interaction with the metal centre. This phenomenon is observed in **57** and **69**, which have benzyl and phenyl groups, respectively, located on the pyridine ring. An angle of 50.3° is observed in **69** between the phenyl group and the pyridine ring. The combination of bulk on the pyridine ring and phosphinimine group appears to form a protective pocket around the metal atom; a requirement for late transition metal olefin polymerisation.

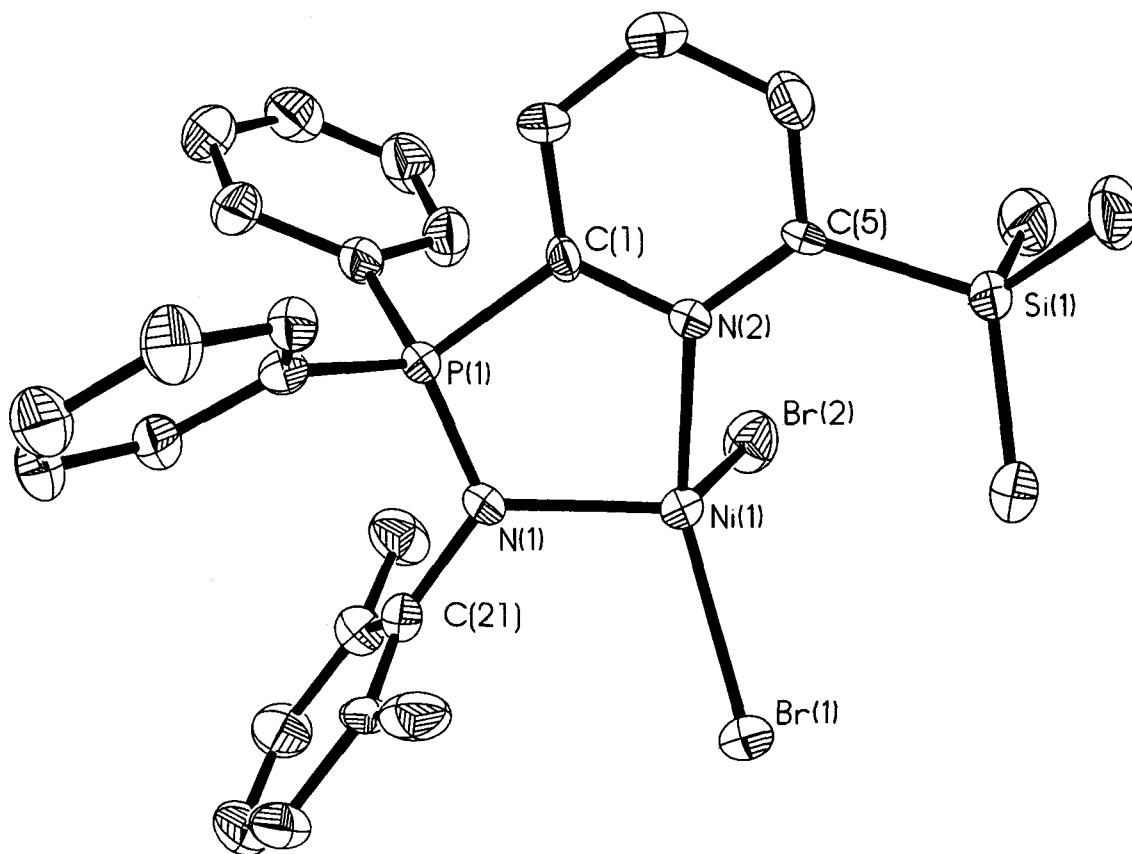


Figure 2.3 ORTEP drawing of **54-CH₂Cl₂**, 30% thermal ellipsoids are shown. Hydrogen atoms have been omitted for clarity. Ni(1)-N(1) 1.996(8) Å, Ni(1)-N(2) 2.092(8) Å, Ni(1)-Br(1) 2.379(2) Å, Ni(1)-Br(2) 2.395(2) Å, P(1)-N(1) 1.586(9) Å, P(1)-C(1) 1.821(9) Å, N(2)-C(1) 1.379(12) Å, Si(1)-C(5) 1.930(10) Å, N(1)-C(21) 1.454(13) Å, N(1)-Ni(1)-N(2) 88.4(3)°, N(1)-Ni(1)-Br(1) 106.0(2)°, N(2)-Ni(1)-Br(1) 139.4(2)°, N(1)-Ni(1)-Br(2) 113.7(2)°, N(2)-Ni(1)-Br(2) 100.6(2)°, Br(1)-Ni(1)-Br(2) 107.36(7)°, N(2)-C(5)-Si(1) 123.4(7)°, C(1)-N(2)-Ni(1) 114.2(6)°, N(2)-C(1)-P(1) 115.5(7)°, N(1)-P(1)-C(1) 105.2(4)°, P(1)-N(1)-Ni(1) 115.2(4)°, C(21)-N(1)-Ni(1) 123.3(6)°.

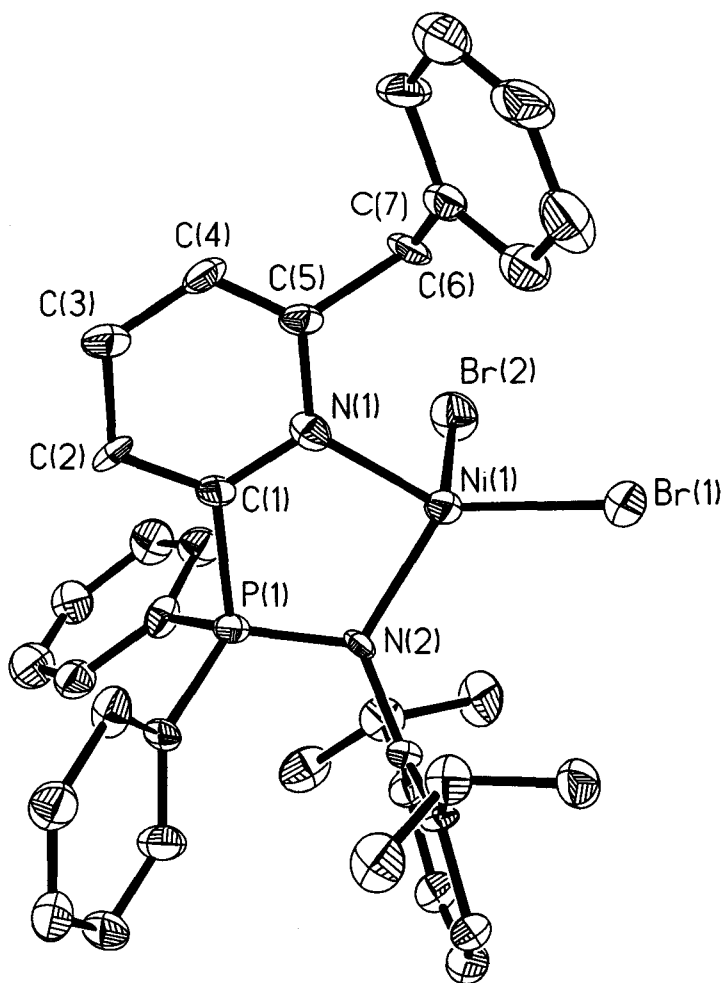


Figure 2.4 ORTEP drawing of **57**, 30% thermal ellipsoids are shown. Hydrogen atoms have been omitted for clarity. Ni(1)-N(2) 2.011(7) Å, Ni(1)-N(1) 2.061(8) Å, Ni(1)-Br(1) 2.351(2) Å, Ni(1)-Br(2) 2.3996(19) Å, P(1)-N(2) 1.615(7) Å, P(1)-C(1) 1.840(9) Å, N(1)-C(1) 1.337(10) Å, N(1)-C(5) 1.414(11) Å, C(5)-C(6) 1.531(11) Å, C(6)-C(7) 1.473(11) Å, N(2)-Ni(1)-N(1) 87.6(3)°, N(2)-Ni(1)-Br(1) 120.4(2)°, N(1)-Ni(1)-Br(1) 126.2(2)°, N(2)-Ni(1)-Br(2) 116.0(2)°, N(1)-Ni(1)-Br(2) 102.4(2)°, Br(1)-Ni(1)-Br(2) 103.55(7)°, N(2)-P(1)-C(1) 103.9(4)°, C(1)-N(1)-C(5) 116.2(8)°, C(1)-N(1)-Ni(1) 116.8(7)°, C(5)-N(1)-Ni(1) 126.4(7)°, P(1)-N(2)-Ni(1) 113.5(5)°, N(1)-C(1)-P(1) 114.7(7)°, N(1)-C(5)-C(6) 118.0(9)°, C(7)-C(6)-C(5) 113.9(8)°.

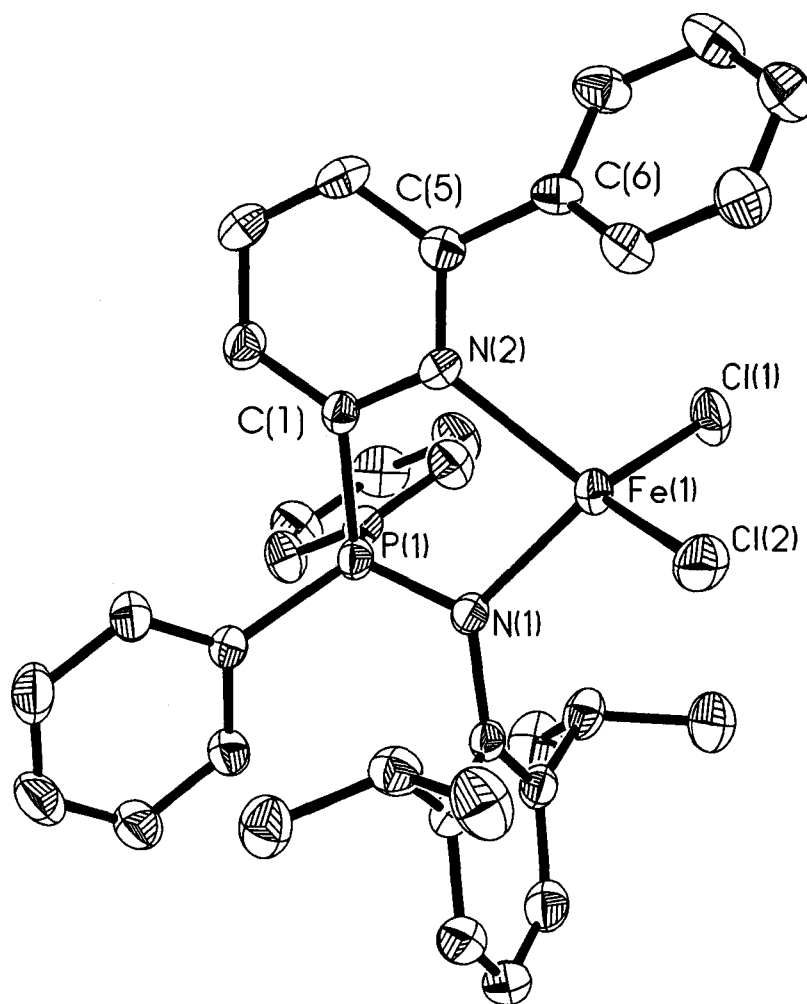


Figure 2.5 ORTEP drawing of **69-H₂O**, 30% thermal ellipsoids are shown. Hydrogen atoms have been omitted for clarity. Fe(1)-N(1) 2.072(5) Å, Fe(1)-N(2) 2.233(5) Å, Fe(1)-Cl(1) 2.2742(19) Å, Fe(1)-Cl(2) 2.2742(19) Å, P(1)-N(1) 1.603(5) Å, P(1)-C(1) 1.827(6) Å, N(2)-C(1) 1.360(7) Å, C(5)-C(6) 1.492(9) Å, N(1)-Fe(1)-N(2) 83.08(18)°, N(1)-Fe(1)-Cl(2) 110.15(14)°, N(2)-Fe(1)-Cl(2) 125.54(14)°, N(1)-Fe(1)-Cl(1) 119.15(14)°, N(2)-Fe(1)-Cl(1) 104.92(14)°, Cl(2)-Fe(1)-Cl(1) 111.95(8)°, N(1)-P(1)-C(1) 105.5(3)°, C(1)-N(2)-C(5) 117.6(5)°, C(1)-N(2)-Fe(1) 116.4(4)°, C(5)-N(2)-Fe(1) 125.6(4)°, N(2)-C(5)-C(6) 117.8(5)°, N(2)-C(1)-P(1) 114.2(4)°.

Ethylene Polymerisation Studies of Pyridyl-phosphinimine Metal Complexes

Preliminary ethylene polymerisations were performed to determine the catalytic potential of pyridyl-phosphinimine containing-transition metal catalysts. Initial testing of complex **59** at room temperature and atmospheric ethylene pressure in a Buchi reactor showed no polymerisation activity. Complexes **54**, **55**, **58**, **59**, **64**, **65**, **68**, and **69** were then activated with MAO in toluene at 35°C and 300 psi ethylene (Table 2.2) in a Parr high pressure reactor; however, no polymer was recovered after each trial. Similar trials were performed by NOVA using hexane as the solvent, and no polymer was detected after workup.

Table 2.2 Ethylene polymerisation by Cp_2ZrCl_2 and nickel/iron pyridyl-phosphinimine complexes **54**, **55**, **58**, **59**, **64**, **65**, **68**, and **69**.

Trial	Compound	Solvent	Activity (g PE/mmol cat·hr·atm)	M_w	M_w/M_n
LSPB1-4 ^a	Cp_2ZrCl_2	toluene	40	-	-
LSPB5-6 ^a	54	toluene	-	-	-
LSPB7-8 ^a	55	toluene	Trace	-	-
LSPB9-10 ^a	58	toluene	-	-	-
NOVA1 ^b	59	hexane	2.4	^c	^c
LSPB11-12 ^a	59	toluene	-	-	-
LSPB13-14 ^a	64	toluene	-	-	-
LSPB15-16 ^a	65	toluene	-	-	-
LSPB17-18 ^a	68	toluene	-	-	-
NOVA2 ^b	69	hexane	1.8	^c	^c
LSPB19-20 ^a	69	toluene	-	-	-

^a300 psig ethylene, 35°C, Al:M ratio of 500:1, MAO. ^bperformed by NOVA, 300 psig, 35°C, Al:M ratio of 500:1. ^cno detectable polymer.

The work of Keim²⁸ and de Souza and Reau⁵⁰ prompted interest in the potential of these metal complexes as ethylene oligomerisation catalysts. Complexes **59** and **69** were

evaluated for ethylene oligomerisation at 35°C and 300 psi ethylene. The *in situ* generation of the active species was performed by two different methods: (1) MAO activation in toluene; and (2) diethylaluminum chloride (DEAC) activation in chlorobenzene. Under these reaction conditions, the nickel species **59**, when activated by DEAC, was found to give the highest activity (Table 2.3). GC and NMR identification of products suggested that only C₄ alkenes are formed, with varying degrees of alkene selectivity. These findings are not surprising in light of results from de Souza and Reau,⁵⁰ who also found that DEAC activation of several Ni-bisphosphinimine catalysts in the presence of ethylene primarily produced C₄ alkenes with varying amounts of C₆, and C₈ alkenes. These results suggest a modest activity for the oligomerisation of ethylene, although **54** displays an activity roughly one order of magnitude less than previously reported Ni-bisphosphinimine complexes (344.3 g·mmol⁻¹·hr⁻¹·atm⁻¹).⁵⁰

Table 2.3 Ethylene oligomerisation results of activated nickel/iron pyridyl-phosphinimine complexes **59** and **69**.

Trial	Compound	Solvent	Mass of oligomers (g) ^c	Activity ^d
LSPB34-35 ^a	59	toluene	0.807	16.1
LSPB36-37 ^b	59	chlorobenzene	7.95	48.2
LSPB37-38 ^a	69	toluene	0.66	13.2
LSPB39-40 ^b	69	chlorobenzene	0.50	3.0

^a300 psig ethylene, 35°C, Al:M ratio of 500:1, MAO. ^b300 psig ethylene, 35°C, Al:M ratio of 200:1. ^ccalculated from GC peak areas, and NMR. ^dg oligomer·cat⁻¹·hr⁻¹·atm⁻¹.

The phosphinimine-based LTM complexes synthesized in this work do not appear capable of polymerizing ethylene with high catalytic activities. Clearly, compared to the highly active diimine systems, the presence of a phosphinimine fragment exerts a very different influence on the electronic properties of the metal centre. Previous

computational investigations have shown that the electronic effects of the Grubbs-type catalyst, **12**, significantly influence the catalytic performance,^{70a} hence, it was of interest to investigate these phosphinimine-based catalysts for similar effects.

Computational Study of Diimine (NCCN) and Phosphinimine-imine (NPCN) Ligands and Nickel(II) Complexes

Density functional theory (DFT) has been successfully used to study olefin polymerisation with simple cationic nickel-diimine complexes.⁷⁰⁻⁷⁷ Recently, Tomita *et al.* have suggested that σ -donation of ethylene participates in the coordinate nickel bond to a greater extent than π -back donation.⁷⁷ Furthermore, the σ -donating ability of incoming ethylene is related to the influence of the ligand coordinated to the metal *trans* to the incoming ethylene; the *trans* influence. In addition, they suggest that the energy of the lone pair on the ligand affects its *trans* influence; the greater the energy of the lone pair orbital, the more electron donating the ligand is to the metal centre. Electron donation from the ligand suppresses electron donation from ethylene to the metal centre, creating a weak metal-ethylene coordinate bond. Tomita *et al.* further suggested that the agostic interaction formed through charge transfer (Scheme 1.1) from the C—H bonding orbital to the empty *d*-orbital of the metal is also affected. The increased electron density on the metal centre suppresses charge transfer and leads to a weak agostic interaction between ethylene and nickel.

DFT calculations as described in section 2.2 were performed to examine orbital energies of NCCN and NPCN-based ligands. The HOMO-1 and the HOMO-2 correspond to the lone pair of the imine and phosphinimine fragments, as shown in Figures 2.6a and 2.6b, respectively. Results in Table 2.4 indicate that the lone pair

Figures 2.6a and 2.6b, respectively. Results in Table 2.4 indicate that the lone pair energies are highest in the NPCN ligand. This suggests that the presence of a phosphorus atom in NPCN not only increases the lone pair energy of the phosphinimine fragment (P=N), but also that of the imine fragment (C=N). Therefore, both isomers of the cationic nickel methyl NPCN complex are expected to have a weak metal-ethylene coordinate bond. This weak interaction might result in olefin oligomerisation rather than the preferred polymerisation of ethylene. The lone pair energy of the diimine ligand is slightly misleading, since this ligand has a symmetrical nature, leading to a bonding (Figure 2.7a) and antibonding (Figure 2.7b) combination of lone pair energies. It is also apparent that there is a noticeable decrease in lone pair energy when electron-withdrawing fluorine atoms are substituted on the phosphorus atom. This suggests that the presence of such groups on phosphorus should allow a stronger metal-ethylene coordinate bond in both $[\text{NiCH}_3(\text{NPCN})]^+$ isomers.

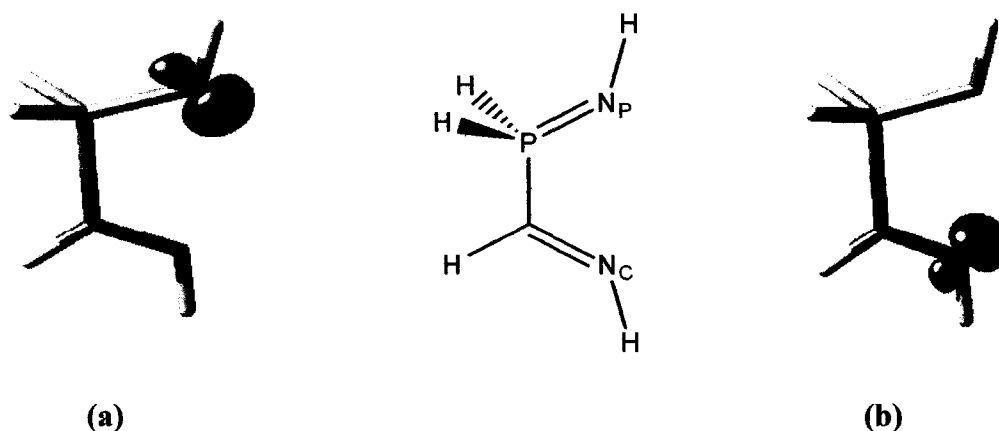
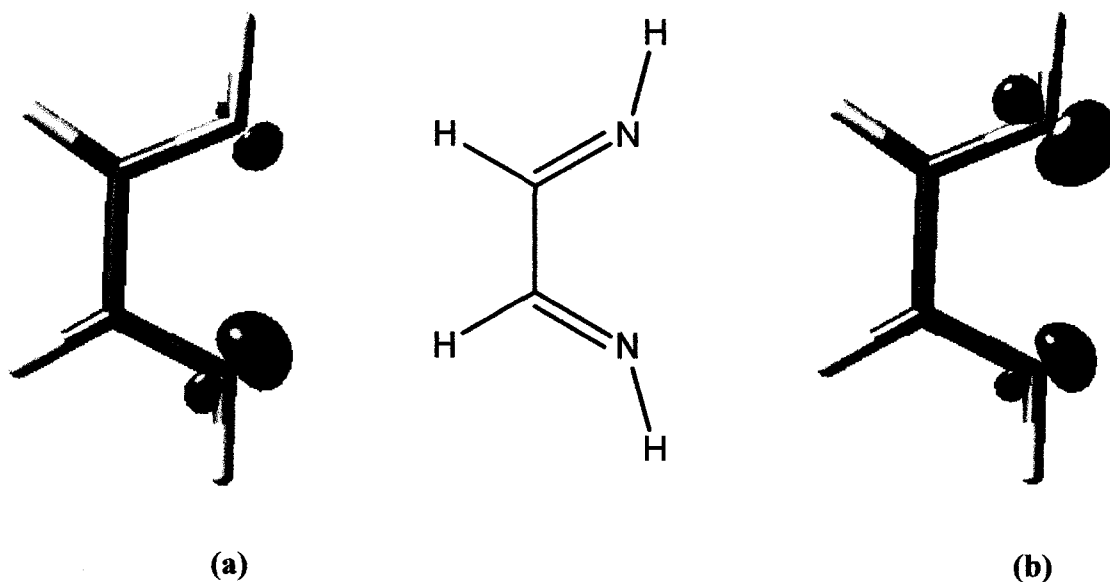


Figure 2.6 Illustration of the lone pairs on (a) P=N, and (b) C=N fragments in the NPCN ligand.

Table 2.4 The lone pair energies and nickel atomic charge of ligands and cationic metal complexes.

	NCCN	NPCN	NPF ₂ CN
E_{HOMO}	-10.5		
$E_{\text{lone pair (N}_C\text{)}}$ (HOMO-2)	-11.6 ^c -11.3 ^d	-11.5	-12.5
$E_{\text{lone pair (N}_P\text{)}}$ (HOMO-1)		-9.2	-11.2
Symmetry of [NiCH ₃ (ligand)] ⁺	C _s	C ₁	C ₁
[NiCH ₃ (ligand)] ⁺ ^b	0.858	0.832 ^e 0.816 ^f	0.856 ^e 0.861 ^f

^aEnergies measured in eV. ^bNBO charge of nickel. ^cAntibonding combination of lone pairs. ^dBonding combination of lone pairs. ^eNBO of nickel with CN *cis* to Ni—CH₃ bond. ^fNBO of Ni with PN *cis* to Ni—CH₃ bond.

**Figure 2.7** Illustration of the (a) bonding and (b) antibonding combinations of lone pairs on the NCCN ligand.

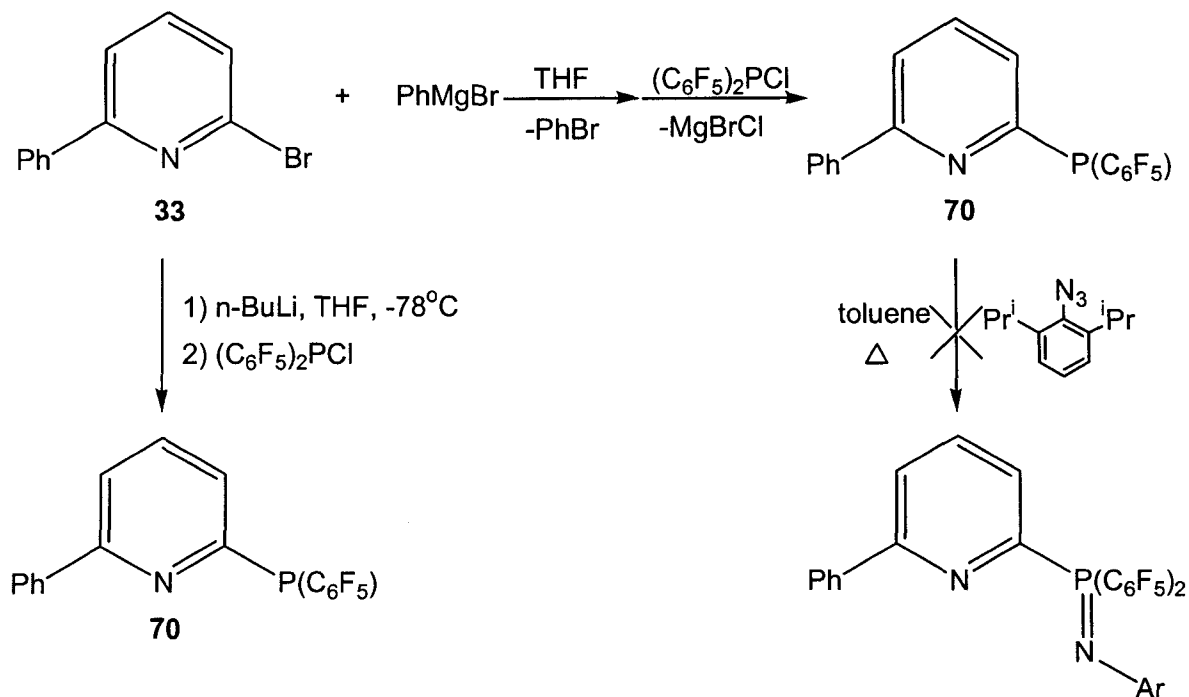
NBO analysis of $[\text{NiCH}_3(\text{ligand})]^+$ showed that NPCN-metal complex had the lowest positive charge on the nickel atom (Table 2.4). Since the lone pair energy orbital is highest in the NPCN case, this ligand is the most electron donating and increases electron density on the nickel atom. Thus, the metal centre becomes less electrophilic, suppressing σ -donation from the incoming ethylene resulting in a weak ethylene-metal interaction. Furthermore, this prevents charge transfer from the C—H bonding orbital to the empty d -orbital, leading to a weaker agostic interaction between nickel and one of the protons on the ethylene. Substitution of highly electronegative fluorine atoms on the phosphorus atom appears to make the NPCN ligand behave more like the NCCN ligand. Fluorine atoms remove electron density from the phosphinimine and imine fragments, and increase the positive charge on nickel. This should allow a stronger interaction between the incoming ethylene and nickel.

Comparison of calculations with polymerisation results obtained above suggests phosphinimine-based ligands may be poor olefin polymerisation catalysts. However, the catalytic potential for such ligands may be improved if electron-withdrawing substituents are present on the phosphorus atom.

Attempted Synthesis of Fluorinated Pyridyl-phosphinimine Ligands

In light of the above computational results, the synthesis of fluorinated phosphine ligands was attempted. Bis(pentafluorophenyl)chlorophosphine **27** offers the desired electronic characteristics and has been prepared by several different methods.^{56,78} Initial attempts to synthesize the corresponding pyridyl-phosphine from the lithiated 6-phenyl-pyridyl species suffered from very low yields, possibly due to *ortho*-metallation of the

phenyl ring. As an alternative, the Grignard analog was prepared by the reaction of **33** with PhMgBr (Scheme 2.6). This reagent could then be reacted with **27** to form the desired phosphine **70**.



Scheme 2.6 Attempted synthesis of a fluorinated-phosphinimine ligand utilizing **70**.

Attempts to oxidize the fluorinated pyridyl-phosphinimine ligand were unsuccessful, even at elevated temperatures. Earlier reports suggested similar difficulties with pyrrolyl and indolyl-phosphine oxidation,⁷⁹ and it is believed that in this case, oxidation cannot occur as a result of the weakly basic nature of the electron deficient phosphorus atom. Further experiments with different electron-withdrawing groups may allow oxidation and aid in the progress towards effective LTM phosphinimine olefin polymerisation catalysts.

2.4 Summary and Conclusions

A synthetic methodology for the preparation of group VIII and X pyridyl-phosphinimine complexes has been developed. Activation of several of these complexes with DEAC results in moderate activity for the oligomerisation of ethylene rather than polymerisation. Computational calculations on model systems of the active nickel(II) species suggest that the phosphinimine ligand creates a greater negative charge on the metal centre than a diimine ligand, which translates into a weakened ethylene-metal interaction. Removing the negative charge can be accomplished by the substitution of electron-withdrawing groups on the phosphorus atom; however, successful application is awaiting discovery.

Chapter Three

Syntheses of Selected Group VI and VIII-X Imidazolyl and Imidazolate-Phosphinimine Complexes

3.1 Introduction

In the search for novel LTM polymerisation catalysts, our research has led us to examine imidazole-based phosphinimine metal complexes. This class of ligand may be manipulated to possess a steric environment similar to successful diimine-based catalysts, but with different electronic properties. In contrast to the analogous pyridyl-compounds, imidazoles may be manipulated to possess either anionic or neutral character. In light of results from the previous chapter, group VI, VIII and X imidazolyl- or imidazolate-phosphinimine complexes, in the presence or absence of a cocatalyst, may have the catalytic potential to polymerise or oligomerise ethylene.

In this chapter, we examine the synthesis of both imidazolyl- and imidazolate-phosphinimine ligands and their metal complexes with several first- and second-row group VI, VIII, IX, and X transition metals. Iron(II) and nickel(II) metal complexes with the neutral imidazolyl ligand are evaluated for their potential to polymerise and oligomerise ethylene, in addition to chromium(III) and nickel(II) phosphinimine-imidazolate complexes.

3.2 Experimental section

General Data All preparations ^1H , $^{13}\text{C}\{^1\text{H}\}$, $^{31}\text{P}\{^1\text{H}\}$, IR spectroscopy, EA, GC analysis, and magnetic susceptibility measurements were carried out under conditions similar to

those described in Section 2.2. 1-H-2-(Diphenylphosphino)imidazole **71**,⁸⁰ 1-methyl-2-(diphenylphosphino)-4-*tert*-butylimidazole **72**,^{81,82} and $[(\eta^3\text{-C}_3\text{H}_5)\text{NiBr}]_2$ ⁸³ were prepared according to literature techniques.

Synthesis of 1-methyl-2-(diphenylphosphino)imidazole [1-Me-2-PPh₂]imid **73, [1-Me-4,5-Ph₂-2-PPh₂]imidazole **74**, [1-Me-2-PPh₂]benzimidazole **75**** Compounds **73** to **75** were prepared by similar methods, thus only one representative procedure is described. To a cooled (-78°C) THF (50 mL) solution of 1-methyl-2-diphenylphosphinoimidazole (5.0 g, 60.9 mmol) was added dropwise 26.8 mL of n-BuLi (2.5 M in hexanes). The solution was stirred at reduced temperature for 1 hour and 12.0 mL (67.1 mmol) of Ph₂PCl was added dropwise. The solution was gradually warmed to room temperature and stirred overnight. The solvent was removed *in vacuo* and diethyl ether was added (75 mL) along with water (50 mL). The organic layer was collected and the aqueous layer washed with ether (30 mL). The ether layer was dried with anhydrous MgSO₄, filtered, and the solvent removed to give a white solid. The product was recrystallized with CH₂Cl₂/hexane to give a microcrystalline solid (90% yield). **73**: ³¹P{¹H} NMR (CDCl₃, 25°C, δ): -30.0(s). ¹H NMR (CDCl₃, 25°C, δ): 3.75 (s, 3H, -NCH₃), 7.05 (m, 1H, -imidH), 7.27 (d, 1.2 Hz, 1H, -imidH), 7.27-7.37 (m, 6H, -*meta*PPh₂, -*para*PPh₂), 7.43-7.49 (m, 4H, -*ortho*PPh₂). ¹³C{¹H} NMR (CDCl₃, 25°C, δ): 34.2 (d, J_{C-P} 13.5 Hz), 123.8, 128.8 (d, J_{C-P} 7.6 Hz), 129.3, 131.1, 134.1 (d, J_{C-P} 20.3 Hz), 135.0 (d, J_{C-P} 3.8 Hz), 146.0.

74: 85% yield, white microcrystalline solid. ³¹P{¹H} NMR (CDCl₃, 25°C, δ): -29.5 (s). ¹H NMR (CDCl₃, 25°C, δ): 3.55 (s, 3H, -CH₃), 7.13 (m, 1H, -imidH), 7.19 (m, 2H, -

ArH), 7.35-7.40 (m, 8H, *-metaPPh₂*, *paraPPh₂*, *-ArH*), 7.45-7.47 (m, 3H, ArH, *-imidH*), 7.51 (m, 2H, *-ArH*), 7.67-7.70 (m, 4H, *-orthoPPh₂*). $^{13}\text{C}\{^1\text{H}\}$ NMR (CDCl_3 , 25°C, δ): 32.5 (d, $J_{\text{C-P}}$ 14.9 Hz), 126.2, 126.7, 128.0, 128.4 (d, $J_{\text{C-P}}$ 7.6 Hz), 128.6, 128.9, 129.0, 130.8, 131.3, 132.1, 134.0 (d, $J_{\text{C-P}}$ 20.4 Hz), 134.9, 135.5 (d, $J_{\text{C-P}}$ 4.6 Hz), 139.8, 145.0.

75: 86% yield, white powder. $^{31}\text{P}\{^1\text{H}\}$ NMR (CDCl_3 , 25°C, δ): -24.9 (s). ^1H NMR (CDCl_3 , 25°C, δ): 3.83 (s, 3H, *-CH₃*), 7.27 (m, 2H, *-benzimidH*), 7.32 (m, 1H, *-benzimidH*), 7.36-7.38 (m, 7H, *-metaPPh₂*, *-paraPPh₂*, *-benzimidH*), 7.51-7.54 (m, 4H, *-orthoPPh₂*), 7.83 (d, 1H, *-benzimidH*). $^{13}\text{C}\{^1\text{H}\}$ NMR (CDCl_3 , 25°C, δ): 31.3 (d, $J_{\text{C-P}}$ 13.6 Hz), 109.4, 120.7, 122.2, 123.2, 129.0 (d, $J_{\text{C-P}}$ 7.8 Hz), 129.7, 133.9 (d, $J_{\text{C-P}}$ 4.5 Hz), 134.3 (d, $J_{\text{C-P}}$ 20.4 Hz), 137.2, 144.4 (d, $J_{\text{C-P}}$ 6.9 Hz), 154.3 (d, $^2J_{\text{C-P}}$ 3.4 Hz).

Synthesis of [1-Me-2-PPh₂N-2,6-Me₂C₆H₃]imid 76, [1-Me-2-PPh₂N-2,6-ⁱPrC₆H₃]imid 77, [1-Me-4,5-Ph₂-2-PPh₂N-2,6-Me₂C₆H₃]imid 78, [1-Me-4,5-Ph₂-2-PPh₂N-2,6-ⁱPrC₆H₃]imid 79, [1-Me-2-PPh₂N-2,6-Me₂C₆H₃]benzimid 80, [1-Me-2-PPh₂N-2,6-ⁱPrC₆H₃]benzimid 81, [1-Me-4-^tBu-2-PPh₂N-2,6-ⁱPrC₆H₃]imid 82 Compounds 76 to 82 were prepared by similar methods thus only one representative procedure is described. To a THF solution (50 mL) of 1-methyl-2-(diphenylphosphino)imidazole (1.50 g, 5.6 mmol) was added 1.7 g (10.2 mmol) of 2,6-dimethylphenyl azide. The solution was heated at 60°C overnight, and the solvent was removed to give a brown oil. Petroleum ether was added and the mixture was stirred and stored at -30°C overnight. Filtration gave a 2.0 g (93%) of a cream-colored solid, $\nu_{\text{P=N}}$ 1352 cm^{-1} . **76:** $^{31}\text{P}\{^1\text{H}\}$ NMR (CDCl_3 , 25°C, δ): -16.0 (s). ^1H NMR (CDCl_3 , 25°C, δ): 1.96 (s, 6H, *-CH₃*), 3.68 (s, 3H, *-NCH₃*), 6.67 (dt, 7.5, 2.1 Hz, 1H, *-NArH*), 6.90 (d, 7.2 Hz, 2H, *-NArH*), 7.05 (m, 1H, *-imidH*),

7.23 (m, 1H, -imidH), 7.41-7.47 (m, 4H, -metaPPh₂), 7.53 (dt, 5.7, 1.8 Hz, 2H, -paraPPh₂), 7.69-7.77 (m, 4H, -orthoPPh₂). ¹³C{¹H} NMR (CDCl₃, 25°C, δ): 18.2, 34.9, 119.6, 125.3, 127.5 (d, J_{C-P} 11.9 Hz), 127.9, 128.7 (d, J_{C-P} 12.8 Hz), 130.0 (d, J_{C-P} 14.9 Hz), 131.9, 132.2 (d, J_{C-P} 9.9 Hz), 132.7, 143.0 (J_{C-P} 128.0 Hz), 145.8.

77: Yield = 95%, cream-colored solid, ν_{P=N} 1358 cm⁻¹. ³¹P{¹H} NMR (CDCl₃, 25°C, δ): -16.3 (s). ¹H NMR (CDCl₃, 25°C, δ): 0.88 (d, 6.9 Hz, 12H, -CH(CH₃)₂), 3.22 (sept, 6.8 Hz, 2H, -CH(CH₃)₂), 3.67 (s, 3H, -CH₃), 6.85 (m, 1H, -NArH), 6.96 (m, 2H, -NArH), 7.04 (s, 1H, -imidH), 7.21 (s, 1H, -imidH), 7.42-7.46 (m, 4H, -metaPPh₂), 7.52 (m, 2H, -paraPPh₂), 7.66-7.70 (m, 4H, -orthoPPh₂). ¹³C{¹H} NMR (CDCl₃, 25°C, δ): 23.0, 27.5, 34.9, 119.0, 124.9, 127.5 (d, J_{C-P} 11.9 Hz), 127.9, 128.9 (d, J_{C-P} 12.7 Hz), 130.9 (d, J_{C-P} 15.5 Hz), 131.0, 132.0 (d, J_{C-P} 9.9 Hz), 132.0, 144.0 (J_{C-P} 128.9 Hz), 146.2.

78: Yield = 92%, slightly yellow solid, ν_{P=N} 1361 cm⁻¹. ³¹P{¹H} NMR (CDCl₃, 25°C, δ): -16.6 (s). ¹H NMR (CDCl₃, 25°C, δ): 2.03 (s, 6H, -CH₃), 3.46 (s, 3H, -NCH₃), 6.92 (m, 1H, -NArH), 6.93 (d, 7.2 Hz, 2H, -NArH), 7.15-7.18 (m, 3H, -ArH), 7.31-7.34 (m, 2H, -ArH), 7.46-7.55 (m, 11H, -metaPPh₂, -paraPPh₂, -ArH), 7.89-7.95 (m, 4H, -orthoPPh₂). ¹³C{¹H} NMR (CDCl₃, 25°C, δ): 20.2, 33.0, 119.1, 126.7, 127.9, 128.2 (d, ²J_{C-P} 12.8 Hz), 128.5, 129.1, 129.2, 130.3, 130.8, 131.7, 132.4 (d, J_{C-P} 9.9 Hz), 132.6, 134.3, 138.7 (d, J_{C-P} 13.7 Hz), 142.5 (d, J_{C-P} 127.7 Hz), 146.5 (some quaternary carbons not observed).

79: Yield = 91%, cream-colored solid, ν_{P=N} 1372 cm⁻¹. ³¹P{¹H} NMR (CDCl₃, 25°C, δ): -16.3 (s). ¹H NMR (CDCl₃, 25°C, δ): 0.94 (d, 6.9 Hz, 12H, -CH(CH₃)₂), 3.32 (sept, 6.9 Hz, 2H, -CH(CH₃)₂), 3.44 (s, 3H, -CH₃), 6.82 (dt, 6.9 Hz, 2.1 Hz, 1H, -NArH), 6.97 (m, 2H, -NArH), 7.13-7.27 (m, 3H, -ArH), 7.30-7.33 (m, 2H, -ArH), 7.42-7.58 (m, 11H, -metaPPh₂, -paraPPh₂, -ArH), 7.82-7.90 (m, 4H, -orthoPPh₂). ¹³C{¹H} NMR (CDCl₃,

25°C, δ): 23.7, 28.5, 32.8, 119.5, 122.7, 126.5, 126.8, 128.2 (d, J_{C-P} 11.2 Hz), 128.4, 130.4 (d, J_{C-P} 8.7 Hz), 130.6, 131.5, 132.0, 132.4 (d, J_{C-P} 9.8 Hz), 133.1, 134.4, 138.7 (d, J_{C-P} 13.9 Hz), 141.7, 142.7 (d, J_{C-P} 7.9 Hz), 142.9 (d, J_{C-P} 115.2 Hz), 143.3 (d, J_{C-P} 13.4 Hz) (some quaternary carbons are not observed).

80: Yield = 88%, beige solid, $\nu_{P=N}$ 1362 cm^{-1} . $^{31}\text{P}\{^1\text{H}\}$ NMR (d_8 -THF, 25°C, δ): -19.0 (s) ^1H NMR (CDCl_3 , 25°C, δ): 1.95 (s, 6H, $-\text{CH}_3$), 3.83 (s, 3H, $-\text{NCH}_3$), 6.49 (dt, 7.5, 1.5 Hz, 1H, $-\text{NArH}$), 6.77 (d, 7.5 Hz, 2H, $-\text{NArH}$), 7.24-7.32 (m, 2H, $-\text{benzimidH}$), 7.41-7.52 (m, 7H, $-\text{metaPPh}_2$, $-\text{paraPPh}_2$, $-\text{benzimidH}$), 7.32 (d, 7.8 Hz, 1H, $-\text{benzimidH}$), 7.86-7.93 (m, 4H, $-\text{orthoPPh}_2$). $^{13}\text{C}\{^1\text{H}\}$ NMR (CDCl_3 , 25°C, δ): 21.1, 25.8, 32.1, 111.1, 119.6, 122.0, 123.5, 125.1, 128.7, 129.3 (d, J_{C-P} 12.8 Hz), 132.5, 132.6, 133.2 (d, J_{C-P} 10.0 Hz), 134.2, 138.1 (d, J_{C-P} 3.1 Hz), 144.2 (d, J_{C-P} 16.1 Hz), 147.5, 150.5 (d, J_{C-P} 121.6 Hz).

81: Yield = 92%, cream-colored solid, $\nu_{P=N}$ 1370 cm^{-1} . $^{31}\text{P}\{^1\text{H}\}$ NMR (CDCl_3 , 25°C, δ): -15.5 (s) ^1H NMR (CDCl_3 , 25°C, δ): 0.83 (d, 12 H, 6.9 Hz, $-(\text{CH}(\text{CH}_3)_2)_2$), 3.23 (sept, 2H, 6.9 Hz, $-(\text{CH}(\text{CH}_3)_2)_2$), 3.84 (s, 3H, $-\text{NCH}_3$), 6.80-6.86 (m, 1H, $-\text{NArH}$), 6.95 (d, 2H, $-\text{NArH}$), 7.25-7.35 (m, 1H, $-\text{benzimidH}$), 7.40 (m, 2H, $-\text{benzimidH}$), 7.44-7.50 (m, 4H, $-\text{metaPPh}_2$), 7.53-7.58 (m, 2H, $-\text{paraPPh}_2$), 7.73-7.80 (m, 4H, $-\text{orthoPPh}_2$), 7.86 (m, 1H, $-\text{benzimidH}$). $^{13}\text{C}\{^1\text{H}\}$ NMR (CDCl_3 , 25°C, δ): 23.6, 28.7, 31.6, 109.6, 119.8, 121.6, 122.7, 124.4, 128.6 (d, J_{C-P} 12.9 Hz), 130.6 (d, J_{C-P} 111.5 Hz), 132.3 (d, J_{C-P} 9.9 Hz), 133.1, 133.9, 137.0, 142.6 (d, J_{C-P} 7.4 Hz), 142.8, 143.4 (d, J_{C-P} 17.5 Hz), 150.7 (d, J_{C-P} 121.0 Hz).

82: Yield = 90%, yellow solid, $\nu_{P=N}$ 1377 cm^{-1} . $^{31}\text{P}\{^1\text{H}\}$ NMR (CDCl_3 , 25°C, δ): -18.8 (s) ^1H NMR (CDCl_3 , 25°C, δ): 0.85 (d, 12H, 6.9 Hz, $-(\text{CH}(\text{CH}_3)_2)_2$), 1.21 (s, 9H, $-(\text{CH}_3)_3$), 3.25 (sept, 2H, $-(\text{CH}(\text{CH}_3)_2)_2$), 3.36 (s, 3H, $-\text{NCH}_3$), 6.65 (s, 1H, $-\text{imidH}$), 6.80 (m, 1H, -

NArH), 6.92 (m, 2H, -NArH), 7.37-7.40 (m, 4H, -*meta*PPh₂), 7.44 (m, 2H, -*para*PPh₂), 7.76-7.80 (m, 4H, -*ortho*PPh₂). ¹³C{¹H} NMR (CDCl₃, 25°C, δ): 22.6, 28.7, 30.2, 31.9, 34.1, 118.7, 119.1, 122.6, 128.1 (d, J_{C-P} 12.5 Hz), 131.1, 132.3 (d, J_{C-P} 9.6 Hz), 132.5 (d, J_{C-P} 112.6 Hz) 141.5 (d, J_{C-P} 131.3 Hz), 142.6 (d, J_{C-P} 8.4 Hz), 143.6, 152.9 (d, J_{C-P} 14.1 Hz).

Synthesis of [1-Me-2-PPh₂N-2,6-¹Pr₂C₆H₃]imidPdCl₂-CH₃CN 83 To a stirred solution of PdCl₂(PhCN)₂ (44 mg, 0.11 mmol) in toluene was added a toluene solution (5 mL) of **77** (50 mg, 0.11 mmol). The red solution was stirred for 2 hours, and an orange precipitate gradually formed. After 2 hours, the solution was cooled to -30°C, filtered and the solid washed with cold toluene several times. The orange solid was recrystallized by dissolving in CH₃CN and cooling to -30°C to give orange crystals. ³¹P{¹H} NMR (d₆-DMSO, 25°C, δ): 28.2 (s). ¹H NMR (d₆-DMSO, 25°C, δ): 0.27 (d, 6.9 Hz, 6H, -CH(CH₃)₂), 1.32 (d, 6.9 Hz, 6H, -CH(CH₃)₂), 3.30 (s, 3H, -NCH₃), 3.32 (sept, 6.6 Hz, 2H, -CH(CH₃)₂), 6.76 (d, 7.5 Hz, 2H, -NArH), 6.96 (dt, 8.1 Hz, 2.1 Hz, 1H, -NArH), 7.65-7.72 (m, 8H, -*meta*PPh₂, -*para*PPh₂, -imidH), 7.77-7.82 (m, 4H, -*ortho*PPh₂). ¹³C{¹H} NMR (d₆-DMSO, 25°C, δ): 22.5, 25.1, 28.3, 35.8, 122.0, 123.1, 123.3, 125.3, 128.6, 129.9 (d, J_{C-P} 14.6 Hz), 132.5 (d, J_{C-P} 10.3 Hz), 134.5, 137.2, 140.0 (d, J_{C-P} 164.5 Hz), 147.2 (d, J_{C-P} 5.3 Hz). Anal. Calcd. for C₃₀H₃₅Cl₂N₄PPd (659.93): C, 54.60; H, 5.35; N, 8.49. Found: C, 54.13; H, 5.29; N, 8.39.

Synthesis of [1-Me-2-PPh₂N-2,6-Me₂C₆H₃]imidNiBr₂ **84**, [1-Me-2-PPh₂N-2,6-ⁱPr₂C₆H₃]imidNiBr₂ **85**, [1-Me-2-PPh₂N-2,6-Me₂C₆H₃]benzimidNiBr₂ **86**, [1-Me-2-PPh₂N-2,6-ⁱPr₂C₆H₃]benzimidNiBr₂ **87**, [1-Me-4,5-Ph₂-2-PPh₂N-2,6-Me₂C₆H₃]imidNiBr₂ **88**, [1-Me-4,5-Ph₂-2-PPh₂N-2,6-ⁱPr₂C₆H₃]imidNiBr₂ **89**, [1-Me-4-^tBu-2-PPh₂N-2,6-ⁱPr₂C₆H₃]imidNiBr₂ **90** Compounds **84** to **90** were prepared by similar methods, thus only one representative procedure is described. To a slight excess of **75** (1.05 eq., 150 mg, 0.39 mmol) and NiBr₂(DME) adduct (114 mg, 0.37 mmol) was added 10 mL CH₂Cl₂. The blue suspension was stirred overnight, and concentrated to several mL's *in vacuo*. Diethyl ether (10 mL) was added and the mixture was filtered to give a light blue powder. **84**: Yield = 95%, purple powder, $\nu_{P=N}$ 1225 cm⁻¹, μ_{eff} 3.01. Anal. Calcd. for C₂₄H₂₄Br₂N₃NiP (603.94): C, 47.73; H, 4.01; N, 6.96. Found: C, 47.68; H, 4.00; N, 6.82.

85-CH₂Cl₂: Yield = 90%, blue-green powder, $\nu_{P=N}$ 1214 cm⁻¹, μ_{eff} 2.94. Anal. Calcd. for C₂₉H₃₄Br₂Cl₂N₃NiP (744.98): C, 46.75; H, 4.60; N, 5.64. Found: C, 46.47; H, 4.44; N, 6.07.

86-CH₂Cl₂: Yield = 86%, purple powder, $\nu_{P=N}$ 1219 cm⁻¹, μ_{eff} 3.41. Anal. Calcd. for C₂₉H₂₈Br₂Cl₂N₃NiP (738.93): C, 47.14; H, 3.82; N, 5.69. Found: C, 47.42; H, 3.66; N, 5.84.

87: Yield = 87%, blue-green powder, $\nu_{P=N}$ 1243 cm⁻¹, μ_{eff} 3.24. Anal. Calcd. for C₃₂H₃₂Br₂N₃NiP (708.09): C, 54.28; H, 4.56; N, 5.93. Found: C, 54.57; H, 4.10; N, 5.81.

88: Yield = 90%, purple powder, $\nu_{P=N}$ 1217 cm⁻¹, μ_{eff} 2.99. Anal. Calcd. for C₃₆H₃₂Br₂N₃NiP (756.13): C, 57.18; H, 4.27; N, 5.56. Found: C, 56.83; H, 4.47; N, 5.33.

89: Yield = 87%, blue-green powder, $\nu_{\text{P=N}}$ 1196 cm^{-1} , μ_{eff} 3.15. Anal. Calcd for $\text{C}_{40}\text{H}_{40}\text{Br}_2\text{N}_3\text{NiP}$ (812.24): C, 59.15; H, 4.96; N, 5.17. Found: C, 59.41; H, 5.13; N, 5.01.

90: Yield = 91%, blue-green powder, $\nu_{\text{P=N}}$ 1244 cm^{-1} , μ_{eff} 3.07. Anal. Calcd for $\text{C}_{32}\text{H}_{40}\text{Br}_2\text{N}_3\text{NiP}$ (716.16): C, 53.67; H, 5.63; N, 5.87. Found: C, 53.14; H, 5.44; N, 5.83.

Synthesis of [1-Me-2-PPh₂N-2,6-Me₂C₆H₃]imidFeCl₂ 91, [1-Me-2-PPh₂N-2,6-ⁱPr₂C₆H₃]imidFeCl₂ 92, [1-Me-2-PPh₂N-2,6-Me₂C₆H₃]benzimidFeCl₂ 93, [1-Me-2-PPh₂N-2,6-ⁱPr₂C₆H₃]benzimidFeCl₂ 94, [1-Me-4,5-Ph₂-2-PPh₂N-2,6-Me₂C₆H₃]imidFeCl₂ 95, [1-Me-4,5-Ph₂-2-PPh₂N-2,6-ⁱPr₂C₆H₃]imidFeCl₂ 96, [1-Me-4-^tBu-2-PPh₂N-2,6-ⁱPr₂C₆H₃]imidFeCl₂ 97 Compounds 91 to 97 were prepared by similar

methods, thus only one representative procedure is described. To a slight excess of **76** (1.05 eq, 150 mg, 0.39 mmol) and FeCl₂ (47 mg, 0.37 mmol) was added 10 mL THF. The orange suspension was stirred overnight, and concentrated to several mL's *in vacuo*. Diethyl ether (10 mL) was added and the mixture was filtered to give an orange powder.

91: Yield = 88%, orange solid, $\nu_{\text{P=N}}$ 1211 cm^{-1} , μ_{eff} 4.98. Anal. Calcd. for $\text{C}_{24}\text{H}_{24}\text{Cl}_2\text{N}_3\text{FeP}$ (512.19): C, 56.28; H, 4.72; N, 8.20. Found: C, 55.97; H, 4.80; N, 7.86.

92: Yield = 95%, yellow-orange solid, $\nu_{\text{P=N}}$ 1198 cm^{-1} , μ_{eff} 5.10. Anal. Calcd. for $\text{C}_{28}\text{H}_{32}\text{Cl}_2\text{N}_3\text{FeP}$ (568.30): C, 59.18; H, 5.68; N, 7.39. Found: C, 58.89; H, 6.00; N, 7.43.

93: Yield = 89%, orange solid, $\nu_{\text{P=N}}$ 1215 cm^{-1} , μ_{eff} 5.24. Anal. Calcd. for $\text{C}_{28}\text{H}_{26}\text{Cl}_2\text{N}_3\text{FeP}$ (562.25): C, 59.81; H, 4.66; N, 7.47. Found: C, 59.65; H, 5.06; N, 7.77.

94: Yield = 92%, yellow-orange solid, $\nu_{\text{P=N}}$ 1191 cm^{-1} , μ_{eff} 5.21. Anal. Calcd. for $\text{C}_{32}\text{H}_{34}\text{Cl}_2\text{N}_3\text{FeP}$ (618.36): C, 62.16; H, 5.54; N, 6.80. Found: C, 61.78; H, 5.85; N, 7.11.

95: Yield = 84%, yellow crystals, $\nu_{\text{P=N}}$ 1217 cm^{-1} , μ_{eff} 5.01. Anal. Calcd for $\text{C}_{36}\text{H}_{32}\text{Cl}_2\text{N}_3\text{FeP}$ (664.38): C, 65.08; H, 4.85; N, 6.32. Found: C, 64.91; H, 4.52; N, 5.82.

96-2CH₂Cl₂: Yield = 85%, yellow crystals, $\nu_{\text{P=N}}$ 1120 cm^{-1} , μ_{eff} 4.99. Anal. Calcd. for $\text{C}_{42}\text{H}_{44}\text{Cl}_6\text{FeN}_3\text{P}$ (890.35): C, 56.66; H, 4.98; N, 4.72. Found: C, 56.55; H, 4.64; N, 4.93.

97: Yield = 80%, yellow crystals, $\nu_{\text{P=N}}$ 1193 cm^{-1} , μ_{eff} 5.12. Anal. Calcd for $\text{C}_{32}\text{H}_{40}\text{Cl}_2\text{N}_3\text{FeP}$ (624.40): C, 61.55; H, 6.46; N, 6.73. Found: C, 61.15; H, 6.38; N, 6.88.

Synthesis of [1-H-2-PPh₂N-2,6-Me₂C₆H₃]imid **98**

To a stirred THF (20 mL) solution of **71** (1.01 g, 4.0 mmol) was added a THF solution of 2,6-dimethylphenylazide (1.2 g, 8.0 mmol) over a period of 30 minutes at room temperature. Gas evolution was noted during the addition of the azide. The yellow solution was then stirred overnight, and the solvent removed *in vacuo*. The residue was dissolved in several mL's of THF and petroleum ether added (bp. 30-60°C) to precipitate a creamy white solid. The solid was filtered and washed with petroleum ether several times to give a white solid (95%). ³¹P NMR (*d*₈-THF, 25°C, δ): -21.4 (s) ¹H NMR (*d*₈-THF, 25°C, δ): 1.97 (s, 6H, -CH₃), 6.48 (m, 1H, -NArH), 6.78 (d, 7.2 Hz, 2H, -NArH), 7.25 (m, 2H, -imidH), 7.34-7.46 (m, 6H, -*meta*PPh₂, -*para*PPh₂), 7.84-7.91 (m, 4H, -*ortho*PPh₂). ¹³C{H} NMR (*d*₈-THF, 25°C, δ): 18.5, 116.2, 122.8, 125.6, 125.8 (d, J_{C-P} 2.7 Hz), 126.0 (d, J_{C-P} 12.5 Hz), 129.1, 129.9 (d, J_{C-P} 9.9 Hz), 130.0 (d, J_{C-P} 7.8 Hz), 132.0 (d, J_{C-P} 88.7 Hz), 140.0 (d, J_{C-P} 155.0 Hz), 144.9.

Synthesis of Na[2-PPh₂N-2,6-Me₂C₆H₃]imid·THF 99

To a stirred suspension of NaH (24 mg, 0.96 mmol) in THF (10 mL) was added dropwise a THF solution (10 mL) of **98** (300 mg, 0.81 mmol). Gas evolution occurred immediately and the suspension was stirred overnight. The solution was filtered through Celite and the solvent removed *in vacuo* to give a white solid. This was recrystallized with THF/pentane to give colourless crystals (85%). ¹H NMR (*d*₈-THF, 25°C, δ): -4.7 (s) ¹H NMR (*d*₈-THF, 25°C, δ): 1.75 (m, 2H, -coord. THF), 1.93 (s, 6H, -CH₃), 3.61 (m, 2H, -coord. THF), 6.48 (m, 1H, -NArH), 6.74 (d, 7.5 Hz, 2H, -NArH), 7.15-7.37 (m, 6H, -*meta*PPh₂, -*para*PPh₂), 7.24-7.26 (m, 2H, -imidH), 7.68-7.56 (m, 4H, -*ortho*PPh₂). ¹³C{H} NMR (*d*₈-THF, 25°C, δ): 21.4, 26.6, 68.4, 117.3, 119.4 (d, J_{C-P} 3.0 Hz), 128.1 (d, J_{C-P} 11.2 Hz), 128.3 (d, J_{C-P} 2.1 Hz), 130.6, 131.1 (d, J_{C-P} 16.6 Hz), 133.1 (d, ³J_{C-P} 9.1 Hz), 134.4 (d, J_{C-P} 7.4 Hz), 138.0 (d, J_{C-P} 89.6 Hz), 144.5 (d, J_{C-P} 187.2 Hz), 150.5.

Synthesis of [2-PPh₂N-2,6-Me₂C₆H₃]imidRhCp*Cl 100, [2-PPh₂N-2,6-Me₂C₆H₃]imidCrCp*Cl 101 Compounds **100** and **101** were prepared by similar methods, thus only one representative procedure is described. To a benzene (10 mL) solution of [Cp*RhCl₂]₂ (41 mg, 0.066 mmol) was added a benzene (5 mL) suspension of **99** (57 mg, 0.13 mmol). The suspension gradually dissolved giving a deep red solution, which was stirred overnight, filtered through Celite, and the solvent removed. Recrystallization with benzene/pentane gave deep red crystals (75%). **100**: ¹H NMR (CDCl₃, 25°C, δ): 13.1 (s) ¹H NMR (CDCl₃, 25°C, δ): 1.35 (s, 15H, -C₅Me₅), 1.95 (br s, 3H, -CH₃), 2.05 (br s, 3H, -CH₃), 6.98 (m, 3H, -NArH), 7.18-7.24 (m, 4H, -*meta*PPh₂), 7.33 (m, 2H, -*para*PPh₂), 7.61 (d, 1.5 Hz, 1H, -imidH), 7.67-7.74 (m, 4H, -*ortho*PPh₂),

7.77 (d, 3.0 Hz, 1H, -imidH). $^{13}\text{C}\{\text{H}\}$ NMR (CDCl_3 , 25°C, δ): 8.3, 20.8, 22.0, 92.6 (d, $J_{\text{Rh-C}}$ 13.7 Hz), 116.5, 117.5 (d, $J_{\text{C-P}}$ 3.5 Hz), 127.5 (d, $J_{\text{C-P}}$ 12.5 Hz), 128.0 (d, $J_{\text{C-P}}$ 2.5 Hz), 131.5, 132.3 (d, $J_{\text{C-P}}$ 15.5 Hz), 133.0 (d, $J_{\text{C-P}}$ 8.5 Hz), 134.0 (d, $J_{\text{C-P}}$ 7.2 Hz), 137.5 (d, $J_{\text{C-P}}$ 89.0 Hz), 146.4 (d, $J_{\text{C-P}}$ 156.0 Hz), 151.4. Anal. Calcd. For $\text{C}_{33}\text{H}_{36}\text{ClN}_3\text{PRh}$ (644.0): C, 61.55; H, 5.63; N, 6.52. Found: C, 61.45; H, 5.75; N, 6.72.

101: Anal. Calcd. For $\text{C}_{33}\text{H}_{36}\text{ClCrN}_3\text{P}$ (644.0): C, 66.83; H, 6.12; N, 7.09. Found: C, 66.90; H, 6.14; N, 6.96.

Synthesis of [2-PPh₂N-2,6-Me₂C₆H₃]imidRhCOD 102

To a stirred benzene (10 mL) solution of [(COD)RhCl]₂ (67 mg, 0.14 mmol) was added a benzene (5 mL) suspension of **99** (126 mg, 0.28 mmol). The suspension was stirred overnight, filtered through Celite, and the solvent removed. Recrystallization with benzene/pentane gave a yellow solid. Suitable X-ray quality crystals were grown from a layered CH_2Cl_2 /pentane solution (95 %). $^{31}\text{P}\{\text{H}\}$ NMR (d_8 -THF, 25°C, δ): 17.9 (s). ^1H NMR (d_8 -THF, 25°C, δ): 1.73 (m, 2H, -CH₂CH), 1.89 (m, 2H, -CH₂CH), 2.25-2.40 (m, 4H, -(CH₂)₂CH), 3.65 (m, 2H, -CH=CH), 4.33 (m, 2H, -CH=CH), 6.80-6.90 (m, 4H, -NArH and -imidH), 7.25 (m, 1H, -imidH), 7.31-7.37 (m, 4H, -metaPPh₂), 7.46-7.54 (m, 2H, -paraPPh₂), 7.54-7.61 (m, 4H, -orthoPPh₂). $^{13}\text{C}\{\text{H}\}$ NMR (d_8 -THF, 25°C, δ): 14.5, 31.6 (d, $J_{\text{Rh-C}}$ 14.0 Hz), 74.5 (d, $J_{\text{Rh-C}}$, 14.0 Hz), 83.7 (d, $J_{\text{Rh-C}}$ 12.3 Hz), 124.5, 126.7 (d, $J_{\text{C-P}}$ 9.9 Hz), 129.2 (d, $J_{\text{C-P}}$ 11.9 Hz), 129.4, 130.5 (d, $J_{\text{C-P}}$ 131.6 Hz), 132.9, 133.4 (d, $J_{\text{C-P}}$ 9.5 Hz), 134.1 (d, $J_{\text{C-P}}$ 17.0 Hz), 137.5 (d, $J_{\text{C-P}}$ 5.2 Hz), 144.7, 145.0 (d, $J_{\text{C-P}}$ 195.8 Hz). Anal. Calcd. For $\text{C}_{31}\text{H}_{33}\text{N}_3\text{PRh}$ (581.5): C, 64.03; H, 5.72; N, 7.23. Found: C, 64.43; H, 5.61; N, 7.20.

Synthesis of [2-PPh₂N-2,6-Me₂C₆H₃]imidNi(allyl) 103

To 39 mg of $[(\eta^3\text{-C}_3\text{H}_5\text{NiBr})_2]$ (0.105 mmol) dissolved in 2 mL benzene was added a benzene suspension of **99** (100 mg, 0.21 mmol). The suspension was stirred overnight, filtered through Celite, and the solvent removed to give a brittle dark yellow foam. The foam was recrystallized with benzene/pentane to give a dull yellow solid (95 mg, 95% yield). ^{31}P NMR (C_6D_6 , 25°C, δ): 14.8 (s). ^1H NMR (C_6D_6 , 25°C, δ): 1.72 (d, 1H, 13.1 Hz, -NiCH_{anti}CH), 1.77 (d, 1H, 5.6 Hz, -NiCH_{syn}CH), 1.94 (s, 3H, -CH₃), 2.06 (d, 1H, 12.8 Hz, -NiCH_{anti}CH), 2.13 (s, 3H, -CH₃), 2.93 (d, 1H, 6.2 Hz, -NiCH_{syn}CH), 5.25 (m, 1H, -NiCH_{central}CH), 6.83-6.97 (m, 9H, -metaPPh₂, -paraPPh₂, -NArH), 7.29 (s, 1H, -imidH), 7.64-7.68 (dd, $^2J_{\text{P-H}}$ 12.0 Hz, $^3J_{\text{Ho-Hm}}$ 7.5 Hz, 2H, -orthoPPh₂), 7.80-7.84 (dd, $^2J_{\text{P-H}}$ 12.0 Hz, $^3J_{\text{Ho-Hm}}$ 7.5 Hz, 2H, -orthoPPh₂), 7.94 (d, 1H, 2.7 Hz, -imidH). $^{13}\text{C}\{\text{H}\}$ NMR (C_6D_6 , 25°C, δ): 20.3, 47.7, 56.1, 109.3, 123.1(d, $J_{\text{C-P}}$ 2.5 Hz), 128.4, 129.4 (d, $J_{\text{C-P}}$ 5.3 Hz), 130.6 (d, $J_{\text{C-P}}$ 5.6 Hz), 131.5 (d, $J_{\text{C-P}}$ 9.4 Hz), 131.7 (d, $J_{\text{C-P}}$ 9.4 Hz), 132.1 (d, $J_{\text{C-P}}$ 11.5 Hz), 132.3 (d, $J_{\text{C-P}}$ 11.5 Hz), 135.1, 135.3 (d, $J_{\text{C-P}}$ 17.6 Hz), 135.9 (d, $J_{\text{C-P}}$ 4.8 Hz), 144.5 (d, $J_{\text{C-P}}$ 192.2 Hz), 147.9 (d, $J_{\text{C-P}}$ 3.1 Hz). Anal. Calcd. for $\text{C}_{26}\text{H}_{26}\text{N}_3\text{NiP}$ (470.17): C, 66.42; H, 5.57; N, 8.94. Found: C, 66.09; H, 5.51; N, 8.80.

Procedure for ethylene polymerisation and oligomerisation

The procedure for ethylene polymerisation and oligomerisation were carried out under conditions similar to those described in Section 2.2.

Table 3.1 Crystallographic Parameters for 83, 96, 97, 99, 100, 101 and 102.

	83-CH ₃ CN	96-2CH ₂ Cl ₂	97
Formula	C ₃₀ H ₃₅ Cl ₂ N ₄ PPd	C ₄₂ H ₄₄ Cl ₆ FeN ₃ P	C ₃₂ H ₄₀ Cl ₂ FeN ₃ P
MW	659.89	890.32	624.39
a(Å)	10.333(8)	16.006(9)	12.376(6)
b(Å)	11.302(8)	18.784(11)	15.765(8)
c(Å)	13.339(10)	16.330(9)	17.919(8)
α(deg)	73.674(14)		
β(deg)	87.098(13)	113.890(11)	109.685(9)
γ(deg)	85.621(14)		
Cryst syst	Triclinic	Monoclinic	Monoclinic
Space group	P-1	P2 ₁ /n	P2 ₁ /c
Vol(Å) ³	1490.0(19)	4489(4)	3292(3)
D _{calcd} (gcm ⁻³)	1.471	1.317	1.260
Z	2	4	4
Abs. coeff., μ, mm ⁻¹	0.882	0.761	0.694
Data collected	6266	18964	13827
Data F _o ² >3σ(F _o ²)	4279	6369	4672
Variables	343	478	352
R ^a (%)	4.3	5.2	3.0
R _w ^a (%)	10.5	13.7	7.9
Goodness of Fit	1.047	1.030	1.021

^aAll data collected at 20°C with Mo Kα radiation (λ = 0.71073 Å), R = Σ||F_o| - |F_c|| / Σ|F_o|, R_w = [Σ[ω(F_o² - F_c²)²] / Σ[ωF_o²]^{0.5}

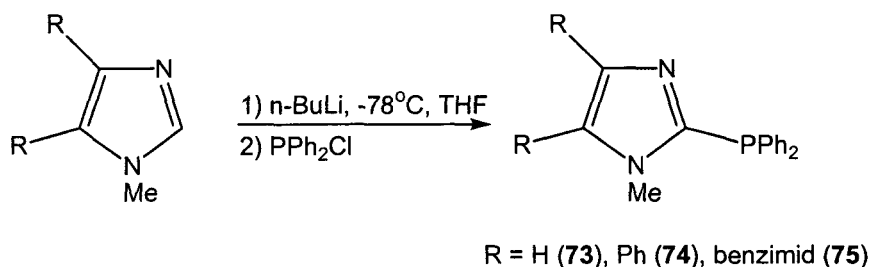
	99	100	101	102
Formula	C ₃₀ H ₃₅ N ₃ NaOP	C ₃₃ H ₃₆ ClN ₃ PRh	C ₃₃ H ₃₆ ClCrN ₃ P	C ₃₁ H ₃₃ N ₃ PRh
MW	507.57	643.98	593.07	581.48
a(Å)	9.167(5)	17.510(11)	9.187(5)	8.459(5)
b(Å)	12.033(6)	9.149(6)	10.503(6)	9.056(5)
c(Å)	25.300(13)	18.916(11)	16.696(9)	19.201(11)
α(deg)			82.522(11)	80.602(12)
β(deg)	93.553(9)	91.891(12)	89.486(10)	78.983(11)
γ(deg)			69.885(9)	73.660(10)
Cryst syst	Monoclinic	Monoclinic	Triclinic	Triclinic
Space group	P2 ₁ /c	P2 ₁ /c	P-1	P-1
Vol(Å) ³	2785(2)	3029(3)	1498.7(14)	1376.0(13)
D _{calcd} (g cm ⁻³)	1.210	1.412	1.314	1.403
Z	4	4	2	2
Abs. coeff., μ, mm ⁻¹	0.141	0.731	0.551	0.703
Data collected	11613	12668	6420	5903
Data F _o ² > 3σ(F _o ²)	3982	4339	4261	3899
Variables	325	352	352	325
R ^a (%)	4.5	3.8	4.7	2.7
R _w ^a (%)	11.4	4.9	13.7	6.3
Goodness of Fit	1.012	1.025	1.082	1.039

^aAll data collected at 20°C with Mo Kα radiation (λ = 0.71073 Å), $R = \frac{\sum ||F_o| - |F_c||}{\sum |F_o|}$,
 $R_w = [\frac{\sum [\omega(F_o^2 - F_c^2)^2]}{\sum [\omega F_o^2]}]^{0.5}$

3.3 Results and Discussion

Neutral Imidazolyl-phosphinimine Ligands

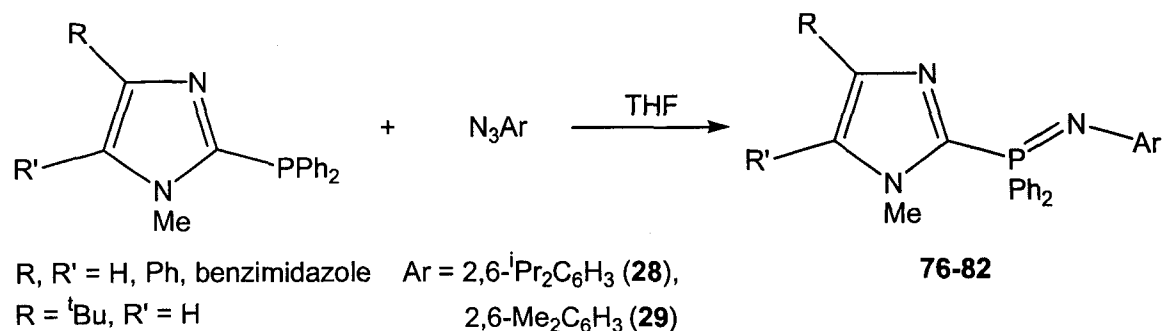
A variety of methods have been reported for the synthesis of imidazolyl-phosphines.⁸⁴⁻⁸⁶ The most convenient route involves the selective lithiation of the C2 position followed by electrophilic attack with a halophosphine (Scheme 3.1). Following this procedure, several substituted imidazolyl-phosphines are synthesized and isolated in greater than 75% yield after recrystallization. ³¹P NMR spectroscopy reveals chemical shifts of approximately -25 to -30 ppm for **73-75**, in agreement with literature reports for other imidazolyl-phosphines.⁸⁴⁻⁸⁶



Scheme 3.1 Synthesis of substituted 1-methyl-2-diphenylphosphinoimidazoles **73-75**.

In a similar fashion to pyridyl-phosphines, oxidation of **73-75** with substituted phenyl azides provides imidazolyl-phosphinimine ligands in excellent yields after recrystallization (Scheme 3.2). ¹H NMR analysis indicates the presence of appropriate ^tBu, Ph, Me, or ⁱPr signals depending upon the substitution on imidazole or phosphinimine groups. ³¹P NMR spectroscopy shows a single resonance for each ligand, at a chemical shift (δ -15 to -19 ppm) downfield from the phosphine. Furthermore, IR

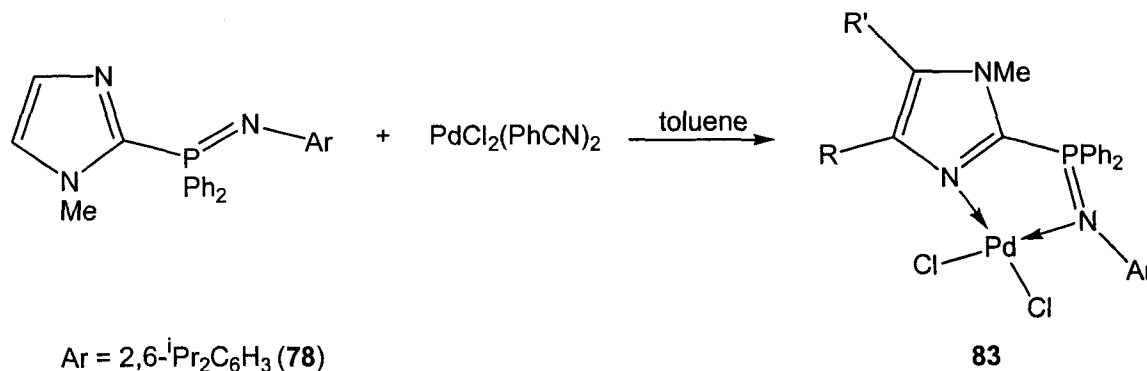
analysis of **76-82** shows strong P=N stretching frequencies between 1352-1377 cm^{-1} , similar to previously described pyridyl-ligands.



Scheme 3.2 Synthesis of neutral substituted imidazolyl-phosphinimine ligands **76-82**.

Phosphinimine complexes **76-82** react with several first- and second-row group VIII and X metal halides and their derivatives to form metal complexes, **83-97**. The reaction between compound **77** and $\text{PdCl}_2(\text{PhCN})_2$ proceeds smoothly in toluene to form the phosphinimine-palladium species **83**, shown in Scheme 3.3. ^1H NMR analysis of **83** shows small chemical shift differences with respect to the free ligand, with the exception of two distinct isopropyl resonances. This occurrence shows a non-inequivalence for both methyl groups in the isopropyl fragment, with one methyl group positioned towards the palladium metal centre in solution while the other is directed away. This methyl orientation separates the two methyl signals by 1.1 ppm, with the upfield signal attributed to the methyl group directed towards the palladium atom. ^{13}C NMR spectroscopy also shows two distinct methyl resonances at 22.5 ppm and 25.1 ppm. This phenomenon has been observed in similar palladium-diimine complexes reported by Brookhart.³¹

Furthermore, ^{31}P NMR spectroscopy shows a singlet at 28.2 ppm, and is similar to the downfield shift observed in the pyridine case (*vide supra*).



Scheme 3.3 Synthesis of the imidazolyl-phosphinimine palladium complex **83**.

The solid state structure of **83** reveals that the phosphinimine ligand coordinates in a bidentate fashion through both nitrogen atoms, similar to the pyridyl-phosphinimine palladium complex **49** and previous reported findings.^{67,68} The geometry at the palladium metal centre is pseudo-square planar as determined from the angles around the metal centre. The five-membered ring formed from coordination of the ligand to the metal also has a mean deviation from the plane of 0.0178 Å. A distorted tetrahedral geometry is evident at the phosphorus atom, and a distorted trigonal planar geometry is present at the phosphinimine nitrogen atom. The two Pd—Cl bond lengths are almost identical, suggesting similar *trans* influences for both donor atoms. However, the Pd—N bond lengths differ by ~0.06 Å, suggesting a different electronic metal-ligand interaction than was found in the pyridine case.

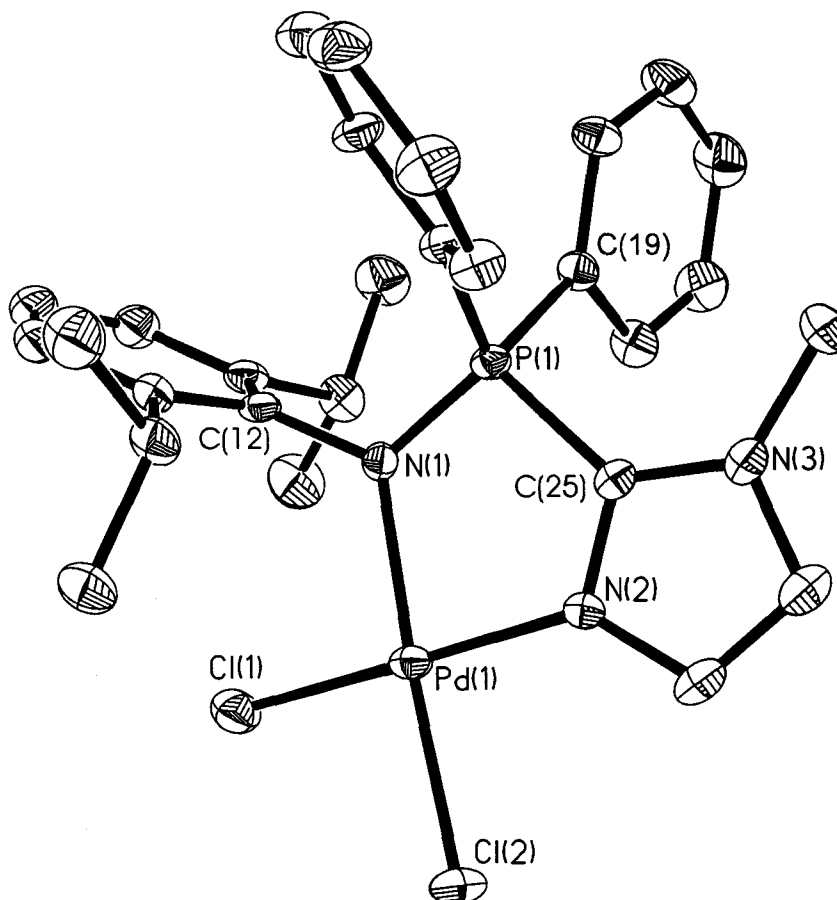
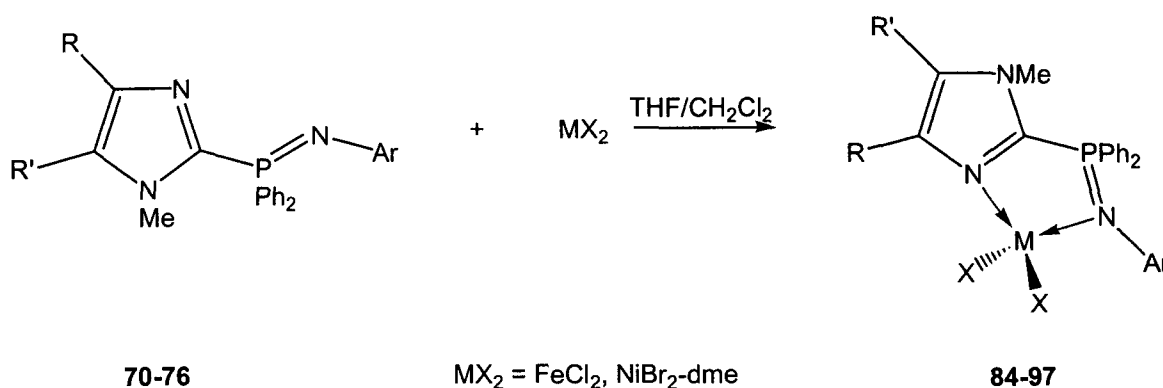


Figure 3.1 ORTEP drawing of **83-CH₃CN**, 30% thermal ellipsoids are shown. Hydrogen atoms have been omitted for clarity. Pd(1)-N(2) 2.026(4) Å, Pd(1)-N(1) 2.086(4) Å, Pd(1)-Cl(1) 2.298(2) Å, Pd(1)-Cl(2) 2.2988(17) Å, P(1)-N(1) 1.614(4) Å, P(1)-C(25) 1.795(5) Å, N(2)-C(25) 1.338(6) Å, P(1)-C(19) 1.798(5) Å, P(1)-C(13) 1.807(5) Å, N(2)-Pd(1)-N(1) 84.70(14)°, N(2)-Pd(1)-Cl(1) 175.56(12)°, N(1)-Pd(1)-Cl(1) 93.74(11)°, N(2)-Pd(1)-Cl(2) 90.91(11)°, N(1)-Pd(1)-Cl(2) 175.34(11)°, Cl(1)-Pd(1)-Cl(2) 90.74(5)°, N(1)-P(1)-C(25) 101.4(2)°, P(1)-N(1)-Pd(1) 117.0(2)°, C(25)-N(2)-Pd(1) 118.8(3)°, C(12)-N(1)-P(1) 118.6(3)°, N(1)-P(1)-C(13) 118.6(2)°, C(19)-P(1)-C(13) 107.5(2)°, N(1)-P(1)-C(19) 115.6(2)°.

Iron(II) and nickel(II) metal complexes were synthesized by the reaction of ligands **76-82** with metal halides. The complexes were identified by IR, EA, and magnetic susceptibility measurements, with NMR spectroscopy suggesting that the metal complexes are also paramagnetic in solution. The solubility of metal complexes further complicates identification as most complexes were insoluble in common organic solvents. IR spectroscopy of **84-97** shows a P=N stretching frequency range of 1190 cm^{-1} to 1250 cm^{-1} . In comparison to free ligands, an average P=N shift of 160 cm^{-1} to lower wavenumbers is observed in the metal complexes, in agreement with results obtained in the pyridine complexes (*vide supra*). Magnetic susceptibility measurements shows nickel(II) and iron(II) complexes have an average μ_{eff} of 3.12 and 5.09 BM, respectively. These values are similar to the theoretical values of 2.83 BM and 4.90 BM for tetrahedral d_8 nickel(II) and d_6 iron(II) complexes, respectively.



Scheme 3.4 General synthesis of metal complexes **85-97**.

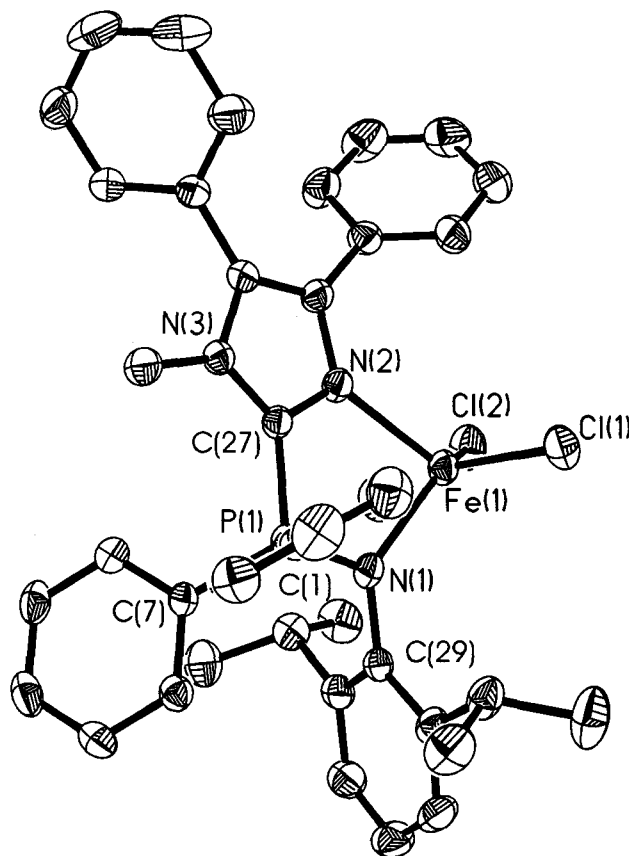


Figure 3.2 ORTEP drawing of **96**, 30% thermal ellipsoids are shown. Hydrogen atoms have been omitted for clarity. Fe(1)-N(1) 2.105(3) Å, Fe(1)-N(2) 2.114(4) Å, Fe(1)-Cl(2) 2.2588(17) Å, Fe(1)-Cl(1) 2.2843(15) Å, P(1)-N(1) 1.600(3) Å, P(1)-C(27) 1.809(4) Å, N(2)-C(27) 1.343(5) Å, P(1)-C(7) 1.801(4) Å, P(1)-C(1) 1.816(4) Å, N(1)-Fe(1)-N(2) 84.76(12)°, N(1)-Fe(1)-Cl(2) 127.04(10)°, N(2)-Fe(1)-Cl(2) 108.10(9)°, N(1)-Fe(1)-Cl(1) 105.15(10)°, N(2)-Fe(1)-Cl(1) 110.34(10)°, Cl(2)-Fe(1)-Cl(1) 116.49(6)°, N(1)-P(1)-C(7) 115.60(18)°, N(1)-P(1)-C(27) 102.37(18)°, P(1)-N(1)-Fe(1) 115.88(18)°, C(27)-N(2)-Fe(1) 114.8(3)°, C(29)-N(1)-Fe(1) 124.6(2)°.

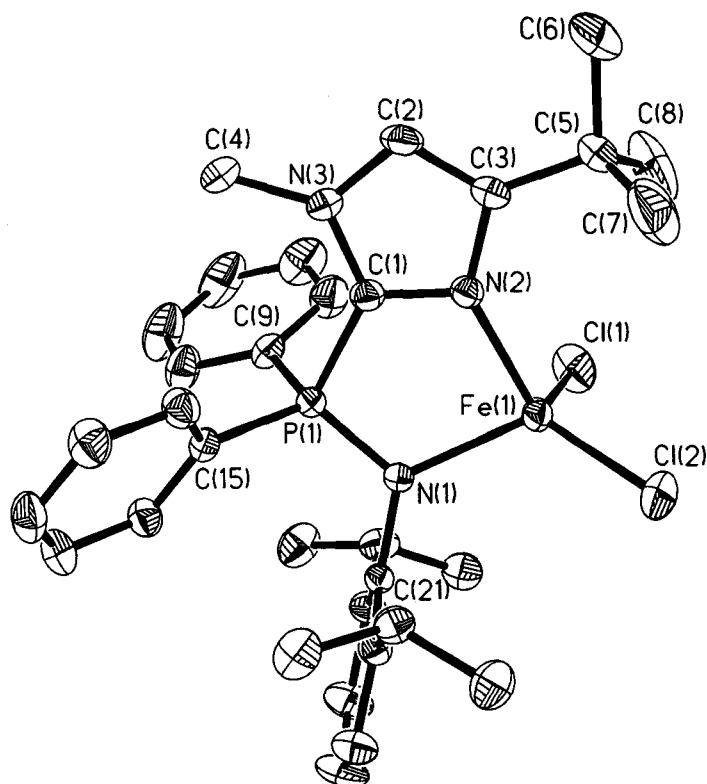


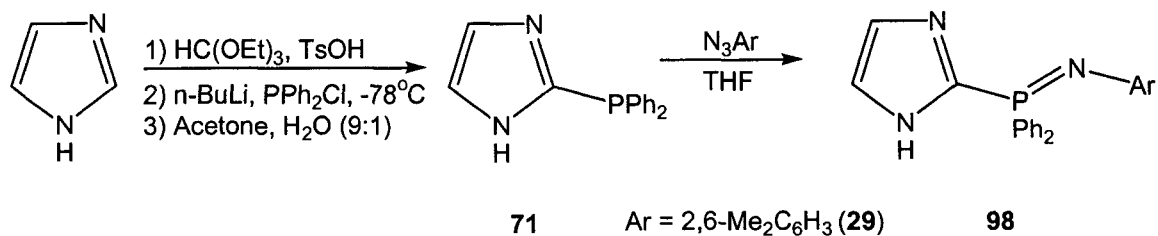
Figure 3.3 ORTEP drawing of **97**, 30% thermal ellipsoids are shown. Hydrogen atoms have been omitted for clarity. Fe(1)-N(1) 2.0979(19) Å, Fe(1)-N(2) 2.141(2) Å, Fe(1)-Cl(2) 2.2530(13) Å, Fe(1)-Cl(1) 2.2795(10) Å, N(1)-P(1) 1.5972(18) Å, N(2)-C(1) 1.341(3) Å, P(1)-C(1) 1.804(2) Å, P(1)-C(15) 1.804(2) Å, P(1)-C(9) 1.827(3) Å, C(3)-C(5) 1.517(3) Å, N(1)-Fe(1)-N(2) 85.02(7)°, N(1)-Fe(1)-Cl(2) 117.51(6)°, N(2)-Fe(1)-Cl(2) 115.63(6)°, N(1)-Fe(1)-Cl(1) 109.86(6)°, N(2)-Fe(1)-Cl(1) 109.23(6)°, Cl(2)-Fe(1)-Cl(1) 115.62(4)°, C(21)-N(1)-P(1) 120.09(14)°, C(21)-N(1)-Fe(1) 125.28(13)°, P(1)-N(1)-Fe(1) 114.62(9)°, C(1)-N(2)-Fe(1) 112.66(13)°, N(1)-P(1)-C(1) 102.30(10)°, N(1)-P(1)-C(15) 115.02(10)°, C(1)-P(1)-C(15) 110.33(10)°, C(15)-P(1)-C(9) 107.78(11)°.

Suitable X-ray quality crystals of **96** and **97** can be grown from saturated solutions of CH₃CN. Attempts to recover crystals from nickel(II) compounds failed due to their insolubility in common organic solvents. Single crystal diffraction studies indicate the iron(II) centre adopts a pseudo-tetrahedral geometry with two chloride atoms and a bidentate imidazolyl-phosphinimine ligand filling the coordination sphere. The P=N bond lengths of both complexes are similar (~1.600 Å), and compare well with previously discussed pyridyl-phosphinimine metal compounds, and literature cases.^{44,46} These values are slightly longer than reported for the ligand CH₂(Ph₂P=NC₆H₄Me-4)₂,⁴³ suggesting that metal coordination to the ligand reduces P=N double bond character. Much like the pyridine examples, the five-membered ring adopts a non-planar arrangement with a mean deviation from the plane of 0.0807 Å and 0.1057 Å for **96** and **97**, respectively. Phenyl groups attached to the imidazole ring in **96** make a 49.1° angle relative to the imidazole ring, similar to the observed angle in **69**.

Anionic Imidazolyl-phosphinimine Ligands

The synthesis of anionic imidazolate ligands is not as straightforward as for the neutral ligands. The phosphorylation of 1-H-imidazolyl-phosphines at the 2-position requires protecting one of the imidazole nitrogen atoms prior to lithiation. *N*-Benzyl,⁸⁷ *N*-alkoxymethyl,⁸⁸ *N*-tosyl,⁸⁹ and *N*-trityl⁹⁰ protecting groups have been previously used for imidazole; however, such groups suffer from either low yields,⁸⁸ harsh conditions required to remove such groups,⁸⁷ or poorly described procedures.^{89,90} Diethylorthoformate appears to be a suitable protecting group, and can be removed by hydrolysis after phosphorylation.⁸⁰ Oxidation of the phosphine with organic azides

proceeds smoothly to give phosphinimines in high yield (>90%). Both ^{31}P and ^1H NMR spectroscopy confirm the synthesis of **98**, with a ^{31}P chemical shift at -21.5 ppm, slightly downfield from the 1-methyl neutral analogues. Previous studies have shown that phosphinimine molecules possess the ability to deprotonate other functional groups to form zwitterionic-like compounds.⁵² Such a case is expected with an acidic imidazolyl proton present; however, no proton exchange is observed between the basic phosphinimine functionality and the acidic imidazole proton.



Scheme 3.5 Synthesis of 1-H-imidazolyl-phosphinimine ligand **98**.

The neutral imidazoles (1-H) can be deprotonated with NaH at room temperature in THF to give the imidazolate-phosphinimine, **99**, in good yield (90% yield). ^{31}P NMR spectroscopy shows a downfield shift to -4.7 ppm, while ^1H NMR shows a slight downfield shift of imidazole protons.

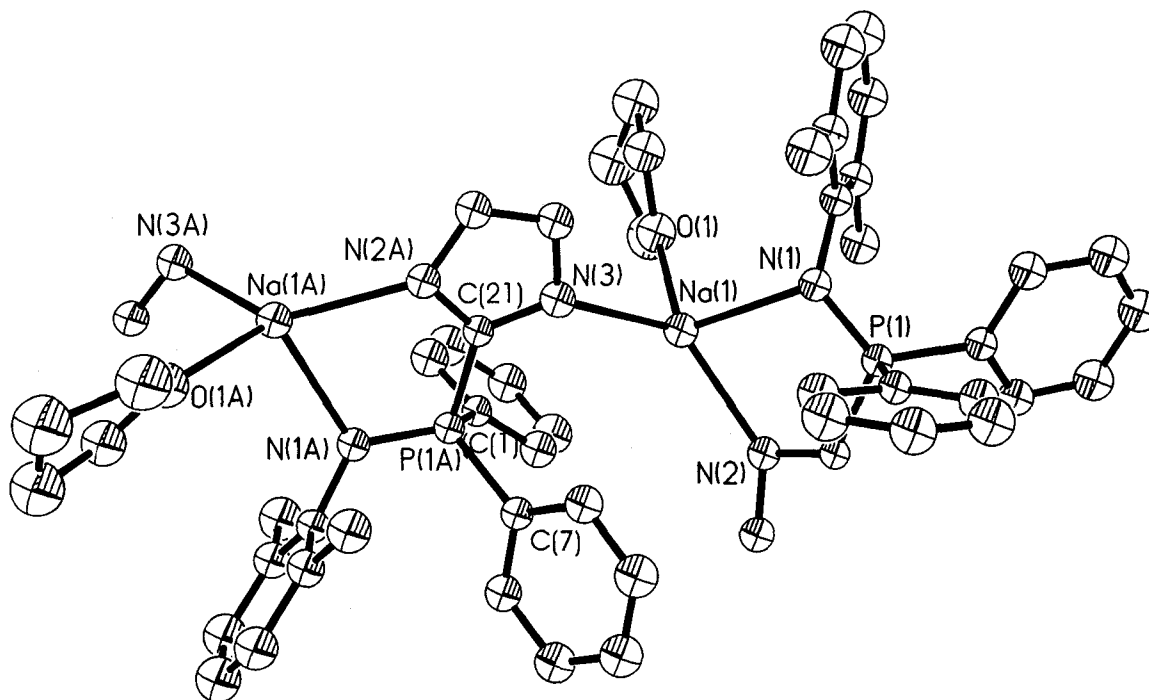
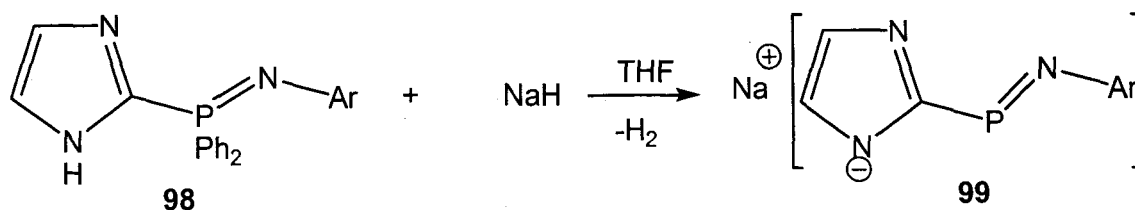


Figure 3.4 ORTEP drawing of **99**, 30% thermal ellipsoids are shown. Hydrogen atoms have been omitted for clarity. Na(1)-O(1) 2.368(3) Å, Na(1)-N(2) 2.425(2) Å, Na(1)-N(3) 2.441(3) Å, Na(1)-N(1) 2.461(2) Å, Na(1)-P(1) 3.4188(18) Å, P(1)-N(1) 1.573(2) Å, P(1)-C(21) 1.785(3) Å, P(1)-C(7) 1.816(3) Å, P(1)-C(1) 1.825(3) Å, N(2A)-C(21) 1.349(3) Å, N(3)-C(21) 1.356(3) Å, O(1)-Na(1)-N(2) 128.26(9)°, O(1)-Na(1)-N(3) 97.13(9)°, N(2)-Na(1)-N(3) 130.60(9)°, O(1)-Na(1)-N(1) 103.43(9)°, N(2)-Na(1)-N(1) 77.03(8)°, N(3)-Na(1)-N(1) 114.17(9)°, N(1A)-P(1A)-C(21) 108.84(12)°, N(1A)-P(1A)-C(7) 114.53(12)°, C(21)-P(1A)-C(7) 109.74(12)°, N(1A)-P(1A)-C(1) 114.71(12)°, P(1A)-N(1A)-Na(1) 114.05(11)°, C(21)-N(2A)-Na(1A) 114.45(17)°, C(21)-N(3)-Na(1) 137.57(19)°.

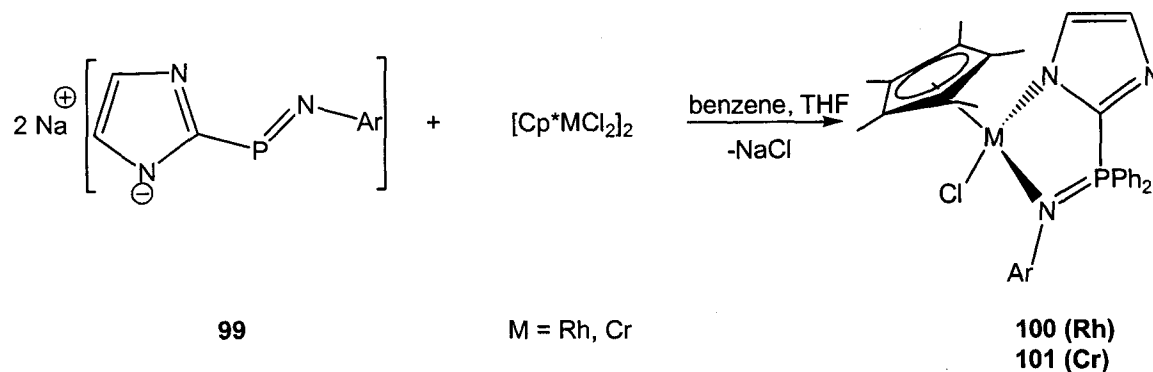


Scheme 3.6 Synthesis of phosphinimine-imidazolate ligand **99**.

The formulation of **99** was determined crystallographically and shows a polymeric solid state organization with the bidentate imidazolate-phosphinimine ligand chelated to a sodium atom with pseudo-tetrahedral geometry and an additional sodium interaction with a second imidazolyl nitrogen atom. The bond lengths of Na(1)-N(1), Na(1)-N(2), and Na(1)-N(3) are all similar (~ 0.02 Å) suggesting a relatively equal sharing of electron density between the sodium atom and imidazolate anions.

The anionic ligand **99** displays a versatile bonding nature, reacting cleanly with different chromium(III), rhodium(I), rhodium(III) and nickel(II) metal halide complexes. The reactions with $[\text{Cp}^*\text{RhCl}_2]_2$ and $[\text{Cp}^*\text{CrCl}_2]_2$ and 2 equivalents of **99** form Rh(III) (**100**) and Cr(III) (**101**) complexes in good yields ($>80\%$) after recrystallization (Scheme 3.7). The ^{31}P NMR spectrum of **100** confirms the presence of one product; however, no ^{103}Rh - ^{31}P coupling is observed. ^1H NMR spectroscopy indicates only one set of imidazole and Cp* resonances, with two broad methyl signals at 1.95 and 2.05 ppm. The inequivalent methyl signals result from the pseudo-tetrahedral environment of the metal centre, with one methyl group directed towards the chlorine atom while the other is located towards the Cp* ring. The NMR spectrum of **101** reveals broad signals indicating a paramagnetic complex, as is expected for a Cr(III) species. The solid state

structure of complexes **100** and **101** were determined by X-ray crystallography; crystals were grown from a saturated benzene solution (**100**) or tetrahydrofuran solution (**101**) (Figures 3.5 and 3.6, respectively).



Scheme 3.7 Synthesis of Rh(III) and Cr(III) phosphininimine-imidazolate metal complexes.

X-ray crystallography of **100** and **101** shows that the compounds are isostructural. The imidazolate-phosphinimine ligand coordinates in a bidentate fashion to the pseudo-tetrahedral metal centres. The geometries at the phosphorus and nitrogen atoms appear to be distorted tetrahedral and trigonal planar, respectively, as was seen for previous complexes. The M(1)-N(2) bond length is significantly shorter than the M(1)-N(1) bond distance ($\sim 0.12 \text{ \AA}$ for **100**, and $\sim 0.07 \text{ \AA}$ for **101**) indicating that N(2) has significant anionic character compared to N(1). The P=N bond lengths of **100** and **101** are $1.617(3) \text{ \AA}$ and $1.624(3) \text{ \AA}$, respectively, which are close to the values obtained in the neutral imidazolyl metal complexes. Furthermore, the N(2)-C(13) bond distance of both rhodium(III) and chromium(III) complexes appears to be similar.

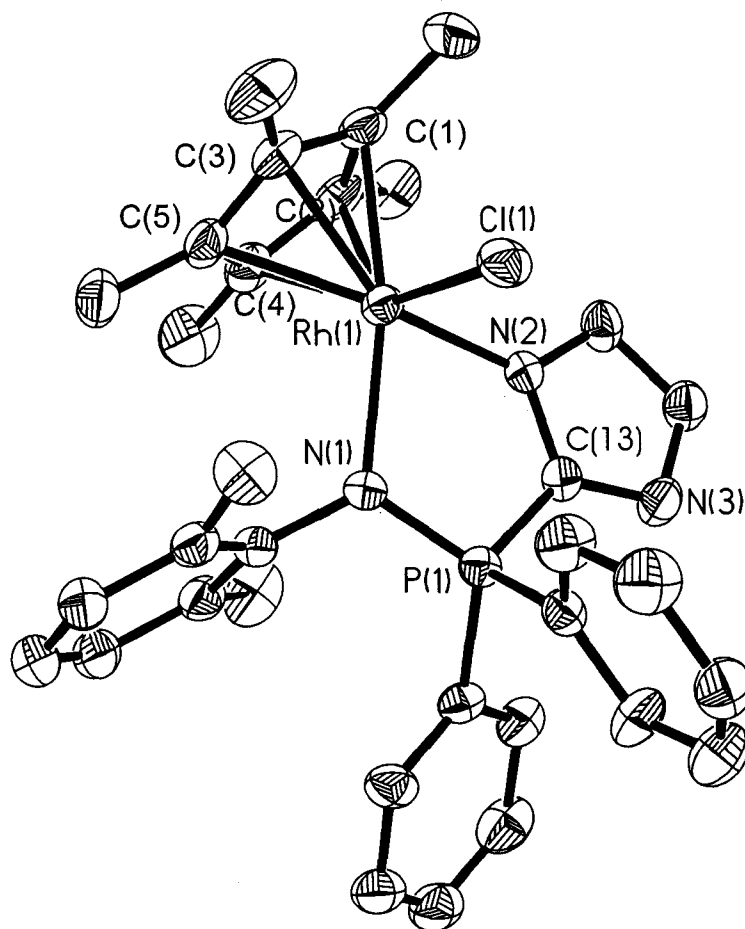


Figure 3.5 ORTEP drawing of **100**, 30% thermal ellipsoids are shown. Hydrogen atoms have been omitted for clarity. Rh(1)-N(2) 2.098(4) Å, Rh(1)-C(1) 2.139(4) Å, Rh(1)-C(2) 2.176(4) Å, Rh(1)-C(3) 2.180(5) Å, Rh(1)-C(5) 2.184(4) Å, Rh(1)-C(4) 2.200(5) Å, Rh(1)-N(1) 2.224(3) Å, Rh(1)-Cl(1) 2.4298(16) Å, P(1)-N(1) 1.617(3) Å, P(1)-C(13) 1.772(4) Å, N(2)-C(13) 1.363(4) Å, C(1)-C(2) 1.422(6) Å, N(2)-Rh(1)-N(1) 79.69(13)°, N(2)-Rh(1)-Cl(1) 85.58(9)°, N(1)-Rh(1)-Cl(1) 90.09(9)°, N(1)-P(1)-C(13) 102.22(19)°, P(1)-N(1)-Rh(1) 116.25(19)°.

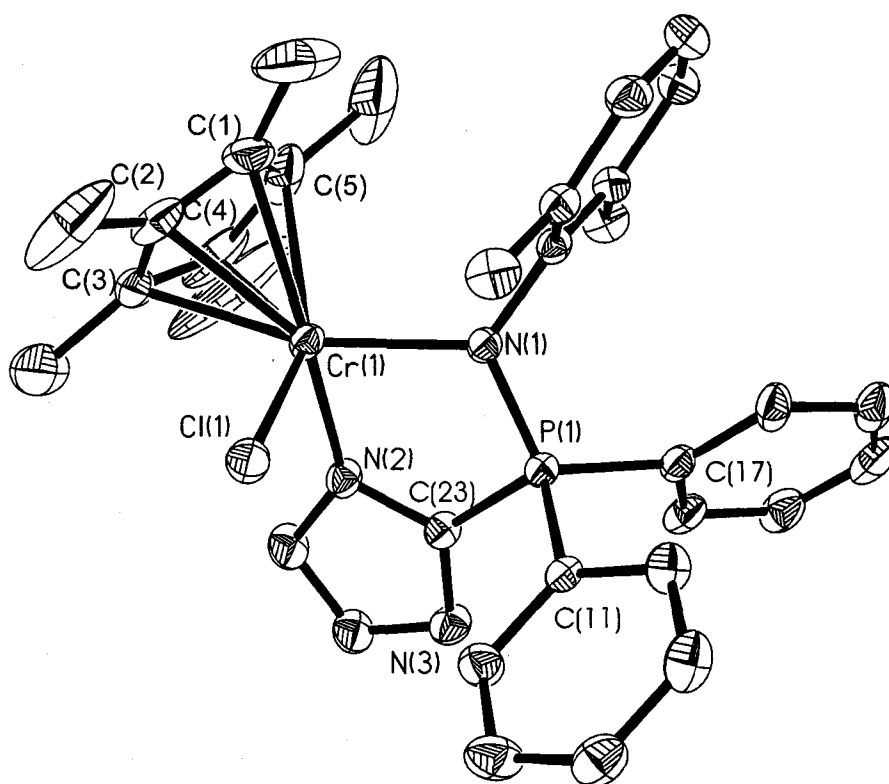
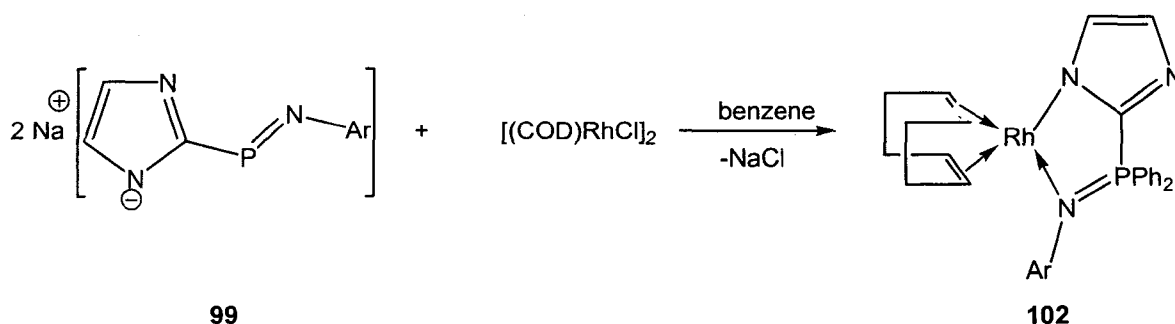


Figure 3.6 ORTEP drawing of 101, 30% thermal ellipsoids are shown. Hydrogen atoms have been omitted for clarity. Cr(1)-N(2) 2.058(3) Å, Cr(1)-N(1) 2.120(3) Å, Cr(1)-Cl(1) 2.3238(16) Å, Cr(1)-C(3) 2.239(4) Å, Cr(1)-C(2) 2.249(4) Å, Cr(1)-C(4) 2.254(4) Å, Cr(1)-C(1) 2.264(5) Å, Cr(1)-C(5) 2.261(5) Å, P(1)-N(1) 1.624(3) Å, N(2)-C(23) 1.357(4) Å, N(3)-C(23) 1.341(4) Å, P(1)-C(17) 1.822(3) Å, P(1)-C(11) 1.817(4) Å, N(2)-Cr(1)-N(1) 82.98(10), N(2)-Cr(1)-Cl(1) 92.57(9), N(1)-Cr(1)-Cl(1) 96.55(8), N(1)-P(1)-C(23) 101.84(15), P(1)-N(1)-Cr(1) 114.02(14), C(23)-N(2)-Cr(1) 118.4(2).

The 16-electron chromium complex **101** was screened for possible olefin polymerisation activity. Previous monodentate Cr(III) phosphinimine complexes supported on silica polymerised ethylene at 90°C, with an activity of 312.9 g PE mmol cat⁻¹ hr⁻¹ atm⁻¹.⁹¹ Surprisingly, activation of **101** with MAO under 1 atm of ethylene showed negligible olefin consumption. The presence of the uncoordinated imidazole nitrogen atom may affect olefin polymerisation, but it is not clear why this catalyst remains inactive.

The anionic imidazolate ligand also reacts with [(COD)RhCl]₂ to form complex **102** in excellent yield (95% yield). Spectroscopic data shows a chemical shift at 17.9 ppm in the ³¹P NMR spectrum, downfield from the ligand **99**; however, no ¹⁰³Rh-³¹P coupling was noted. The ¹H NMR spectrum features six different sets of cyclooctadiene protons as a result of the asymmetric ligand. The two olefinic signals appears as multiplets and have a 1.1 ppm chemical shift difference. Four sets of multiplets are also observed, corresponding to the methylene groups of the cyclooctadiene group. The ¹³C NMR spectrum of **102** confirms the structural assignments as two olefinic doublets at 74.5 and 83.7 ppm were observed with Rh-C coupling of 12.3 Hz and 14.0 Hz, respectively. Similar coupling and resonance values were observed for [Rh(CH₂PPh₂=N-C₆H₄-4)(COD)].⁹²



Scheme 3. Reaction of **99** with [(COD)RhCl]₂.

X-ray crystallography confirmed the structure of **102**, in which cyclooctadiene and a phosphinimine-imidazolate ligand coordinate to a pseudo-square planar rhodium(I) metal centre. The Rh(1)-N(2) bond distance is significantly shorter (0.06 Å) than the Rh(1)-N(1) bond length due to the anionic nature of the imidazolate group. The P(1)-N(1) bond length (1.619(3) Å) is similar to distances described in previous phosphinimine complexes (*vide supra*) and those described in literature.^{28,29,31} The Rh(1)-N(1) distance (2.133(2) Å) resembles distances reported for [Rh(CH₂PPh₂=N-C₆H₄-4)(COD)] (2.132(3) Å),⁹² [Rh(COD)(*p*-tol-N=PPh₂CHPPh₂NH-*p*-tol)] (2.144(9) Å),⁹³ [Rh{CH₂(PPh₂=N-*p*-tol)}₂(COD)] (2.17(1) Å),⁹⁴ and {Rh₂{μ-CPh(NPh)₂}(tfbb)₂} (2.086(6)-2.138(4) Å).⁹⁵ The Rh(1)-N(2) bond length (2.070(3) Å) compares well with the Rh—N_{pyrrolate} value found in the amine-pyrrolate chelated rhodium(I) cyclooctadiene complex, [PyCH₂NHCH₂-NC₄H₄]RhCOD (2.039(3) Å)⁹⁶. In accordance with Rh—N bond lengths, the average distances of Rh-C(28)/C(29) (2.109(3) Å) and Rh-C(24)/C(25) (2.148(3) Å) bond lengths show a significant difference indicating a greater *trans* influence of the imidazole group compared to the phosphinimine fragment. Despite the differences in Rh-C bond lengths, the olefinic distances C(28)-C(29) (1.401(5) Å) and C(24)-C(25) (1.388(5) Å) are similar. This lack of correlation between the C=C bond distances and the Rh—C bond lengths has been attributed to local repulsions in the coordination sphere.^{97,98}

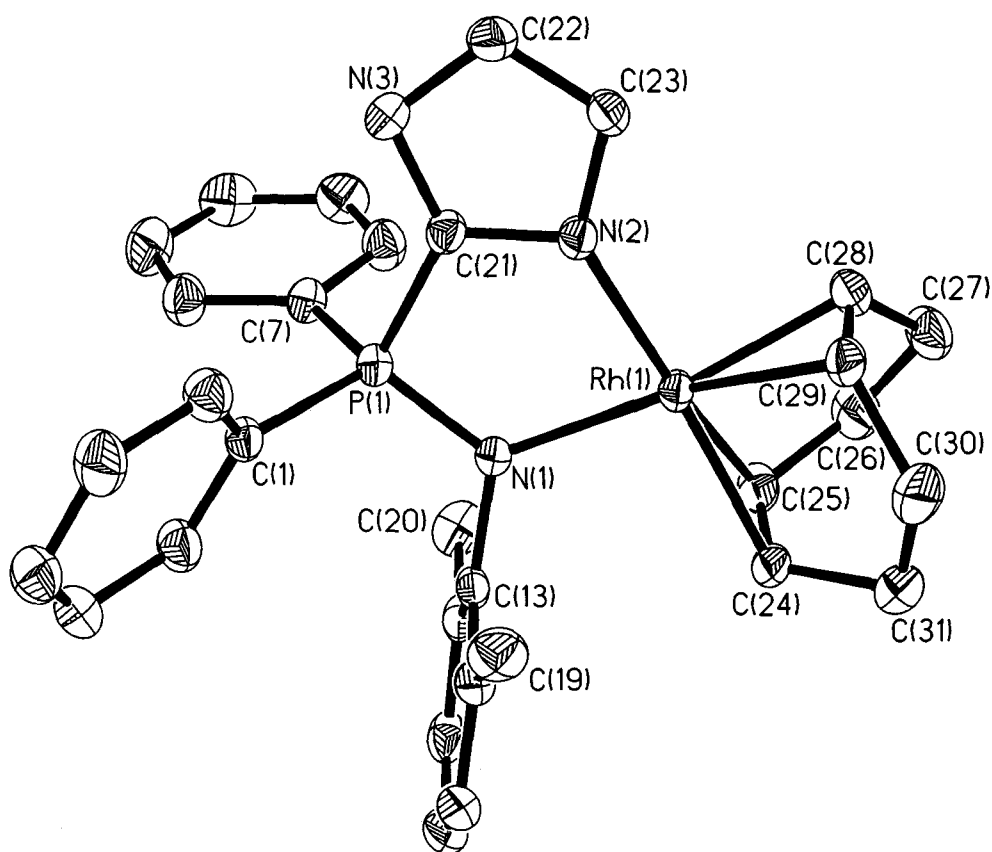
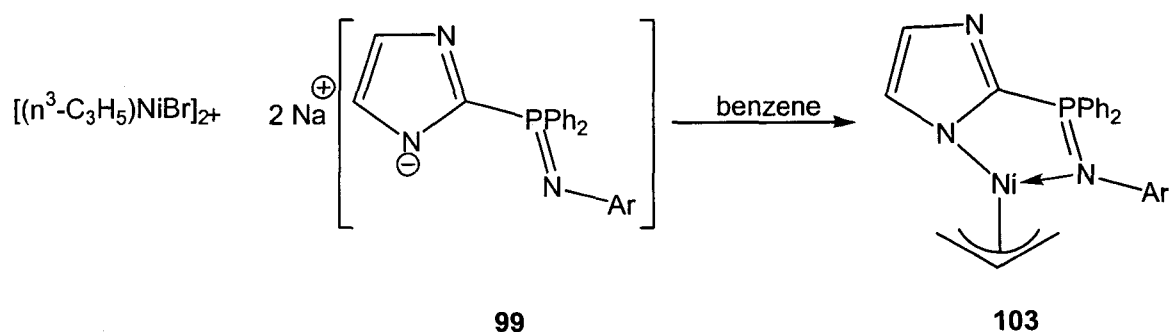


Figure 3.7 ORTEP drawing of **102**, 30% thermal ellipsoids are shown. Hydrogen atoms have been omitted for clarity. Rh(1)-N(2) 2.070(3) Å, Rh(1)-N(1) 2.133(2) Å, Rh(1)-C(29) 2.100(3) Å, Rh(1)-C(28) 2.117(3) Å, Rh(1)-C(25) 2.142(3) Å, Rh(1)-C(24) 2.154(3) Å, N(1)-P(1) 1.619(3) Å, N(2)-C(21) 1.361(4) Å, P(1)-C(21) 1.784(3) Å, C(24)-C(25) 1.388(5) Å, C(28)-C(29) 1.401(5) Å, N(2)-Rh(1)-N(1) 83.30(9)°, C(29)-Rh(1)-C(25) 98.00(14)°, P(1)-N(1)-Rh(1) 116.57(12)°, C(21)-N(2)-Rh(1) 119.65(19)°, N(1)-P(1)-C(21) 103.17(13)°, N(2)-C(21)-P(1) 116.9(2)°, N(1)-P(1)-C(1) 114.56(14)°.

Reactions of compound **99** with nickel(II) complexes were less straightforward than those of rhodium and chromium. Initial attempts to obtain nickel(II) complexes involved the nickel-containing starting materials $\text{NiMe}_2(\text{tmeda})$,⁹⁹ $\text{Ni}(\text{PMe}_3)\text{Cl}(\eta^3\text{-tolyl})$,¹⁰⁰ and $\text{NiBr}(\text{Ph})(\text{PPh}_3)_2$,¹⁰¹ which have been previously shown to react with protonated or anionic ligands. Reactions of these starting materials with **99** (or **98** in the case of $\text{NiMe}_2(\text{tmeda})$) resulted in a mixture of unidentifiable products. Successful coordination of **99** to a nickel(II) centre was accomplished with $[(\eta^3\text{-C}_3\text{H}_5)\text{NiBr}]_2$ to give the expected nickel(II) allyl compound in high yield (>90%). Unfortunately, attempts to isolate crystals for X-ray identification were unsuccessful due to the slow decomposition of **103** in common organic solvents.



Scheme 3.9 Formation of **103** from the reaction between **99** and $[(\text{allyl})\text{NiBr}]_2$.

The identification of **103** was confirmed by NMR spectroscopy and elemental analysis. Assignment of the ^1H and ^{13}C NMR spectrum of **103** shows a similar pattern to previously described square planar metal-allyl compounds.^{41,102,103} The complex exhibits C_1 symmetry in solution, as suggested in the ^1H NMR spectrum by: (1) inequivalent phenyl groups located on the phosphorus atom, (2) inequivalent methyl groups on the

phosphinimine aryl ring, and (3) five distinct allyl signals. ^{13}C NMR spectroscopy also shows this asymmetry, as there are multiple resonances for *ortho* and *meta* carbons on the $-\text{PPh}_2$ moiety. ^{31}P NMR analysis shows a chemical shift at 14.7 ppm, similar to the downfield shifts observed for previous imidizolate complexes.

Ethylene Polymerisation Study of Imidazolyl-phosphinimine Metal Complexes

The iron(II) and nickel(II) complexes described in the previous section, when activated by MAO or DEAC, do not appear to polymerise ethylene. MAO activation of **89** by NOVA yielded polymeric material, which had a molecular weight of 23,100 and a polydispersity index (PDI) of 1.34. Unfortunately, these results could not be duplicated in our lab. The polymer reported by Brookhart *et al.*²⁹ for the most active diimine catalyst has a molecular weight of 72,000 Da; slightly higher than the polymer obtained in this example. However, the polydispersity index (PDI) reported by Brookhart is greater (2.5) than was found with **89**. These values suggest that **89** is not only a single site catalyst but makes a narrower range of polymer molecular weights than the diimine complexes. This may be of use to make a specialized polymer; however, due to its low activity, this is not industrially practical.

Like the analogous pyridine metal complexes, the potential for several nickel(II) and iron(II) complexes to oligomerise ethylene was examined. Nickel(II) catalysts with increased steric bulk appear to possess the highest activity with DEAC activation in chlorobenzene (Table 3.2). Unfortunately, the activated species of **89** appears to have low oligomerisation activity at 35°C and 300 psi of ethylene ($17.9 \text{ g}\cdot\text{mmol}^{-1}\cdot\text{hr}^{-1}\cdot\text{atm}^{-1}$) in comparison with oligomerisations involving **25**.⁵⁰ NMR and GC analysis shows products

are predominantly 1-butene, with minor amounts of *cis*- and *trans*-butene. These results are not surprising as Sun *et al.* have recently reported that activated *P,N*-chelated (diphenylphosphino)quinoline-based nickel complexes selectively produce 1-butene ($490 \text{ g}\cdot\text{mmol}^{-1}\cdot\text{hr}^{-1}\cdot\text{atm}^{-1}$).¹⁰⁴ The iron(II) complexes prepared in this study are essentially inactive for both ethylene oligomerisation and polymerisation.

Table 3.2 Ethylene polymerisation by nickel/iron imidazolyl-phosphinimine complexes **89**, **90**, and **97**.

Trial	Compound	Solvent	Activity (g PE/mmol cat·hr·atm)	M_w	M_w/M_n
LSPB21-22	89	toluene	-	-	-
LSPB23-24	89	hexane	3.6	23,100	1.34
LSPB25-26	89	toluene	-	-	-
LSPB27-28	90	toluene	-	-	-
LSPB29-30	97	hexane	2.5	^c	^c
LSPB31-32	97	toluene	-	-	-

^a300 psig ethylene, 35°C, Al:M ratio of 500:1, MAO. ^bperformed by NOVA, 300 psig, 35°C, Al:M ratio of 500:1. ^cno detectable polymer.

Table 3.3 Ethylene oligomerisation results of activated nickel/iron pyridyl-phosphinimine complexes **89** and **97**.

Trial	Compound	Solvent	Mass of oligomers (g) ^c	Activity ^d
LSPB41-42 ^a	89	toluene	0.52	10.3
LSPB43-44 ^b	89	chlorobenzene	2.98	17.9
LSPB45-46 ^a	97	toluene	0.10	2.0
LSPB47-48 ^b	97	chlorobenzene	0.35	2.1

^a300 psig ethylene, 35°C, Al:M ratio of 500:1, MAO, 5 mmol cat. ^b300 psig ethylene, 35°C, Al:M ratio of 200:1, DEAC, 33 mmol cat. ^ccalculated from GC peak areas, and NMR. ^dg oligomer mmol cat⁻¹ hr⁻¹ atm⁻¹.

The nickel-allyl imidazolate species **103** was examined for the catalytic potential to oligomerise ethylene in the absence of a main group activator. When an aliquot of the

cooled solution was analyzed by GC and NMR, the products identified were internal C₄ alkenes, with very small amounts of C₆ and C₈ alkenes (18.9 g·mmol⁻¹·hr⁻¹·atm⁻¹). This compound shows a much greater activity in contrast to the nickel allyl complex **1** (0.55 g·mmol⁻¹·hr⁻¹·atm⁻¹)²⁸ and the cationic nickel(II) methylallyl species [(Ph₂PCH₂P(O)Ph₂)Ni(η³-CH₃C(CH₃)CH₃)]SbF₆¹⁰⁵ (0.78 g·mmol⁻¹·hr⁻¹·atm⁻¹). When exposed to 30.4 atm of ethylene at 70°C, this methylallyl species oligomerised ethylene with very low activity (0.78 g·mmol⁻¹·hr⁻¹·atm⁻¹) but with good selectivity (C₆ alkenes as the major product).

3.4 Summary and Conclusions

The synthesis of several Group VI, VII, IX and X imidazolyl- and imidazolate-phosphinimine complexes has been accomplished. Activation of several nickel(II) and iron(II) imidazolyl-phosphinimine complexes with DEAC or MAO resulted in low ethylene oligomerisation activity. In the presence of ethylene, the single component catalyst **103** exhibited a modest ability to oligomerise ethylene (18.9 g·mmol⁻¹·hr⁻¹·atm⁻¹). Contrary to very active nickel(II) diimine catalysts,^{39-31,33-35} phosphinimine-based LTM precursors appear to oligomerise ethylene with modest activities for C₄ alkene synthesis.

Chapter Four

Summary and Outlook

The research described herein has provided insight into the catalytic use of phosphinimine-based ligands in LTM ethylene polymerisation. The primary objective of this work was to develop a phosphinimine alternative to previously successful α -diimine ligands. Group VIII and X metal complexes with these types of ligand were evaluated as possible catalysts for olefin polymerisation.

In Chapter Two, the synthesis of several bulky pyridyl-phosphinimine iron(II) and nickel(II) complexes was performed. Several of these prospective catalysts were activated with MAO in the presence of ethylene to determine their catalytic potential. Unfortunately, nickel(II) and iron(II) complexes were ineffective in polymerizing ethylene. However, during catalytic screening, ethylene consumption was noted, which in conjunction with polymerisation results, suggested activated species may be oligomerizing ethylene. The most active species was **60**, when activated by DEAC in chlorobenzene, and had a modest activity of $48.2 \text{ g}\cdot\text{mmol}^{-1}\cdot\text{hr}^{-1}\cdot\text{atm}^{-1}$. These results drastically differ from the activities and types of polymer obtained from nickel(II) diimine complexes. Calculations were performed in an attempt to explain the effect that both types of ligand have on the cationic nickel(II) centre. Results showed that the presence of a phosphorus atom in the chelating metallacycle causes an increase in negative charge on the metal, suppressing ethylene electron donation. As a result, a weakened metal-ethylene interaction forms, which may explain the lack of alkyl chain

growth in the phosphinimine complexes. Removal of the negative charge on the metal centre could be accomplished with substitution of electron-withdrawing groups on the phosphorus atom. Unfortunately, initial attempts to apply this theory have failed due to an inability to oxidize a poorly basic fluorinated phosphine derivative.

The synthesis of imidazolyl-phosphinimine metal complexes was pursued in Chapter Three. The imidazole fragment allowed manipulation of the ligand to possess anionic or neutral features, thus permitting the synthesis of different LTM complexes. When activated, iron(II) and nickel(II) halides complexes formed with the neutral ligand showed ethylene oligomerisation activity, similar to pyridine catalysts. The anionic ligand was used to synthesize isostructural chromium(III) and rhodium(III) imidazolate complexes. The chromium(III) phosphinimine-imidazolate complex showed no catalytic activity, as opposed to previous unpublished findings for chromium(III) phosphinimine complexes. Rhodium(I) and nickel(II) imidazolate complexes could also be synthesized. Single component olefin polymerisation of the nickel(II) allyl species **104** showed ethylene oligomerisation capability, with an activity of $18.9 \text{ g}\cdot\text{mmol}^{-1}\cdot\text{hr}^{-1}\cdot\text{atm}^{-1}$. NMR and GC identification of the oligomer formed suggested C_4 internal alkenes were the major product with minor amounts of longer chained alkenes.

The research and calculations described in this thesis have provided valuable insight into the applications of phosphinimines in LTM olefin polymerisation. Continued research will be aimed at optimizing ethylene oligomerisation reaction conditions, in attempts to: (1) maximize the activity of catalysts, and (2) exert greater alkene selectivity. This research will be aided by the inclusion of mass spectrometry (MS) information, in addition to NMR and GC. In light of computational results, the incorporation of electron-

withdrawing groups on the phosphorus atom may also improve the activity of metal catalysts. For this research to continue, a weakly basic substituted phosphine capable of oxidation by bulky phenyl azides must be synthesized. In conclusion, the research presented herein has provided solid groundwork for future applications of phosphinimine ligands in LTM olefin catalysis.

References

- 1) Levowitz, I. L. *Modern Plastics Encyclopedia '99* (McGraw-Hill, New York, 1999), vol. 75, pp. B3-B6.
- 2) Ita, P. *World Polyethylene 1138* (Freedonia Group, Cleveland, OH, 1999)
- 3) Sinn, H.; Kaminsky, W.; Vollmer, H. J.; Woldt, R. *Angew. Chem., Int. Ed. Engl.* **1980**, *19*, 390.
- 4) Sinn, H.; Kaminsky, W. *Adv. Organomet. Chem.* **1980**, *18*, 99.
- 5) Wild, F. R. W. P.; Zsolnai, L.; Huttner, G.; Brintzinger, H. H. *J. Organomet. Chem.* **1982**, *232*, 233.
- 6) Coates, G. W.; Waymouth, R. M. *Science*, **1995**, *267*, 217.
- 7) Kaminsky, W.; Kulper, K.; Brintzinger, H.H.; Wild, F. R. W. P. *Angew. Chem., Int. Ed. Engl.* **1985**, *24*, 507.
- 8) Britovsek, G. J. P.; Gibson, V. C.; Wass, D. F. *Angew. Chem. Int. Ed.* **1999**, *38*, 428; and references therein.
- 9) Ziegler, K. *Angew. Chem.* **1964**, *76*, 545.
- 10) Parshall, G. *Homogeneous Catalysis* (Wiley-Interscience: New York, 1980).
- 11) Eisch, J. J.; Pombrick, S. I.; Zheng, G. X. *Organometallics* **1993**, *12*, 3856.
- 12) Ewen, J. A. *J. Am. Chem. Soc.* **1984**, *106*, 6355.
- 13) *Chem. Eng. News* **1992**, 42.
- 14) Canich, J. A. M.; Turner, H. W. WO-A 92/12162, **1992**.
- 15) Stevens, J. C.; Timmers, F. J.; Wilson, D. R.; Schmidt, G. F.; Nickias, P. N.; Rosen, R. K.; Knight, G. W.; Lai, S. Y. EP-B/0416815, **1990**.

- 16) Chen, Y. X.; Marks, T. J. *Organometallics* **1997**, *16*, 3649.
- 17) Chung, T. C.; Rhubright, D. *Macromolecules* **1993**, *26*, 3019; and references therein.
- 18) Schneider, M. J.; Schafer, R.; Mülhaupt, R. *Polymer* **1997**, *38*, 2455.
- 19) Wilen, C.-E.; Luttkhedde, H.; Hjertberg, T.; Nasman, J. H. *Macromolecules* **1996**, *29*, 8569; and references therein.
- 20) Kesti, M. R.; Coates, G. W.; Waymouth, R. M. *J. Am. Chem. Soc.* **1992**, *114*, 9679.
- 21) Schulz, D. N.; Datta, S.; Waymouth, R. M. *ACS Symp. Ser.* **1998**, *704* (Functional Polymers), 38.
- 22) Stein, K. M.; Kesti, M. R.; Coates, G. W.; Waymouth, R. *Polym. Prepr. (Am. Chem. Soc., Div. Polym. Chem.)* **1994**, *35* (1), 480.
- 23) Waymouth, R. M.; Kesti, M. R.; Coates, G. W. WO-A 94/12547, **1994**.
- 24) Lofgren, B.; Aaltonen, P. *Metallocenes '85, Int. Congr. Metallocene Polym.* **1995**, *101*, 1.
- 25) Aaltonen, P.; Fink, G.; Lofgren, B.; Seppala, J. *Macromolecules* **1996**, *29*, 5255; and references therein.
- 26) Galimberti, M.; Giannini, U.; Albizzati, E.; Caldari, S.; Abis, L. *J. Mol. Catal.* **1995**, *101*, 1.
- 27) Keim, W.; Kowaldt, H.; Goddard, R.; Kruger, C. *Angew. Chem., Int. Ed. Engl.* **1978**, *17*, 466.
- 28) Keim, W.; Appel, R.; Storeck, A.; Krüger, C.; Goddard, R. *Angew. Chem., Int. Ed. Engl.*, **1981**, *20*, 116.

- 29) Johnson, L. K.; Killian, C. M.; Brookhart, M. *J. Am. Chem. Soc.* **1995**, *117*, 6414.
- 30) Killian, C. M.; Tempel, C. M.; Johnson, M. J.; Brookhart, M. *J. Am. Chem. Soc.* **1996**, *118*, 11664.
- 31) Brookhart, M. S.; Johnson, L. K.; Killian, C. M.; Arthur, S. D.; Feldman, J.; McCord, E. F.; McLain, S. J.; Kreutzer, K. A.; Bennett, A. M. A.; Coughlin, E. B.; Ittel, S. D.; Parthasarathy, A.; Tempel, D. J. WO-A 96/23010, **1995**.
- 32) Thompson, D. T. *Plat. Metals Rev.* **1996**, *40* (2), 78.
- 33) Johnson, L. K.; Killian, C. M.; Brookhart, M. *Book of Abstracts, 210th ACS National Meeting*, Chicago, IL, August 20-24, 1995 (Pt. 1), INOR-243.
- 34) Brookhart, M.; Johnson, L. K.; Killian, C. M.; Mecking, S.; Tempel, D. *Book of Abstracts, 211th ACS National Meeting*, New Orleans, LA, March 24-28, 1996.
- 35) Brookhart, M. S.; Johnson, L. K.; Killian, C. M.; Mecking, S.; Tempel, D. *J. Polym. Prepr. (Am. Chem. Soc., Div. Polym. Chem.)* **1996**, *37* (1), 254-255.
- 36) Abu-Surrah, A. S.; Rieger, B. *Angew. Chem., Int. Ed. Engl.* **1996**, *35* (21), 2475.
- 37) Britovsek, G. J. P.; Gibson, V. C.; Kimberly, B. S.; Maddox, P. J.; McTavish, S. J.; Solan, G. A.; White, J. P.; Williams, D. J. *Chem. Commun.* **1998**, 849.
- 38) Small, B. L.; Brookhart, M.; Bennett, A. M. A. *J. Am. Chem. Soc.* **1998**, *120*, 4049.
- 39) Small, B. L.; Brookhart, M. *J. Am. Chem. Soc.* **1998**, *120*, 7143.
- 40) Younkin, T. R.; Connor, E. F.; Henderson, J. I.; Friedrich, S. K.; Grubbs, R. H.; Bansleben, D. A. *Science* **2000**, *287*, 460.
- 41) Hicks, F. A.; Brookhart, M. *Organometallics* **2001**, *20*, 3217.
- 42) Liu, W.; Malinoski, J. M.; Brookhart, M. *Organometallics* **2002**, *21*, 2836.

- 43) Imhoff, P.; van Asselt, R.; Elsevier, C. J.; Vrieze, K.; Goubitz, K.; van Malssen, K. F.; Stam, C. H. *Phosphorus, Sulfur Silicon Relat. Elem.* **1990**, *147*, 401.
- 44) (a) Imhoff, P.; van Asselt, R.; Elsevier, C. J.; Zoutberg, M. C.; Stam, C. H. *Inorg. Chim. Acta* **1991**, *184*, 73; and references therein. (b) Avis, M. W.; Goosen, M.; Elsevier, C. J.; Veldman, N.; Kooijman, H.; Spek, A. L. *Inorg. Chim. Acta* **1997**, *264*, 43.
- 45) (a) Hankin, D. M.; Danopoulos, A. A.; Wilkinson, G.; Sweet, T. K. N.; Hurtshouse, M. B. *J. Chem. Soc., Dalton Trans.* **1996**, 4063. (b) Falvello, L. R.; Fernandez, S.; Garcia, M. M.; Navarro, R.; Urriolabeita, E. P. *J. Chem. Soc., Dalton Trans.* **1998**, 3745.
- 46) Al-Benna, S.; Sarsfield, M. J.; Thorton-Pett, M.; Ormsby, D. L.; Maddox, P. J.; Bres, P.; Bochmann, M. *J. Chem. Soc., Dalton Trans.* **2000**, 4247.
- 47) Ong, C. M.; Stephan, D. W. *Inorg. Chem.* **1999**, *38*, 5189.
- 48) Kasani, A.; Kamalesh Babu, R. P.; McDonald, R.; Cavell, R. G. *Angew. Chem., Int. Ed. Engl.* **1999**, *10*, 1483.
- 49) Kasani, A.; McDonald, R.; Ferguson, M.; Cavell, R. G. *Organometallics* **1999**, *18*, 4241.
- 50) Sauthier, M.; Leca, F.; de Souza, R. F.; Bernardo-Gusmao, K.; Fernando, L.; Queiroz, T.; Toupet, L.; Reau, R. *New. J. Chem.* **2002**, *26*, 630.
- 51) Staudinger, H.; Meyer, J. *Helv. Chim. Acta* **1919**, *2*, 635.
- 52) For a review of phosphazides and phosphinimines: Gololobov, Y. G.; Zhmurova, I. N.; Kasukhin, L. F. *Tetrahedron* **1981**, *37*, 437; and references therein.

- 53) (a) Derkach, G. I.; Gubnitskaya, E. S.; Shokol, A.; Kirsanov, A. V. *Zh. Obshch. Khim.* **1962**, *32*, 1201. (b) Derkach, G. I.; Samarai, L. I.; Shtepanek, A. S.; Kirsanov, A. V. *Zh. Obshch. Khim.* **1962**, *32*, 3759. (c) Derkach, G. I.; Gubnitskaya, E. S.; Samarai, L. I.; Shokol, A. *Zh. Obshch. Khim.* **1963**, *33*, 557.
- 54) Perrin, D. D.; Armarego, W. L. F. *Purification of Laboratory Chemicals 3rd ed.* BH: London, **1994**.
- 55) (a) Maisonnnet, A.; Farr, J. P.; Olmstead, M. M.; Hunt, C. T.; Balch, A. *Inorg. Chem.* **1982**, *21*, 3961. (b) Newkome, G. R.; Hager, D. C. *J. Org. Chem.* **1978**, *43* (5), 947.
- 56) RajanBabu, T. V.; Radetich, B.; You, K. K.; Ayers, T. A.; Casalnouvo, A. L.; Calabrese, J. C. *J. Org. Chem.* **1999**, *64* (10), 3429.
- 57) Minato, A.; Tamao, K.; Hayashi, T.; Suzuki, K.; Kumada, M. *Tetrahedron Lett.* **1980**, *21* (9), 845.
- 58) Jutzi, P.; Lorey, O. *J. Organomet. Chem.* **1976**, *104* (2), 153.
- 59) Uchida, Y.; Echikawa, N.; Oae, S. *Heteroatom. Chem.* **1994**, *5* (4), 409.
- 60) (a) Frisch, M. J.; Trucks, G. W.; Schlegel, H. B.; Scuseria, G. E.; Robb, M. A.; Cheeseman, J. R.; Zakrzewski, V. G.; Montgomery, J. A. Jr.; Stratmann, R. E.; Burant, J. C.; Dapprich, S.; Millam, J. M.; Daniels, A. D.; Kudin, K. N.; Strain, M. C.; Farkas, O.; Tomasi, J.; Barone, V.; Cossi, M.; Cammi, R.; Mennucci, B.; Pomelli, C.; Adamo, C.; Clifford, S.; Ochterski, J.; Petersson, G. A.; Ayala, P. Y.; Cui, Q.; Morokuma, K.; Salvador, P.; Dannenberg, J. J.; Malick, D. K.; Rabuck, A. D.; Raghavachari, K.; Foresman, J. B.; Cioslowski, J.;

- Ortiz, J. V.; Baboul, A. G.; Stefanov, B. B.; Liu, G.; Liashenko, A.; Piskorz, P.; Komaromi, I.; Gomperts, R.; Martin, R. L.; Fox, D. J.; Keith, T.; Al-Laham, M. A.; Peng, C. Y.; Nanayakkara, A.; Challacombe, M.; Gill, P. M. W.; Johnson, B.; Chen, W.; Wong, M. W.; Andres, J. L.; Gonzalez, C.; Head-Gordon, M.; Replogle, E. S.; Pople, J. A. *GAUSSIAN 98*; Gaussian, Inc., Pittsburgh PA, 2001. (b) Stephens, P. J.; Devlin, F. J.; Chabalowski, C. F.; Frisch, M. J. *J. Phys. Chem.* **1994**, *98*, 11623.
- 61) Becke, A. D.; *J. Chem. Phys.* **1993**, *98*, 5648.
- 62) Hay P. J.; Wadt, W. R. *J. Chem. Phys.* **1985**, *82*, 270.
- 63) Dunne, B. J.; Orpen, A. G. *Acta Cryst. Sect. C* **1991**, *C47* (2), 345.
- 64) Herring, D. L. *J. Org. Chem.* **1961**, *26*, 3998.
- 65) Smolinsky, G. *J. Org. Chem.* **1961**, *26*, 4108.
- 66) (a) King, R. B.; Cloyd, J. C. *Inorg. Chem.* **1975**, *14*, 1550. (b) Hietkamp, S.; Stufkens, D. J.; Vrieze, K.; *J. Organomet. Chem.* **1979**, *169*, 107. (c) MacLeod, I.; Manojlovic-Muir, L.; Millington, D.; Muir, K. W.; Sharp, D. W. A.; Walker, R. *J. Organomet. Chem.* **1975**, *97*, C7. (d) Appleton, T. G.; Bennett, M. A. *Inorg. Chem* **1978**, *17*, 738.
- 67) Arques, A.; Molina, P.; Aunon, D.; Vilaplana, M. J.; Velasco, M. D.; Martinez, F.; Bautista, D.; Lahoz, F. J. *J. Organomet. Chem.* **2000**, *598*, 329.
- 68) Liu, C.; Chen, D.; Cheng, M.; Peng, S.; Liu, S. *Organometallics*, **1995**, *15*, 1983.
- 69) Corbridge, D. E. C. *Phosphorus* (Elsevier: Amsterdam, 1978).

- 70) (a) Fan, L.; Krzywicki, A.; Somogyvari, A.; Ziegler, T. *Inorg. Chem.* **1994**, *33*, 5287. (b) Fan, L.; Krzywicki, A.; Somogyvari, A.; Ziegler, T. *Inorg. Chem.* **1996**, *35*, 4003.
- 71) (a) Chan, M. S. W.; Deng, L.; Ziegler, T. *Organometallics* **2000**, *19*, 2741. (b) Margl, P.; Ziegler, T. *J. Am. Chem. Soc.* **1996**, *118*, 7337.
- 72) (a) Deng, L.; Margl, P.; Ziegler, T. *J. Am. Chem. Soc.* **1997**, *119*, 1094. (b) Michalak, A.; Ziegler, T. *Organometallics* **2001**, *20*, 1521.
- 73) (a) Deng, L.; Woo, T. K.; Cavallo, L.; Margl, P.; Ziegler, T. *J. Am. Chem. Soc.* **1997**, *119*, 6177. (b) Woo, T. K.; Blochl, P. E.; Ziegler, T. *J. Phys. Chem. A* **2000**, *104*, 121.
- 74) (a) Musaev, D. G.; Froese, R. D. J.; Svensson, M.; Morokuma, K. *J. Am. Chem. Soc.* **1997**, *119*, 367. (b) Musaev, D. G.; Svensson, M.; Morokuma, K.; Stromberg, S.; Zetterberg, K.; Siegbahn, P. E. M. *Organometallics* **1997**, *16*, 1933.
- 75) Musaev, D. G.; Froese, R. D. J.; Morokuma, K. *New J. Chem.* **1997**, *21*, 1269.
- 76) Deubel, D. V.; Ziegler, T. *Organometallics* **2002**, *21*, 1603.
- 77) Tomita, T.; Takahama, T.; Sugimoto, M.; Sakaki, S. *Organometallics* **2002**, *21*, 4138.
- 78) Ali, R.; Dillon, K. B. *J. Chem. Soc., Dalton Trans.* **1990**, 2593.
- 79) Barnard, T. S.; Mason, M. R. *Inorg. Chem.* **2001**, *40*, 5001.
- 80) Curtis, N. J.; Brown, R. S. *J. Org. Chem.* **1980**, *45*, 4038.
- 81) Lipshutz, B. H.; Morey, M. C. *J. Org. Chem.* **1983**, *48*, 3745.

- 82) Hilf, C.; Bosold, F.; Harms, K.; Lohrenz, J. C.; Marsch, M. *Chem. Ber.* **1997**, *130*, 1201.
- 83) Corey, E. J.; Semmelhack, M. F.; Hegedus, L. S. *J. Am. Chem. Soc.* **1968**, *90*(9), 2416.
- 84) Moore, S. S.; Whitesides, G. M. *J. Org. Chem.* **1982**, *47*(8), 1489.
- 85) Abdul-Jalil, M.; Yamada, T.; Fujinami, S.; Honjo, T.; Nishikawa, H. *Polyhedron* **2001**, *20*(7-8), 627.
- 86) Tolmachev, A. A.; Yurchenko, A. A.; Semenova, M. G.; Feshchenko, N. G. *Zh. Obshh. Khim.* **1993**, *63*(3), 714.
- 87) Jones, R. G. *J. Am. Chem. Soc.* **1949**, *71*, 383.
- 88) Tang, C. C.; Davalian, D.; Huang, P.; Breslow, R. *J. Am. Chem. Soc.* **1978**, *100*, 3918.
- 89) (a) Sakakibara, S.; Fujii, T. *Bull. Chem. Soc. Jpn.* **1969**, *42*, 1466. (b) van der Eijk, J. M.; Nolte, R. J. M.; Zwikker, J. W. *J. Org. Chem.* **1980**, *45*, 547.
- 90) (a) Kirk, K. L. *J. Org. Chem.* **1978**, *43*, 4381. (b) Giesemann, H.; Oelschlagel, A.; Pfau, H. *Chem. Ber.* **1960**, *93*, 576.
- 91) Wei, P. R.; Stephan, D. W. *Unpublished results.*
- 92) Imhoff, P.; Nefkens, S. C. A.; Elsevier, C. J.; Goubitz, K.; Stam, C. H. *Organometallics* **1991**, *10*, 1421.
- 93) Imhoff, P.; Elsevier, C. J. *J. Organomet. Chem.* **1989**, *361*, C61.
- 94) Imhoff, P.; van Asselt, R.; Ernsting, J. M.; Vrieze, K. Elsevier, C. J. *Organometallics* **1993**, *12*, 1523.

- 95) Lahoz, F. J.; Tiripicchio, A.; Tiripicchio-Camellini, M.; Ono, L.A. Pinillos, M. T. *J. Chem. Soc., Dalton Trans.* **1985**, 1487.
- 96) Bruin, B.; Kicken, R. J. N. A. M.; Suos, F. A.; Donners, M. P. J.; Reijer, C. J.; Sandee, A. J.; Gelder, R.; Smits, J. M. M.; Gal, A. G.; Spek, A. L. *Eur. J. Inorg. Chem.* **1999**, 1581.
- 97) Keim, W. *J. Organomet. Chem.* **1968**, *14*, 179.
- 98) (a) Murray, B. D.; Hope, H.; Hvoslef, J.; Power, P. P. *Organometallics* **1984**, *3*, 657. (b) Brunner, H.; Beier, P.; Riepl, G.; Bernal, I.; Reisner, G. M.; Benn, R.; Rufinska, A. *Organometallics* **1985**, *4*, 1732. (c) Dick, D. G.; Stephan, D. W. *Can. J. Chem.* **1986**, *64*, 1870.
- 99) Karschube, W.; Porschke, K. R.; Wilke, G. *J. Organomet. Chem.* **1988**, *355*, 525.
- 100) Carmona, E.; Panaque, M.; Poveda, M. L. *Polyhedron* **1989**, *8*, 285.
- 101) Hidai, M.; Kashiwagi, T.; Ikeuchi, T.; Uchida, Y. *J. Organomet. Chem.* **1971**, *30*, 279.
- 102) Pregosin, P. S.; Salzmann, R. *Coord. Chem. Rev.* **1996**, *155*, 35-68; and references therein.
- 103) Elschenbroich, C. A.; Salzer, A. *Organometallics* (VCH; New York, 1992).
- 104) Sun, W.; Zilong, L.; Hu, H.; Wu, B.; Yang, H.; Zhu, N.; Leng, X.; Wang, H. *New J. Chem.* **2002**, *26*, 1474.
- 105) Brassat, I.; Keim, W.; Killat, S.; Mothrath, M.; Mastrorilli, P.; Nobile, C. F.; Suranna, G. P. *J. Mol. Catal. A* **2000**, *157*, 41.

Curriculum Vitae

Liam P. Spencer

Education

- M. Sc. in Synthetic Organometallic Chemistry
from the University of Windsor (Supervisor: Dr. D. W. Stephan)
Thesis Working Title: *Syntheses and Applications of Group VI and VIII-X Heterocyclic-Phosphinimine Complexes*
In progress.
- Bachelor of Science (Hons.) in Chemistry
from the University of Victoria (Honours Thesis Supervisor: Dr. G. Poulton)
Honours Thesis Title: *The Use of Organometallic Reagents in the Synthesis of Unsymmetric Ketones*
April 2000

Publications

- Liam P. Spencer, Ramadan Altwier, Pingrong Wei, James W. Gault, Douglas W. Stephan*, "Pyridine and Imidazole-Phosphinimine Bidentate Ligand Complexes: Considerations for Ethylene Oligomerization Catalysts" *In preparation*, **2002**.
- Liam P. Spencer, Douglas W. Stephan*, "Imidazolate-Phosphinimine Complexes: Synthesis and the potential for ethylene oligomerization" *In preparation*, **2002**.
- Liam P. Spencer, Gerry A. Poulton, "The Use of Organometallic Reagents in the Synthesis of Unsymmetric Ketones" honours thesis, submitted to the University of Victoria, Victoria, B. C. Canada, April **2000**.
- George X. Pan, Liam P. Spencer, Gordon J. Leary, "A comparative study on reactions of hydrogen peroxide and peracetic acid with lignin chromophores. Part 1. The reaction of coniferaldehyde model compounds" *Holzforschung*, **2000**, *54* (2), 144.
- George X. Pan, Liam P. Spencer, Gordon J. Leary, "A comparative study on reactions of hydrogen peroxide and peracetic acid with lignin chromophores: Part 2. The reaction of stilbene-type model compounds" *Holzforschung*, **2000**, *54*(2), 153.

- George X. Pan, Liam P. Spencer, Gordon J. Leary, "Reactivity of ferulic acid and its derivatives toward hydrogen peroxide and peracetic acid" *J. Agric. Food Chem.*, **1999**, 47(8), 3325.

Conferences

- Liam P. Spencer, Gerry A. Poulton*, "The Use of Organometallic Reagents in the Synthesis of Unsymmetric Ketones" Organic Discussion Weekend, Victoria, B. C. April 2000 (oral presentation).

Awards

- Gladys Estella Laird Fellowship, University of British Columbia, January **2003**.
- Charles A. McDowell Fellowship, University of British Columbia, January **2003**.
- Ontario Graduate Scholarship, May **2002**.
- Ontario Graduate Scholarship for Science and Technology, May **2001**.
- University of Windsor Tuition Scholarship (May 2001)
- B.W. Pearse Chemistry Scholarship, University of Victoria, Sept. **2000**.
- NSERC Undergraduate Summer Research Scholarship, University of Victoria, Sept. **1998**.
- University of Victoria Entrance Scholarship, University of Victoria, Sept. **1995**.
- B.C. Teacher's Association Scholarship, University of Victoria, Sept. **1995**.
- B.C. Provincial Scholarship, University of Victoria, Sept. **1995**.
- B.C. Credit Union Bursary, University of Victoria, Sept. **1995**.